Cell Genomics

Article

The shared genetic landscape of blood cell traits and risk of neurological and psychiatric disorders

Graphical abstract

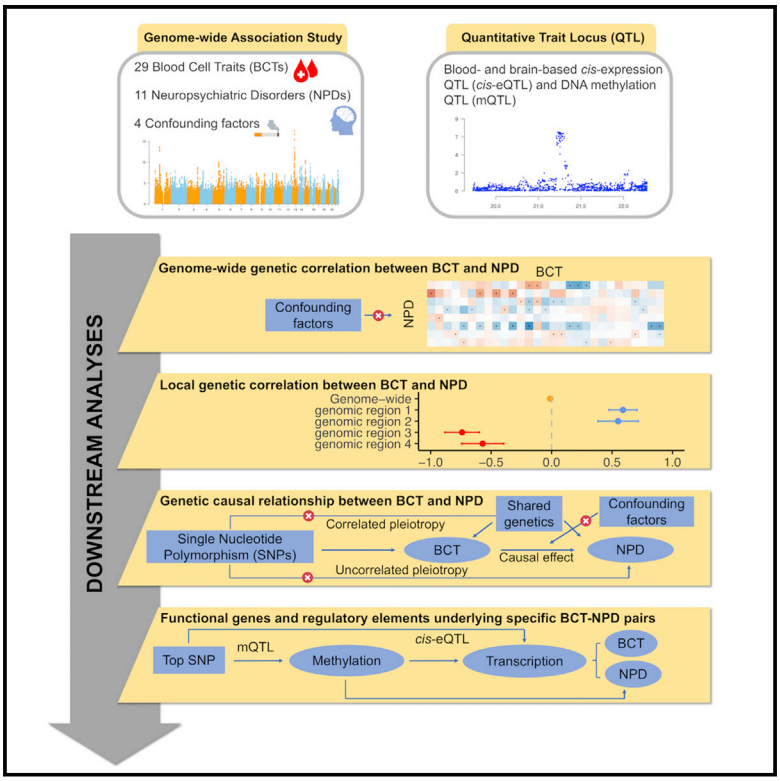

Highlights

- Extensive genome-wide and local genetic correlations between BCTs and NPDs
- Evidence for a causal effect of platelet distribution width on Parkinson's disease
- Multiple functional genes and regulatory elements shared by specific BCT-NPD pairs
- Genetic evidence for potential drug re-purposing candidates for common NPDs

Authors

Yuanhao Yang, Yuan Zhou, Dale R. Nyholt, ..., Zhihong Zhu, Bruce V. Taylor, Jacob Gratten

Correspondence

yuanhao.yang@mater.uq.edu.au (Y.Y.), jacob.gratten@mater.uq.edu.au (J.G.)

In brief

Yang et al. report a broad landscape of genetic overlap between 29 blood cell traits (BCTs) and 11 neurological and psychiatric disorders (NPDs), including previously unreported genome-wide and local genetic correlations, a causal effect of platelet distribution width on Parkinson's disease, and numerous functional genes and regulatory elements shared by specific BCT-NPD pairs. These results shine light on the close relationship of BCTs with risk for NPDs and provide a foundation for improving the prognosis and treatment of common NPDs.

Yang et al., 2023, Cell Genomics 3, 100249
February 8, 2023 © 2023 The Authors.
https://doi.org/10.1016/j.xgen.2022.100249

CellPress

Cell Genomics

CellPress
OPEN ACCESS

Article

The shared genetic landscape of blood cell traits and risk of neurological and psychiatric disorders

Yuanhao Yang,[1,2,9,*] Yuan Zhou,[3] Dale R. Nyholt,[4] Chloe X. Yap,[1,2] Rudolph K. Tannenberg,[1] Ying Wang,[5,6,7] Yang Wu,[2] Zhihong Zhu,[2,8] Bruce V. Taylor,[3] and Jacob Gratten[1,*]

[1]Mater Research Institute, The University of Queensland, Woolloongabba, QLD 4102, Australia
[2]Institute for Molecular Bioscience, The University of Queensland, St Lucia, QLD 4072, Australia
[3]Menzies Institute for Medical Research, University of Tasmania, Hobart, TAS 7000, Australia
[4]School of Biomedical Sciences, Faculty of Health, and Centre for Genomics and Personalised Health, Queensland University of Technology, Kelvin Grove, QLD 4059, Australia
[5]Analytic and Translational Genetics Unit, Massachusetts General Hospital, Boston, MA 02114, USA
[6]Stanley Center for Psychiatric Research, Broad Institute of MIT and Harvard, Cambridge, MA 02142, USA
[7]Program in Medical and Population Genetics, Broad Institute of MIT and Harvard, Cambridge, MA 02142, USA
[8]National Centre for Register-based Research, Aarhus University, Aarhus 8210, Denmark
[9]Lead contact
*Correspondence: yuanhao.yang@mater.uq.edu.au (Y.Y.), jacob.gratten@mater.uq.edu.au (J.G.)
https://doi.org/10.1016/j.xgen.2022.100249

SUMMARY

Phenotypic associations have been reported between blood cell traits (BCTs) and a range of neurological and psychiatric disorders (NPDs), but in most cases, it remains unclear whether these associations have a genetic basis and, if so, to what extent genetic correlations reflect causality. Here, we report genetic correlations and Mendelian randomization analyses between 11 NPDs and 29 BCTs, using genome-wide association study summary statistics. We found significant genetic correlations for four BCT-NPD pairs, all of which have prior evidence for a phenotypic correlation. We identified a previously unreported causal effect of increased platelet distribution width on susceptibility to Parkinson's disease. We identified multiple functional genes and regulatory elements for specific BCT-NPD pairs, some of which are targets of known drugs. These results enrich our understanding of the shared genetic landscape underlying BCTs and NPDs and provide a robust foundation for future work to improve prognosis and treatment of common NPDs.

INTRODUCTION

Variation in the functional and physiological properties of blood cells has been associated with a range of neurological and psychiatric disorders (NPDs), including major depressive disorder (MDD),[1] schizophrenia (SCZ),[2] multiple sclerosis (MS),[3] stroke,[4] and Parkinson's disease (PD).[5] Some phenotypic associations between blood cell traits (BCTs) and NPD diagnoses have been shown to have a genetic basis,[6] in some cases consistent with the presence of a causal effect of hematological indices on disease. For example, Astle et al.[7] reported that elevated lymphocyte count (LYMPH#) causally increases the risk for MS and SCZ, Harshfield et al.[8] reported a causal role of higher plateletcrit (PCT) and eosinophil percentage of white blood cells (EO%) in susceptibility to ischemic stroke and its subtypes (i.e., cardioembolic stroke, large-artery atherosclerotic stroke), and Sealock et al.[1] reported a causal effect of increased white blood cell count (WBC) on risk for depression. Previous studies have also identified specific genes shared by pairs of BCTs and NPDs, such as tyrosine kinase 2 (*TYK2*) underlying MS and T lymphocyte polarization,[9] and the well-established PD risk gene *SNCA* (encoding the protein alpha-synuclein), which also plays a role in development of red blood cells.[10] These discoveries improve understanding of disease etiology and potential points of intervention through re-purposing of drugs.

Despite this progress, the genetic relationships between BCTs and many NPDs remain unclear. There is also uncertainty in relation to whether genetic correlations between BCTs and NPDs predominantly reflect horizontal pleiotropy, whereby genetic variants have effects on both members of a trait pair via one (correlated horizontal pleiotropy) or more (uncorrelated horizontal pleiotropy) independent pathways. Alternatively, a causal relationship may exist between BCT and NPD, potentially involving other traits downstream of the exposure but on the same causal pathway linking the exposure to the outcome (referred to as "vertical pleiotropy").[11] A more comprehensive understanding of genetic overlap and causal relationships between BCTs and NPDs is needed to determine whether

This is an open access article under the CC BY-NC-ND license (http://creativecommons.org/licenses/by-nc-nd/4.0/).

Table 1. GWAS datasets for BCTs used in the study

BCT	Class	Abbreviation
Basophil count	White cells	BASO#
Basophil percentage of white cells	White cells	BASO%
Eosinophil count	White cells	EO#
Eosinophil percentage of white cells	White cells	EO%
Lymphocyte count	White cells	LYMPH#
Lymphocyte percentage of white cells	White cells	LYMPH%
Monocyte count	White cells	MONO#
Monocyte percentage of white cells	White cells	MONO%
Neutrophil count	White cells	NEUT#
Neutrophil percentage of white cells	White cells	NEUT%
White blood cell count	White cells	WBC
Mean platelet volume	Platelets	MPV
Plateletcrit	Platelets	PCT
Platelet distribution width	Platelets	PDW
Platelet count	Platelets	PLT#
Hematocrit	Red cells	HCT
Hemoglobin	Red cells	HGB
High light scatter reticulocyte count	Red cells	HLSR#
High light scatter percentage of red cells	Red cells	HLSR%
Immature fraction of reticulocytes	Red cells	IRF
Mean corpuscular hemoglobin	Red cells	MCH
Mean corpuscular hemoglobin concentration	Red cells	MCHC
Mean corpuscular volume	Red cells	MCV
Mean reticulocyte volume	Red cells	MRV
Mean spheric corpuscular volume	Red cells	MSCV
Red blood cell count	Red cells	RBC#
Red cell distribution width	Red cells	RDW
Reticulocyte count	Red cells	RET#
Reticulocyte fraction of red cells	Red cells	RET%

n samples = 408,112; n SNPs[a] = 9.58M; Vuckovic et al.[26] BCT, blood cell traits; GWAS, genome-wide association study.
[a]SNPs with minor allele frequency < 1%.

hematological measures (which are more accessible and well established than brain-based markers) represent meaningful predictive or prognostic biomarkers for risk of common brain disorders,[12–15] and if hematopoietic pathways may even represent legitimate targets for development of disease-modifying treatments.

In this study, we used large-scale genome-wide association study (GWAS) summary statistics for 29 BCTs and 11 common NPDs (Tables 1 and 2) to estimate global and local genetic correlations between BCT-NPD pairs using high-definition likelihood (HDL)[16] and heritability estimation from summary statistics (ρ-HESS),[17] respectively. We then performed multiple Mendelian randomization (MR) analyses[18–24] to explore evidence for causality between BCTs and NPDs, and we applied summary data-based MR (SMR)[25] to identify putatively functional genes and regulatory elements shared between pairs of BCTs and NPDs. A flowchart of the main analytic steps is provided in Figure 1.

RESULTS

Genetic correlations between BCTs and neurological and psychiatric disorders

We observed Bonferroni significant ($p < 1.57 \times 10^{-4}$) genetic correlations (r_g) for two (of 319) BCT-NPD pairs using the HDL method (MS and LYMPH#: $r_g = 0.09$, SE = 0.02, $p = 3.86 \times 10^{-6}$; SCZ and monocyte percentage of white cells [MONO%]: $r_g = -0.03$, SE = 0.01, $p = 2.11 \times 10^{-5}$), and a further two trait pairs (migraine and platelet count [PLT#]: $r_g = 0.08$, SE = 0.02, $p = 3.94 \times 10^{-4}$; MS and WBC: $r_g = 0.06$, SE = 0.02, $p = 4.78 \times 10^{-4}$) surpassed a less stringent 5% Benjamini-Hochberg false discovery rate (FDR) (Figure 2; Table S1). Notably, each of these four trait pairs had prior evidence for a significant phenotypic correlation in the same direction.[39–42] We then re-estimated each of these four genetic correlations after using multi-trait-based conditional and joint analysis (mtCOJO)[23] to condition each trait on each of four potential confounding factors, including cigarettes per day,[43] drinks per week,[43] educational attainment,[44] and household income.[45] The r_g estimates from these conditional HDL analyses were highly consistent with our original estimates, suggesting that these confounding factors have negligible effects on the shared genetics underlying the focal pairs of BCTs and NPDs (Figure S1; Table S2).

The magnitude of r_g estimates between pairs of BCTs and NPDs were weak to moderate, ranging from −0.11 to 0.13. The HDL r_g estimates were highly consistent with those estimated by linkage disequilibrium (LD) score regression (LDSC; R = 0.81, 95% confidence interval [CI] = 0.76–0.84; Figures S2 and S3). Considering all nominally significant genetic correlations, HDL identified 56 pairs of BCTs and NPDs and LDSC identified 28, of which 14 were not seen with HDL (Table S3; Figure S2). We also estimated the r_g among 406 BCT pairs, and whereas most BCTs were genetically distinct (322 of 406 pairs with absolute value of $r_g < 0.2$), we identified strong positive and negative r_g for a subset of BCT pairs (Figures S4 and S5; Tables S4 and S5), consistent with hematopoietic cell type classifications reported by Astle et al.[7] For example, we found strong positive r_g among white blood cell measures (e.g., LYMPH#, monocyte count, neutrophil count, WBC) but negative r_g among ratios of these white blood cell count measures (e.g., lymphocyte percentage of white cells, MONO%, neutrophil percentage of white cells [NEUT%]).

Local genetic correlations between BCTs and neurological and psychiatric disorders

We used ρ-HESS[17] to estimate local genetic correlations between 319 pairs of BCTs and NPDs at 1,693 approximately LD-independent genomic regions (excluding the major histocompatibility complex [MHC] region). The rationale was that a negligible genome-wide genetic correlation may obscure meaningful genetic correlations in defined genomic regions, and the pattern of local genetic correlations in trait-associated regions can reveal putative causal relationships between traits.[17] As a validity check, we first compared the genome-wide sum of local genetic correlations per trait pair to genome-wide r_g estimates (Table S6) from HDL (and LDSC), finding that these were highly

Table 2. GWAS datasets for neurological and psychiatric disorders used in this study

NPDs (abbreviation) by type[a]	Publication	n cases	n controls	Eff. n[b]	n SNPs[c]
Alzheimer's disease (AD)	Jansen et al.[27]	71,880	383,378	121,062	9.74M
Amyotrophic lateral sclerosis (ALS)	Nicolas et al.[28]	20,806	59,804	30,872	8.85M
Migraine (migraine)	Gormlet et al.[29]	59,674	316,078	100,394	8.94M
Multiple sclerosis (MS)	IMSGC[30]	14,802	26,703	19,046	6.52M
Parkinson's disease (PD)	Nalls et al.[31]	37,688 cases, 18,618 proxy cases	1,417,791	108,311	7.52M
Stroke (stroke)	Malik et al.[32]	40,585	406,111	73,795	8.26M
Attention-deficit/hyperactivity disorder (ADHD)	Demontis et al.[33]	19,099	34,194	24,509	6.91M
Autism spectrum disorder (ASD)	Grove et al.[34]	18,381	27,969	22,183	9.11M
Bipolar disorder (BIP)	Stahl et al.[35]	20,352	31,358	24,684	9.64M
Major depressive disorder (MDD)	Wray et al.[36]	116,404	314,990	169,989	9.51M
Schizophrenia (SCZ)	PGC[37]	51,900	71,675	60,205	9.55M

GWAS, genome-wide association study; IMSGC, International Multiple Sclerosis Genetics Consortium; NPD, neurological and psychiatric disorder; PGC, Psychiatric Genomics Consortium.
[a]NPD, neurological and psychiatric disorder
[b]Eff n: Effective sample size calculated from RICOPILI.[38]
[c]SNPs with minor allele frequency < 1%.

correlated (R = 0.83, 95% CI = 0.79–0.86 for ρ-HESS and HDL; R = 0.74, 95% CI = 0.68–0.79 for ρ-HESS and LDSC; Figure S6), as expected.

Next, we considered if there was evidence for specific genomic regions that contribute disproportionately to trait covariance (Tables S7, S8, S9, S10, S11, S12, S13, S14, S15, S16, and S17). We identified 32 genomic regions (involving 74 trait pairs) with a Bonferroni significant ($p < 9.26 \times 10^{-8}$) local genetic correlation and significant local SNP heritability for both traits (Figure S7; Table S18). These included the *APOE* region on chromosome 19 (hg19: 44.7–46.1 Mb) contributing to Alzheimer's disease (AD) and four BCT traits, and two regions on chromosomes 4 (0.7–1.5 Mb) and 17 (43.1–45.9 Mb) contributing to PD and a total of 20 BCT traits, the latter encompassing the highly pleiotropic 17q21 inversion region, which contains the microtubule-associated protein tau (*MAPT*) gene associated with AD[46] and frontotemporal dementia.[47] Additionally, nine and 24 regions were found to contribute to 24 MS-BCT and 26 SCZ-BCT pairs, respectively. A majority (128 of 166) of these significant local genetic correlations involved trait pairs for which there was no evidence of genome-wide r_g from HDL or LDSC. However, most regions contained genome-wide significant SNPs for both traits (141 of 166), for the NPD (141 of 166) or for the BCT (165 of 166).

Finally, we explored if any BCT-NPD pairs exhibited a pattern of local genetic correlations that were consistent with a putative causal relationship between traits: that is, trait pairs for which the average local genetic correlation was significantly different in BCT-versus NPD-associated regions of the genome. We identified no single BCT-NPD trait pair satisfying this criterion after Bonferroni ($p < 1.57 \times 10^{-4}$) or FDR ($p < \sim 1.50 \times 10^{-4}$) correction for multiple testing, irrespective of the p value cut-off (or SBayesR[48]) used to define trait-specific SNPs and genomic regions (Figures S8–S14; Tables S19, S20, S21, S22, S23, S24, and S25).

Putative causal effects of plateletcrit on stroke and platelet distribution width on PD

Next, we used the CAUSE (causal analysis using summary effect estimates)[18] method to perform bi-directional MR analyses for pairs of BCTs and NPDs with evidence for a nominally significant genome-wide r_g (from HDL or LDSC; n = 70 trait pairs; see Figures 2 and S2), recognizing that causal relationships between highly polygenic traits (such as the BCTs and NPDs included in our study) are more likely in the presence of a global genetic correlation. We identified three Bonferroni-significant ($p < 3.57 \times 10^{-4}$, i.e., $\frac{0.05}{70 \times 2}$) causal relationships (increased LYMPH# on risk for MS: odds ratio [OR_{CAUSE}] = 1.20 [i.e., a 1.2-fold increase in risk for MS for each SD increase in LYMPH#], 95% CI = 1.11–1.31, $p = 3.94 \times 10^{-5}$; increased WBC on MS: $OR_{CAUSE} = 1.16$, 95% CI = 1.07–1.26, $p = 2.60 \times 10^{-4}$; increased PCT on stroke: $OR_{CAUSE} = 1.07$, 95% CI = 1.04–1.11, $p = 6.27 \times 10^{-6}$), two of which remained significant after conservatively adjusting for all 319 trait pairs (i.e., LYMPH# and MS, PCT and stroke). Notably, the genetic correlation between LYMPH# and WBC (both measures of white cells) is 0.64 (SE = 0.06, $p = 1.27 \times 10^{-31}$), suggesting that the putative causal effects of these BCTs on MS represents a partly overlapping signal. A further three potential causal relationships were identified at a less stringent 5% FDR significance level: reduced mean spheric corpuscular volume (MSCV) on autism spectrum disorder (ASD; $OR_{CAUSE} = 0.94$, 95% CI = 0.90–0.97, $p = 6.45 \times 10^{-4}$), increased PCT on MS ($OR_{CAUSE} = 1.14$, 95% CI = 1.06–1.22, $p = 4.29 \times 10^{-4}$), and increased platelet distribution width (PDW) on PD ($OR_{CAUSE} = 1.07$, 95% CI = 1.03–1.12, $p = 6.40 \times 10^{-4}$). In the reverse analyses, there was no evidence for a causal effect of any NPD on any BCT (Figure 3; Table S26), suggesting the significant genetic correlations between BCTs and NPDs are unlikely to be driven by reverse causality.

To further assess these potential causal relationships, we performed a series of sensitivity MR analyses, cognizant of the

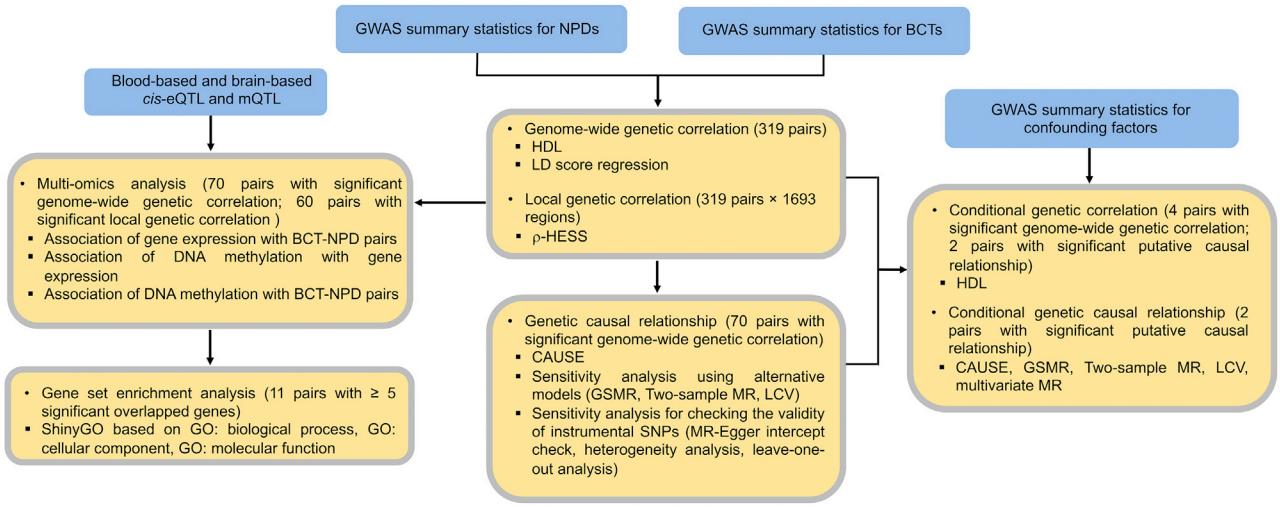

Figure 1. Overview of the main analytic steps performed in the study

strong *a priori* expectation for pleiotropy under the plausible assumption that changes in BCTs are inherent to the disease process. Using six alternative MR methods, we identified consistent evidence for a causal effect of increased PCT on stroke, with $p < 0.05$ for all methods and four of six surpassing the Bonferroni significance threshold (Figure 3; Table S27). Notably, the estimated genetic causality proportion (GCP) from latent causal variable (LCV) analysis for an effect of PCT on stroke was 0.69 (SE = 0.21, $p = 4.43 \times 10^{-23}$), which (to put this in perspective) is roughly equivalent to the GCP estimate for the effect of high cholesterol on risk for myocardial infarction (GCP = 0.70).[24] Consistent with this evidence for a causal relationship, we observed a significant (albeit modest) positive phenotypic correlation (r_P) between PCT and stroke in the UK Biobank (UKB; $r_P = 0.01$ and $p = 2.86 \times 10^{-5}$, assuming prevalence of 5%; see Data S1; Table S28).

We also found consistent evidence for a causal effect of elevated PDW on PD, with $p < 0.05$ for five of six MR methods (Figure 3; Table S27). The exception was LCV (GCP = 0.35, SE = 0.43, $p = 0.17$), which may be explained by the small estimated r_g between PDW and PD ($r_{g(HDL)} = 0.03$, SE = 0.02, $p = 0.09$; $r_{g(LDSC)} = 0.05$, SE = 0.03, $p = 0.04$), given that the LCV method is known to produce conservative p values for traits with low r_g.[24] Again, as would be expected given a causal relationship, we observed a positive r_P between PDW and PD in the UKB, although the estimate was only marginally significant ($r_P \sim 0.01$, $p = 8.44 \times 10^{-4}$ to 0.07 depending on prevalence; Data S1; Table S28), potentially because of the modest number of PD cases in the cohort (n = 1,323 compared with >5,000 for stroke).

To further evaluate the reliability of the inferred causal effects of PCT on stroke and PDW on PD, we performed several additional sensitivity analyses. We first checked the MR-Egger intercept terms in each analysis, confirming there was no evidence for non-zero estimates, and thus no indication that the MR-Egger causal estimates were confounded by pleiotropy (Table S29). Second, we performed leave-one-out analyses for each trait pair using each of the four two-sample MR methods (IVW, MR-Egger, weighted median [WMe], and weighted mode [WMo]). In all instances, there was no evidence that any single instrumental SNP was responsible for the inference of a causal relationship for either PCT-stroke or PDW-PD (Figure S15, Tables S30, S31, S32, and S33). Third, we checked for heterogeneity of instrumental SNP effects in the IVW and MR-Egger analyses, and although there was evidence for heterogeneity, after removing pleiotropic SNPs identified by generalized summary data-based MR (GSMR), the causal estimates from IVW and MR-Egger for PCT-stroke and PDW-PD remained significant and highly consistent with the original estimates (Table S29).

As a final sensitivity analysis, we explored if the causal effects of PCT on stroke and PDW on PD were influenced by common environmental factors associated with disease risk, including smoking,[43] alcohol consumption,[43] educational attainment,[44] and socioeconomic status.[45] We conditioned GWAS statistics for PCT, stroke, PDW and PD on each potential cofounder using mtCOJO and then repeated each of the MR analyses (i.e., CAUSE, GSMR, IVW, MR-Egger, WMe, and WMo) and LCV using the conditioned GWAS summary statistics (see STAR Methods). These conditional MR (and LCV) analyses were all highly consistent with our primary results (Figure S16; Table S34). We also applied multivariable MR (MVMR)[49] analysis to PCT-stroke and PDW-PD, adjusting for potential pleiotropic effects of all four confounders concurrently. Again, these analyses were highly consistent with the causal inference from our primary analyses (Table S35), further supporting unidirectional causal effects of PCT on stroke and PDW on PD.

In addition to PCT-stroke and PDW-PD, we also observed suggestive support for higher LYMPH# on MS, with four of six sensitivity analyses surpassing Bonferroni significance (Figure 3; Table S27). However, effect size estimates varied widely, and contrary to expectations, there was no evidence for a phenotypic correlation between LYMPH# and MS in the UKB ($r_P \sim -0.002$, $p > 0.50$; Data S1; Table S28). These findings suggest that further research will be needed to confirm this putative causal relationship.

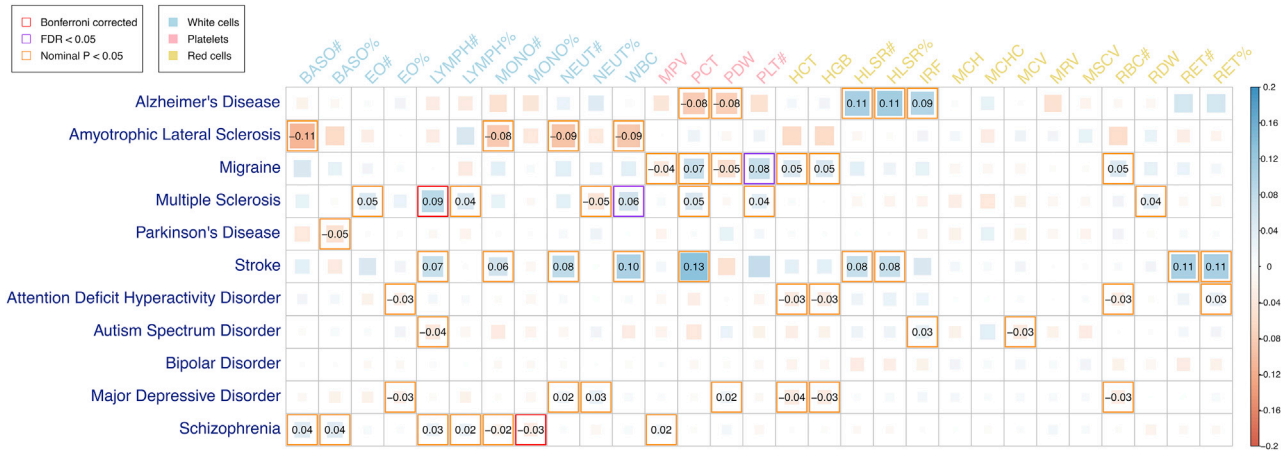

Figure 2. Estimated genetic correlations between BCTs and NPDs using the HDL method

Significant genetic correlations (with estimates provided) are highlighted by red, purple, or orange borders if they were Bonferroni significant ($p < 1.57 \times 10^{-4}$), FDR significant ($p < \sim 7 \times 10^{-3}$), or nominally significant ($p < 0.05$), respectively. See Table S1 for complete details of HDL estimates.

As expected, sensitivity analyses using stroke, PD and MS as exposures for PCT, PDW and LYMPH# (respectively), were universally (or largely) non-significant. Sensitivity analyses of the effect of MSCV on ASD, and of PCT and WBC on MS were highly inconsistent, and thus we could not further determine if their genetic correlations were due to causality or pleiotropy.

Prioritization of putatively functional genes and regulatory elements shared by BCTs and neurological and psychiatric disorders

Finally, we used SMR to identify putatively functional genes and regulatory elements shared by specific pairs of BCTs and NPDs because of causality or pleiotropy.

We first applied SMR to PCT, PDW, stroke and PD to identify functional genes and regulatory elements underlying the putative causal effects of elevated PCT on risk of stroke and increased PDW on risk for PD. In analyses using blood-based *cis*-expression quantitative trait loci (*cis*-eQTL) in eQTLGen[50] (Table S36) or platelet *cis*-eQTLs from GeneSTAR[51] (Table S37), no single gene survived Bonferroni correction ($p_{SMR} < 3.18 \times 10^{-6}$) for both PDW and PD, or PCT and stroke. However, a total of 18 genes were Bonferroni significant for PCT (n = 5), PDW (n = 12), or PD (n = 1), in agreement with evidence for stronger genetic signals for exposures (i.e., PCT, PDW) than outcomes (i.e., stroke, PD). At a less stringent 5% FDR threshold, we identified 56 significant genes (also passing the heterogeneity in dependent instruments [HEIDI] test) for PDW-PD and 20 for PCT-stroke using blood-based *cis*-eQTLs in eQTLGen[50] (Table S36), and a further four genes (*RHD*, *FXYD5*, *MAP1LC3A*, and *SRSF6*) for PDW-PD in analyses using platelet *cis*-eQTLs from GeneSTAR[51] (Table S37). Among these aforementioned genes, 40 of 60 and nine of 20 had consistent direction of SMR effect for PDW-PD and PCT-stroke, respectively (Figure 4). Using brain-based *cis*-eQTLs, none of these genes surpassed the Bonferroni significance threshold ($p_{SMR} < 6.63 \times 10^{-6}$), but a total of 17 genes were FDR significant for PD (Table S38) and three were identified for stroke (*CLBA1*, *IVD*, and *RMC1*), with consistent direction of SMR associations in blood and brain for a large proportion of genes (with the exception of *FXYD5*, *MGAT3*, *RANBP10*, *RHD*, and *UBXN2A*).

Second, we applied SMR to a further 68 BCT-NPD pairs with a nominally significant ($p < 0.05$) genome-wide r_g (from HDL or LDSC). Using data on blood-based *cis*-eQTLs from eQTLGen,[50] we identified 51 pleiotropic genes whose expression level was Bonferroni-significantly ($p_{SMR} < 3.18 \times 10^{-6}$ and $p_{HEIDI} > 0.01$ with $\geq$10 SNPs) associated with both members of specific BCT-NPD pairs (Table S39). We then tested for association of DNA methylation with expression of these 51 genes, using data on DNA methylation quantitative trait loci (mQTL) in blood-derived DNA from the Brisbane Systems Genetics Study (BSGS) and Lothian Birth Cohorts (LBCs).[52] We identified 273 DNA methylation probes that were Bonferroni-significantly associated with expression of one or more of these genes ($p_{SMR} < 5.37 \times 10^{-7}$, $p_{HEIDI} > 0.01$ with $\geq$10 SNPs; Table S40), of which 13 independent probes, associated with a total of 12 genes, were also Bonferroni-significantly associated ($p_{SMR} < 5.37 \times 10^{-7}$, $p_{HEIDI} > 0.01$ with $\geq$10 SNPs) with both members of the respective focal BCT-NPD pair (Figure 5; Tables S41, S42, and S43). These included six genes (*ABCB9*, *AC100854.1*, *BACH2*, *TNFSF14*, *ZC2HC1A*, and *ZMIZ1*) for MS and one or more BCTs on chromosomes 6, 8, 10, and 19, and seven genes (*ABCB9*, *AC091132.16*, *ARL6IP4*, *DND1P1*, *GATAD2A*, *OGFOD2*, and *ZNF664*) for SCZ and one or more BCTs on chromosomes 12, 17, and 19 (including one gene [*ABCB9*] overlapping with MS and related BCTs). Two functional genes (*ARL6IP4* and *GATAD2A*) and regulatory elements for SCZ and reticulocyte fraction of red cells (RET%) surpassed the experiment-wide Bonferroni-corrected thresholds ($p_{SMR} < 9.96 \times 10^{-9}$ [i.e., $\frac{0.05}{15743 \times 29 \times 11}$] using cis-eQTL as exposure and GWAS as outcome; $p_{SMR} < 1.05 \times 10^{-8}$ [i.e., $\frac{0.05}{93122 \times 51}$] using mQTL as exposure and cis-eQTL as outcome; $p_{SMR} < 1.68 \times 10^{-9}$ [i.e., $\frac{0.05}{93122 \times 29 \times 11}$] using mQTL as exposure and GWAS as outcome; $p_{HEIDI} > 0.01$ with $\geq$10 SNPs for each analysis) across all SMR analyses. Notably, there was evidence for involvement

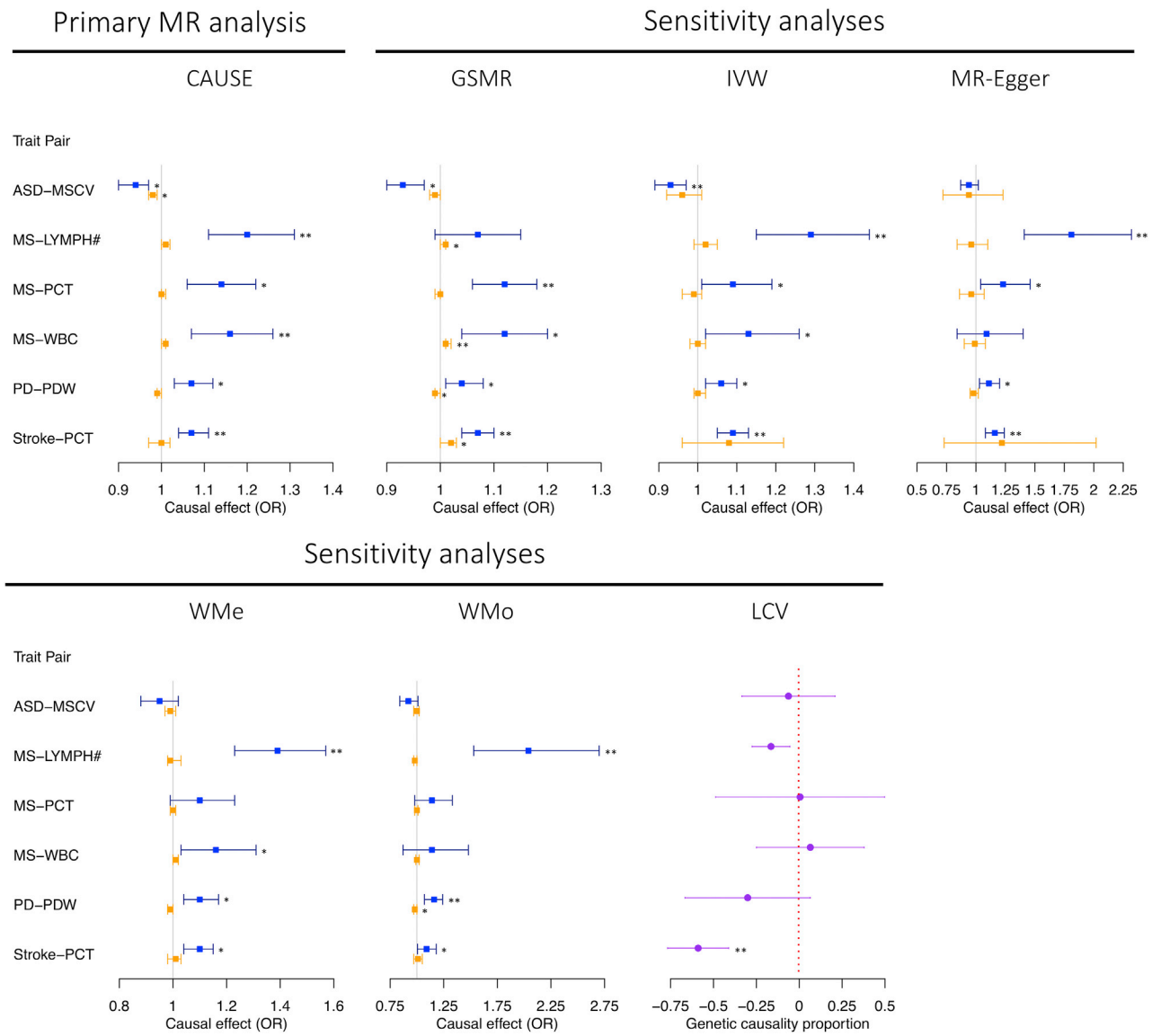

Figure 3. Summary of significant putative causal relationships between BCTs and NPDs identified by CAUSE (primary MR analysis) and of MR sensitivity analyses (including LCV and five two-sample MR methods) for each of these relationships

Results colored in blue represent the estimated causal effect of BCTs on NPDs, while results colored in orange represent the estimated causal effect of NPDs on BCTs. Error bars for CAUSE and the five two-sample MR methods represent 95% confidence intervals, and those for LCV-based GCP point estimates represent standard errors. For LCV, a negative GCP indicates a causal effect of BCT on NPD, and vice versa. Single and double asterisks indicate results surpassing nominal significance ($p < 0.05$) and Bonferroni significance ($p < 3.05 \times 10^{-4}$), respectively. See Tables S26 and S27 for complete details of the estimates.

of regulatory elements located in both promoter and repressor regions for four genes (*ABCB9*, *ARL6IP4*, *GATAD2A*, and *OGFOD2*). For example, reduced methylation in the *OGFOD2* promoter and increased methylation in the *OGFOD2* repressor, in each case associated with up-regulation of this gene, was associated with elevated risk for SCZ and reduced RET% (Table S43). In addition, for all 12 genes that were Bonferroni significant for both members of specific BCT-NPD trait pairs across the three tiers of SMR analyses, the effect of expression on the two traits was concordant with their local genetic correlations (n = 13; Table S43). Additionally, a high proportion (10 of 13) of these local genetic correlations surpassed a 5% nominal significance threshold, indicating a high degree of consistency between SMR and ρ-HESS in relation to shared genetic risk factors.

Third, we performed SMR analyses in regions of Bonferroni-significant local genetic correlation, focusing on the subset of BCT-NPD pairs with negligible genome-wide r_g ($p > 0.05$). On the basis of these criteria, a total of 60 trait pairs and 31 genomic regions were selected for investigation. Using the same multi-step SMR analytic strategy described above, we identified a total of nine Bonferroni-significant genes (*ABCB9*, *ARL6IP4*, *DND1P1*, *GATAD2A*, *OGFOD2*, *ZNF664*, *GNL3*, *LINC02210*,

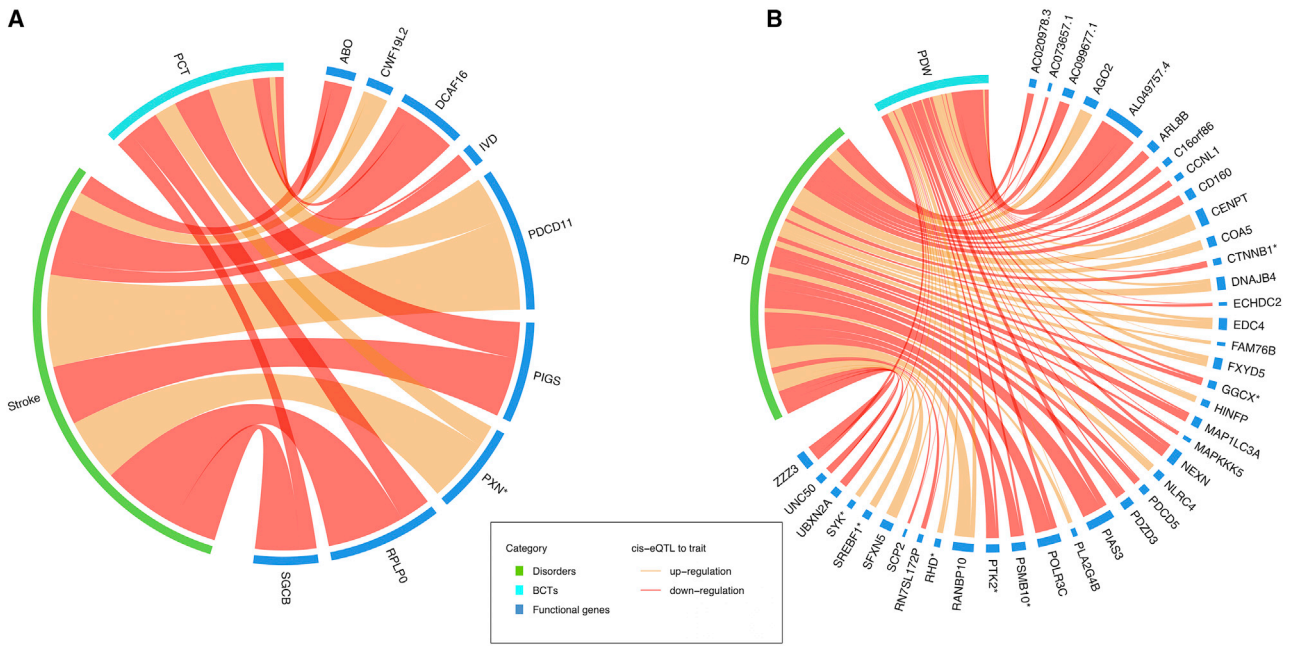

Figure 4. Summary of FDR-significant functional genes associated with PCT-stroke and PDW-PD trait pairs, with consistent direction of SMR effects

(A and B) PCT-stroke (A) and PDW-PD (B) trait pairs. The width of each line represents the SMR association strength. Line color indicates whether upregulation (orange) or downregulation (red) of functional genes is associated with increased disorder risk or BCT values. Genes with an asterisk symbol are known drug targets (Table S49). See Tables S36 and S37 for complete details of the SMR estimates.

and *AC005829.1*) and regulatory elements for SCZ and PD and one or more BCTs (Figure 5; Tables S39, S40, S41, S42, and S44), two of which (*GNL3* and *GATAD2A*; the latter was also reported in pairs of SCZ and RET% of nominally significant genome-wide r_g; Tables S45–S48) were also Bonferroni-significantly associated with their specific NPDs using brain *cis*-eQTLs[53] and mQTLs.[53] In each case, the expression effects of these genes on specific pairs of BCTs and NPDs were consistent with their respective local genetic correlations (Table S44).

Last, we conducted gene set enrichment analysis (GSEA) using ShinyGO[54] to identify biological pathways shared between specific pairs of BCTs and NPDs. We focused on 11 trait pairs with $\geq$5 shared genes identified using SMR applied to blood-based or brain-based *cis*-eQTLs (Table S49). We identified 31 pathways containing $\geq$2 gene set members at an FDR < 0.05, including n = 5 for MS-EO#, n = 2 for MS-RDW, n = 5 for SCZ-LYMPH#, n = 12 for SCZ-MONO%, n = 3 for SCZ-NEUT%, n = 1 for SCZ-RET#, and n = 3 for SCZ-RET% (Table S50). However, whereas the minimum gene set enrichment for these pathway terms was >5-fold, the highest proportion of pathway-specific genes was only 0.04, for tau protein binding in SCZ and MONO% (2 of 45 pathway genes, 338-fold enrichment, FDR p = 4.68×10^{-4}).

DISCUSSION

We generated new insights into the shared genetics of BCTs and neurological and psychiatric disorders using large-scale GWAS summary statistics, and through integration of these data with blood- and brain-based gene expression and DNA methylation QTLs.

We identified a broad landscape of genetic correlations between BCTs and NPDs, including Bonferroni-significant genetic correlations between two BCT-NPD pairs (MS-LYMPH#, SCZ-MONO%), each of which has prior evidence for a significant phenotypic correlation[40,42]; our results provide evidence for a genetic contribution to these previously reported correlations. Overall, the magnitude of HDL-based r_g estimates between BCTs and neurological diseases were greater than those between BCTs and psychiatric disorders (T statistic = 2.68, $p_{\text{two-sample t test}} = 7.87 \times 10^{-3}$); this suggests that neurological diseases (in aggregate) have greater genetic overlap with BCTs than psychiatric disorders, although we acknowledge that not all NPDs are represented in our study. Notwithstanding this caveat, our findings are consistent with evidence for a crucial role of the peripheral immune system in regulating some neurological diseases (e.g., MS, stroke).[55] Interestingly, we failed to replicate some previously reported positive genetic correlations between attention-deficit/hyperactivity disorder (ADHD)-RET%, MDD-WBC, and SCZ-LYMPH#,[6] potentially due to the use of different GWAS summary statistics for some psychiatric disorders (e.g., a subset of the European-based PGC3 SCZ GWAS [n = 123,575] used in this study versus complete PGC3 SCZ GWAS [n = 130,644] in Reay et al.[6]) and BCTs (i.e., our BCT GWAS were obtained from Vuckovic et al.,[26] whereas the previous study used the publicly available blood-based biomarker GWAS from http://www.nealelab.is/uk-biobank), and the use of different LDSC-based SNP sets (i.e., our study focused on

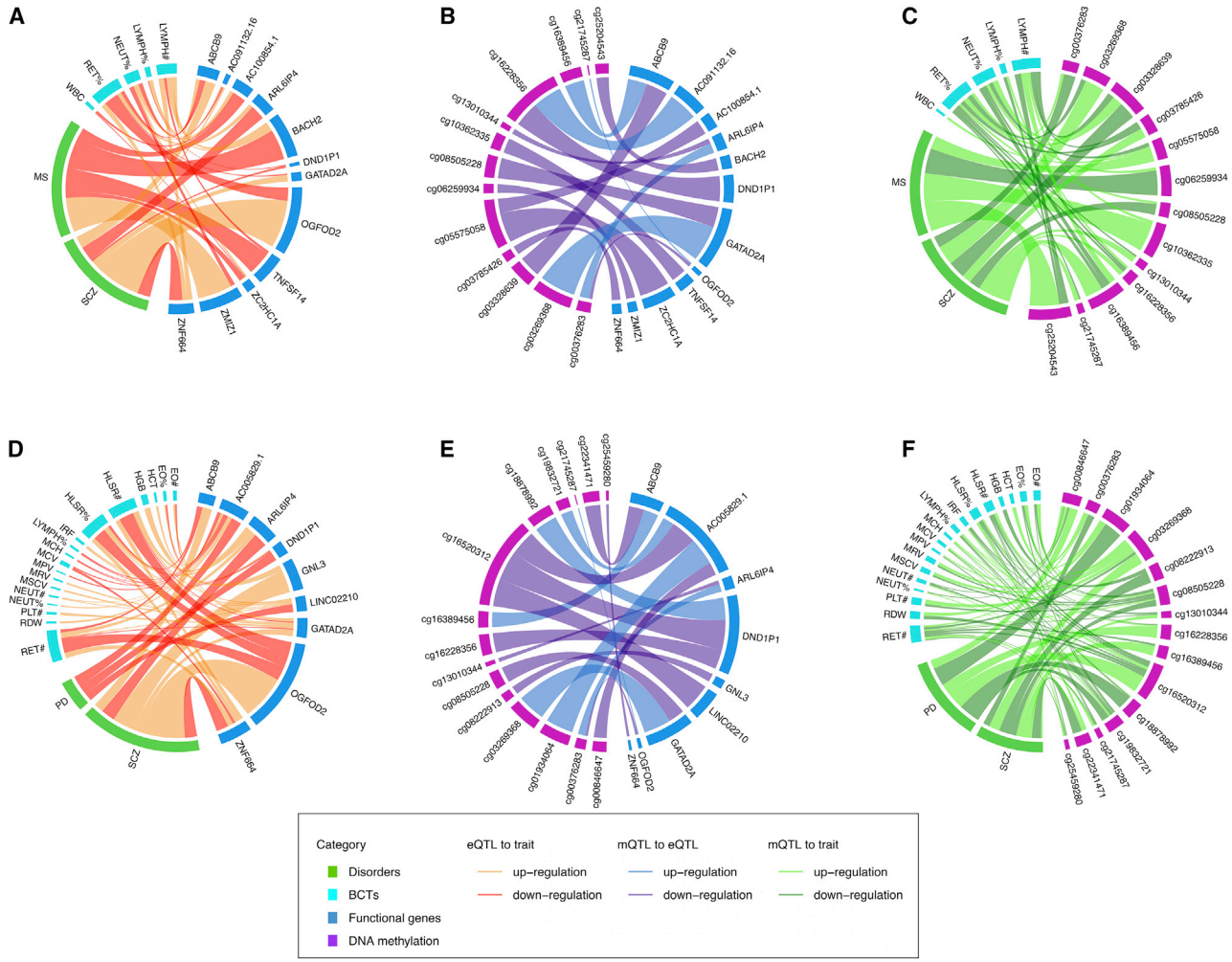

Figure 5. Summary of blood-based Bonferroni-significant functional genes and regulatory elements associated with both members of BCT-NPD trait pairs with significant genome-wide genetic correlations and significant local genetic correlations (but negligible genome-wide genetic correlations)

(A and D) Association of gene expression with each member of the focal BCT-NPD pair. (B and E) Association of DNA methylation with expression of trait-pair-associated genes. (C and F) Association of DNA methylation with BCT-NPD pairs. The width of each line represents the SMR association strength. Line color indicates whether up-regulation or down-regulation of functional genes (or DNA methylation levels) is associated with increased disorder risk or BCT values. See Tables S43 and S44 for complete details of the SMR estimates.

SNP with minor allele frequency [MAF] $\geq$ 0.01, whereas Reay et al.[6] applied MAF $\geq$ 0.05). Further studies will be required to establish these findings conclusively.

Investigation of local genetic correlations between BCTs and NPDs detected 32 Bonferroni-significant local genetic correlations for 74 trait pairs. Interestingly, the majority of these trait pairs (n = 60) did not have a significant genome-wide HDL- or LDSC-based r_g, suggesting that meaningful local genetic correlations are common between traits with negligible genome-wide r_g, and in most cases, a significant genome-wide r_g reflects the presence of moderately significant local genetic correlations across the genome rather than highly significant local genetic correlations in specific genomic regions.

MR analyses identified compelling evidence for two putative causal relationships between BCTs and NPDs: a causal effect of increased PCT on stroke, which has been previously reported by Harshfield et al.,[8] and a causal effect of increased PDW on PD, which to our knowledge has not been previously reported. MR analyses also revealed suggestive evidence for a causal effect of elevated LYMPH# on MS, previously reported by Astle et al.,[7] although the evidence for this relationship remains inconclusive. In relation to increased PCT and stroke, our analyses strengthened the evidence for a causal effect through use of more powerful GWAS summary statistics for BCTs (sample size of 408,000 compared with 173,000 in Harshfield et al.[8]), and the application of additional, and arguably more sophisticated MR methods, including GSMR, LCV, and CAUSE, the latter of which is capable of differentiating causality from both correlated and uncorrelated pleiotropy. High PCT levels may induce stroke via a reduction in blood

flow and vessel patency,[56] which have been associated with stroke severity.[57]

In relation to increased PDW and risk for PD, we found consistent evidence for a causal relationship using six of seven MR methods. Weak genetic correlation has been previously reported between PDW and PD,[58] but our results suggest this is due (at least in part) to a causal effect of PDW on PD. Increased PDW is an indicator of platelet activation, which is known to occur as part of the inflammatory response.[59–61] Platelet activation has also been specifically implicated in neuroinflammation,[62] which is hypothesized to be a core pathogenic mechanism in PD.[63,64] Our findings are consistent with recent evidence that regular use of non-steroidal anti-inflammatory drugs (i.e., anti-platelet medications such as ibuprofen and aspirin) is protective for PD in carriers of mutations in the established PD gene *LRRK2*.[65]

To explore if the inferred causal effect of increased PDW on risk for PD is a signature of underlying inflammation, we adjusted SNP effects for PDW (and PD) using summary data from a large GWAS of C-reactive protein[66] (CRP; see Data S2). Interestingly, the magnitude of the causal effect of PDW on PD remained largely unchanged after adjusting for CRP, suggesting that the causal effect of PDW on PD may involve platelet functions independent of the inflammatory response. Notably, the protein implicated in the primary cellular pathology of PD, alpha-synuclein, is present in large quantities in platelets, where it regulates the Ca^{2+}-dependent release of alpha granules.[67] Irrespective of the mechanism, our findings highlight the potential clinical utility of these platelet parameters as potential risk markers and targets for improving prevention and prognosis of stroke and PD.

With the exception of the PCT-stroke and PDW-PD (and to a lesser extent LYMPH#-MS) associations, there was no consistent evidence for a causal relationship, using multiple MR models or ρ-HESS, for any other BCT-NPD pair, including those with significant genome-wide r_g. This implies, as expected, that pleiotropy is pervasive between BCTs and NPDs, which is consistent with findings reported by previous studies of vascular-neuropsychiatric associations.[7,68]

Using SMR, we identified a total of 60 and 20 FDR-significant genes associated with PDW-PD and PCT-stroke, respectively (Tables S36 and S37). Given evidence for a causal effect of increased PDW on PD risk, and of the well-established role of elevated PCT on susceptibility to stroke, these genes represent especially interesting candidates for mitigating risk for PD and/or stroke via modulation of platelet activity or function. Interestingly, 11 of the 60 PDW-PD genes and two of the 20 PCT-stroke genes are known drug targets (Table S51). For example, the *SYK* (spleen-associated tyrosine kinase) gene, which is targeted by 30 drugs with primary indications for a range of cancers and autoimmune disorders, plays an essential role in platelet activation as part of the collagen receptor glycoprotein (GPV1)-induced signaling pathway.[69] In our analyses, up-regulation of *SYK* was Bonferroni-significantly associated with increased PDW and FDR-significantly associated with higher risk for PD, suggesting that *SYK* inhibitors (e.g., cerdulatinib, apitolisib, fostamatinib, entospletinib, lanraplenib) may represent potential drug re-purposing opportunities for mitigation of PD risk. Another notable example is the catenin beta 1 gene (*CTNNB1*) which codes for β-catenin, a protein that plays essential roles in the Wnt/β-catenin pathway and cadherin-catenin cell adhesion, which in platelets undergoes complete proteolysis during platelet aggregation.[70] Our analyses indicate that up-regulation of *CTNNB1* is associated with reduced PDW and is protective for PD (both at FDR 5% significance level), suggesting that β-catenin inhibitors may be worthy of further investigation in relation to ameliorating risk for PD. Interestingly, although a number of anti-platelet and anticoagulation therapies are commonly used in stroke prevention (e.g., aspirin), the genes targeted by these drugs were not identified in our SMR analyses, an omission that may be attributable to a lack of power in the stroke GWAS and/or the fact that anticoagulation factors produced in the liver may not be captured by blood-based *cis*-eQTLs.

Among the remaining FDR-significant genes (i.e., excluding drug targets), a particularly notable gene for PD is *COA5* (cytochrome *c* oxidase assembly factor 5), which is known to be associated with mitochondrial complex IV deficiency.[71] This is significant given the broad body of evidence implicating mitochondrial dysfunction in degeneration of dopaminergic neurons in PD patients,[72] and the intimate role of mitochondria in platelet activation.[73] Further studies will be required to evaluate the clinical significance of this and other putative functional genes and regulatory elements for PD and stroke. Clarification of the specific genes and molecular mechanism(s) linking PDW to PD may present opportunities for mitigating risk for PD via platelet-targeting therapeutics, as is currently the case for stroke.

Looking beyond PCT-stroke and PDW-PD, the blood-based SMR analyses identified 51 genes for BCT-NPD pairs with at least nominally significant genome-wide r_g (Table S39). Among these, a total of 12 genes (Table S43)—all involving associations between MS and/or SCZ and one or more BCTs—showed Bonferroni-significant evidence for a regulatory pathway linking specific DNA methylation probe(s) to gene expression, gene expression to both members of specific BCT-NPD pairs, and for direct and consistent effects of DNA methylation on the same BCT-NPD pairs. Several of these functional genes are worthy of mention:

GATAD2A (GATA zinc finger domain containing 2A) is a crucial subunit of the nucleosome remodeling and histone deacetylation (NuRD) complex, which is one of the primary chromatin remodeling complexes in mammalian cells.[74] *GATAD2A* has been reported to be implicated in elevated risk for SCZ, potentially via its role as a regulator of gene expression during neurodevelopment.[75–77] The NuRD complex is also centrally involved in hematopoiesis,[78] although the specific role of *GATAD2A* in relation to the seven BCTs associated with this gene in our SMR analyses remains unclear. Interestingly, whereas the SCZ risk allele at *GATAD2A* was associated with up-regulation of this gene in blood, it was associated with down-regulation in brain, consistent with prior reports[79] and the idea that a proportion of risk alleles have different effects on gene expression in different organs.

Another notable gene is *MAPK3* (mitogen-activated protein kinase 3), a key member of the extra-cellular signal-regulated kinase pathway, which plays a central role in cell growth,

differentiation and survival via regulation of transcription and translation. In our analyses, up-regulation of *MAPK3* was Bonferroni-significantly associated with increased risk for SCZ and decreased NEUT%, the latter of which is consistent with neutropenia, a potentially life-threatening condition characterized by reduced neutrophil count and correspondingly higher risk for infection. This is significant, because whereas neutropenia (and the related condition of agranulocytosis) is a well-known side effect of some second-generation anti-psychotics, such as clozapine, our results suggest that some genetic variants associated with increased risk for SCZ also directly increase susceptibility to neutropenia.[80,81] There was no evidence for a causal effect of NEUT% on risk for SCZ in the MR analyses, suggesting that the association of *MAPK3* with SCZ and NEUT% is due to pleiotropy. We also found no evidence for an association of DNA methylation with expression of *MAPK3*, or with risk for schizophrenia or variation in NEUT%. Further study will be needed to decipher the pleiotropic mechanism(s) via which *MAPK3* influences NEUT% and susceptibility to SCZ.

Another gene associated with increased risk for SCZ and reduced NEUT% was *ABCB9* (ATP-binding cassette subfamily B member 9), which is a member of the MDR/TAP subfamily of ABC transporters, responsible for translocation of MHC peptides into lysosomes. Up-regulation of *ABCB9* was also associated with increased risk for MS, increased LYMPH#, and reduced RET%. The association of *ABCB9* with SCZ (among other traits such as cardiometabolic disease) has been previously reported,[76,82,83] but here we provide evidence for a role of this gene in MS, LYMPH#, NEUT%, and RET%. The association of *ABCB9* with both MS and LYMPH# indicates that this is one of the genes underlying the positive genetic correlation between these traits.

The application of gene set enrichment analysis to Bonferroni-significant genes identified through SMR identified multiple FDR-significant biological pathways that were shared by specific pairs of BCTs and NPDs. The top-ranked pathway was tau protein binding for SCZ-MONO%, which is notable given that aberrantly phosphorylated tau protein has been associated with risk for SCZ[84]; and there is evidence that monocyte-derived macrophages play an important role in phagocytosing extra-cellular oligomeric tau protein.[85] Although this observation has potential therapeutic implications, an important caveat is that the proportion of pathway-specific genes was small (<5%). This was also the case for other FDR-significant pathways identified by GSEA, which suggests that larger studies will be needed for robust inference of biological pathways shared by specific pairs of BCTs and NPDs.

In conclusion, we report a broad landscape of genetic overlap between BCTs and common NPDs, finding evidence to suggest that platelet parameters may be useful biomarkers for risk stratification of primary prevention trials of PD. Additionally, we identified multiple functional genes and regulatory elements for specific pairs of BCTs and NPDs, some of which are previously unreported, including known drug targets that may present drug re-purposing opportunities for PD. Our results provide a robust genetic foundation for improving prognosis, prevention, and possibly new avenues for treatment of common NPDs on the basis of readily assayed BCTs.

Limitations of the study

We note several limitations in our analyses. First, potential sample overlap between BCT and NPD GWAS summary statistics (i.e., both AD and PD GWAS included participants of UKB that overlap with the BCT GWAS) may introduce weak instrument bias and thus decrease the power of MR methods for detecting causal relationships.[86] Nevertheless, we believe the magnitude of such bias is minimal for two reasons: (1) the intercept from bivariate LDSC was <0.02 for all pairs of BCTs and NPDs, and (2) we applied multiple MR models with different instrumental SNP sets and observed consistent results. Second, the blood-based *cis*-eQTL summary data used in our SMR analyses were not corrected for blood cell proportions. This has the potential to influence the SMR results for BCTs, although because the eQTLGen dataset is very large, any potential influence of blood cell heterogeneity is likely to be averaged out. Third, although we report a number of statistically significant findings, further investigation will be required to determine if they are clinically meaningful.

STAR★METHODS

Detailed methods are provided in the online version of this paper and include the following:

- KEY RESOURCES TABLE
- RESOURCE AVAILABILITY
  - Lead contact
  - Materials availability
  - Data and code availability
- METHOD DETAILS
  - GWAS summary data
  - *cis*-eQTL and mQTL summary data
  - Estimation of genetic correlations using high-definition likelihood (HDL)
  - Estimation of genetic correlations using LD score regression (LDSC)
  - Investigating potential confounding factors mediating the shared genetics underlying pairs of traits with significant genetic correlations
  - Estimation of local genetic correlations using ρ-HESS
  - Mendelian randomization analyses
  - Multi-omics analysis of putatively functional mechanisms underlying shared genetic loci for BCTs and neurological and psychiatric disorders
  - Gene set enrichment analysis (GSEA)
- QUANTIFICATION AND STATISTICAL ANALYSIS

SUPPLEMENTAL INFORMATION

Supplemental information can be found online at https://doi.org/10.1016/j.xgen.2022.100249.

ACKNOWLEDGEMENTS

We acknowledge funding support from the Australian National Health and Medical Research Council (GNT1127440 and GNT2013281 to J.G.; GNT20098389 to B.V.T.; GNT1173155 to Y.Z.), Mater Foundation (Y.Y., C.X.Y., R.K.T., J.G.), MS Australia (B.V.T.), and the Macquarie Foundation

paired senior research fellowship (B.V.T.). We also thank the International Multiple Sclerosis Genetics Consortium (IMSGC) and the IHGC for providing access to GWAS summary data. This research was enabled using the UK Biobank Resource under application 12505. We are grateful to Professor Naomi Wray for insightful comments and discussion.

AUTHOR CONTRIBUTIONS

Y.Y. and J.G. designed the study and wrote the manuscript. Y.Y. performed the primary analyses, with assistance from Z.Z. (MR analyses) and Y. Wu (SMR analyses). J.G. supervised the study. Y.Y., Y.Z., D.R.N., C.X.Y., R.K.T., Y. Wu, Y. Wang, Z.Z., B.V.T., and J.G. contributed to the interpretation of results and the critical revision of the manuscript.

DECLARATION OF INTERESTS

The authors declare no competing interests.

INCLUSION AND DIVERSITY

One or more of the authors of this paper self-identifies as an underrepresented ethnic minority in their field of research or within their geographical location. One or more of the authors of this paper self-identifies as a gender minority in their field of research. We support inclusive, diverse, and equitable conduct of research.

Received: July 4, 2022
Revised: August 3, 2022
Accepted: December 20, 2022
Published: January 25, 2023

REFERENCES

1. Sealock, J.M., Lee, Y.H., Moscati, A., Venkatesh, S., Voloudakis, G., Straub, P., Singh, K., Feng, Y.C.A., Ge, T., Roussos, P., et al. (2021). Use of the PsycheMERGE network to investigate the association between depression polygenic scores and white blood cell count. JAMA Psychiatr. *78*, 1365–1374. https://doi.org/10.1001/jamapsychiatry.2021.2959.
2. Medema, S., Mocking, R.J.T., Koeter, M.W.J., Vaz, F.M., Meijer, C., de Haan, L., van Beveren, N.J.M., GROUP;Genetic Risk and Outcome of Psychosis investigators; Kahn, R., de Haan, L., et al. (2016). Levels of red blood cell fatty acids in patients with psychosis, their unaffected siblings, and healthy controls. Schizophr. Bull. *42*, 358–368. https://doi.org/10.1093/schbul/sbv133.
3. Sheremata, W.A., Jy, W., Horstman, L.L., Ahn, Y.S., Alexander, J.S., and Minagar, A. (2008). Evidence of platelet activation in multiple sclerosis. J. Neuroinflammation *5*, 27. https://doi.org/10.1186/1742-2094-5-27.
4. Furlan, J.C., Vergouwen, M.D.I., Fang, J., and Silver, F.L. (2014). White blood cell count is an independent predictor of outcomes after acute ischaemic stroke. Eur. J. Neurol. *21*, 215–222. https://doi.org/10.1111/ene.12233.
5. Abbott, R.D., Ross, G.W., Tanner, C.M., Andersen, J.K., Masaki, K.H., Rodriguez, B.L., White, L.R., and Petrovitch, H. (2012). Late-life hemoglobin and the incidence of Parkinson's disease. Neurobiol. Aging *33*, 914–920. https://doi.org/10.1016/j.neurobiolaging.2010.06.023.
6. Reay, W.R., Kiltschewskij, D.J., Geaghan, M.P., Atkins, J.R., Carr, V.J., Green, M.J., and Cairns, M.J. (2022). Genetic estimates of correlation and causality between blood-based biomarkers and psychiatric disorders. Sci. Adv. *8*, eabj8969. https://doi.org/10.1126/sciadv.abj8969.
7. Astle, W.J., Elding, H., Jiang, T., Allen, D., Ruklisa, D., Mann, A.L., Mead, D., Bouman, H., Riveros-Mckay, F., Kostadima, M.A., et al. (2016). The allelic landscape of human blood cell trait variation and links to common complex disease. Cell *167*, 1415–1429.e19. https://doi.org/10.1016/j.cell.2016.10.042.
8. Harshfield, E.L., Sims, M.C., Traylor, M., Ouwehand, W.H., and Markus, H.S. (2020). The role of haematological traits in risk of ischaemic stroke and its subtypes. Brain *143*, 210–221. https://doi.org/10.1093/brain/awz362.
9. Couturier, N., Bucciarelli, F., Nurtdinov, R.N., Debouverie, M., Lebrun-Frenay, C., Defer, G., Moreau, T., Confavreux, C., Vukusic, S., Cournu-Rebeix, I., et al. (2011). Tyrosine kinase 2 variant influences T lymphocyte polarization and multiple sclerosis susceptibility. Brain *134*, 693–703. https://doi.org/10.1093/brain/awr010.
10. Scherzer, C.R., Grass, J.A., Liao, Z., Pepivani, I., Zheng, B., Eklund, A.C., Ney, P.A., Ng, J., McGoldrick, M., Mollenhauer, B., et al. (2008). GATA transcription factors directly regulate the Parkinson's disease-linked gene alpha-synuclein. Proc. Natl. Acad. Sci. USA *105*, 10907–10912. https://doi.org/10.1073/pnas.0802437105.
11. Davies, N.M., Holmes, M.V., and Davey Smith, G. (2018). Reading Mendelian randomisation studies: a guide, glossary, and checklist for clinicians. BMJ *362*, k601. https://doi.org/10.1136/bmj.k601.
12. Chahine, L.M., Stern, M.B., and Chen-Plotkin, A. (2014). Blood-based biomarkers for Parkinson's disease. Park. Relat. Disord. *20* (*Suppl 1*), S99–S103. https://doi.org/10.1016/S1353-8020(13)70025-7.
13. Hampel, H., O'Bryant, S.E., Molinuevo, J.L., Zetterberg, H., Masters, C.L., Lista, S., Kiddle, S.J., Batrla, R., and Blennow, K. (2018). Blood-based biomarkers for Alzheimer disease: mapping the road to the clinic. Nat. Rev. Neurol. *14*, 639–652. https://doi.org/10.1038/s41582-018-0079-7.
14. Henriksen, K., O'Bryant, S.E., Hampel, H., Trojanowski, J.Q., Montine, T.J., Jeromin, A., Blennow, K., Lönneborg, A., Wyss-Coray, T., Soares, H., et al. (2014). The future of blood-based biomarkers for Alzheimer's disease. Alzheimers Dement *10*, 115–131. https://doi.org/10.1016/j.jalz.2013.01.013.
15. Lai, C.Y., Scarr, E., Udawela, M., Everall, I., Chen, W.J., and Dean, B. (2016). Biomarkers in schizophrenia: a focus on blood based diagnostics and theranostics. World J. Psychiatr. *6*, 102–117. https://doi.org/10.5498/wjp.v6.i1.102.
16. Ning, Z., Pawitan, Y., and Shen, X. (2020). High-definition likelihood inference of genetic correlations across human complex traits. Nat. Genet. *52*, 859–864. https://doi.org/10.1038/s41588-020-0653-y.
17. Shi, H., Mancuso, N., Spendlove, S., and Pasaniuc, B. (2017). Local genetic correlation gives insights into the shared genetic architecture of complex traits. Am. J. Hum. Genet. *101*, 737–751. https://doi.org/10.1016/j.ajhg.2017.09.022.
18. Morrison, J., Knoblauch, N., Marcus, J.H., Stephens, M., and He, X. (2020). Mendelian randomization accounting for correlated and uncorrelated pleiotropic effects using genome-wide summary statistics. Nat. Genet. *52*, 740–747. https://doi.org/10.1038/s41588-020-0631-4.
19. Burgess, S., Butterworth, A., and Thompson, S.G. (2013). Mendelian randomization analysis with multiple genetic variants using summarized data. Genet. Epidemiol. *37*, 658–665. https://doi.org/10.1002/gepi.21758.
20. Burgess, S., and Thompson, S.G. (2017). Interpreting findings from Mendelian randomization using the MR-Egger method. Eur. J. Epidemiol. *32*, 377–389. https://doi.org/10.1007/s10654-017-0255-x.
21. Hartwig, F.P., Davey Smith, G., and Bowden, J. (2017). Robust inference in summary data Mendelian randomization via the zero modal pleiotropy assumption. Int. J. Epidemiol. *46*, 1985–1998. https://doi.org/10.1093/ije/dyx102.
22. Bowden, J., Davey Smith, G., Haycock, P.C., and Burgess, S. (2016). Consistent estimation in mendelian randomization with some invalid instruments using a weighted median estimator. Genet. Epidemiol. *40*, 304–314. https://doi.org/10.1002/gepi.21965.
23. Zhu, Z., Zheng, Z., Zhang, F., Wu, Y., Trzaskowski, M., Maier, R., Robinson, M.R., McGrath, J.J., Visscher, P.M., Wray, N.R., and Yang, J. (2018). Causal associations between risk factors and common diseases inferred

from GWAS summary data. Nat. Commun. *9*, 224. https://doi.org/10.1038/s41467-017-02317-2.

24. O'Connor, L.J., and Price, A.L. (2018). Distinguishing genetic correlation from causation across 52 diseases and complex traits. Nat. Genet. *50*, 1728–1734. https://doi.org/10.1038/s41588-018-0255-0.
25. Zhu, Z., Zhang, F., Hu, H., Bakshi, A., Robinson, M.R., Powell, J.E., Montgomery, G.W., Goddard, M.E., Wray, N.R., Visscher, P.M., and Yang, J. (2016). Integration of summary data from GWAS and eQTL studies predicts complex trait gene targets. Nat. Genet. *48*, 481–487. https://doi.org/10.1038/ng.3538.
26. Vuckovic, D., Bao, E.L., Akbari, P., Lareau, C.A., Mousas, A., Jiang, T., Chen, M.H., Raffield, L.M., Tardaguila, M., Huffman, J.E., et al. (2020). The polygenic and monogenic basis of blood traits and diseases. Cell *182*, 1214–1231.e11. https://doi.org/10.1016/j.cell.2020.08.008.
27. Jansen, I.E., Savage, J.E., Watanabe, K., Bryois, J., Williams, D.M., Steinberg, S., Sealock, J., Karlsson, I.K., Hägg, S., Athanasiu, L., et al. (2019). Genome-wide meta-analysis identifies new loci and functional pathways influencing Alzheimer's disease risk. Nat. Genet. *51*, 404–413. https://doi.org/10.1038/s41588-018-0311-9.
28. Nicolas, A., Kenna, K.P., Renton, A.E., Ticozzi, N., Faghri, F., Chia, R., Dominov, J.A., Kenna, B.J., Nalls, M.A., Keagle, P., et al. (2018). Genome-wide analyses identify KIF5A as a novel ALS gene. Neuron *97*, 1268–1283.e6. https://doi.org/10.1016/j.neuron.2018.02.027.
29. Gormley, P., Anttila, V., Winsvold, B.S., Palta, P., Esko, T., Pers, T.H., Farh, K.H., Cuenca-Leon, E., Muona, M., Furlotte, N.A., et al. (2016). Meta-analysis of 375, 000 individuals identifies 38 susceptibility loci for migraine. Nat. Genet. *48*, 856–866. https://doi.org/10.1038/ng.3598.
30. International Multiple Sclerosis Genetics Consortium (2019). Multiple sclerosis genomic map implicates peripheral immune cells and microglia in susceptibility. Science *365*, eaav7188. https://doi.org/10.1126/science.aav7188.
31. Nalls, M.A., Blauwendraat, C., Vallerga, C.L., Heilbron, K., Bandres-Ciga, S., Chang, D., Tan, M., Kia, D.A., Noyce, A.J., Xue, A., et al. (2019). Identification of novel risk loci, causal insights, and heritable risk for Parkinson's disease: a meta-analysis of genome-wide association studies. Lancet Neurol. *18*, 1091–1102. https://doi.org/10.1016/S1474-4422(19)30320-5.
32. Malik, R., Chauhan, G., Traylor, M., Sargurupremraj, M., Okada, Y., Mishra, A., Rutten-Jacobs, L., Giese, A.K., van der Laan, S.W., Gretarsdottir, S., et al. (2018). Multiancestry genome-wide association study of 520, 000 subjects identifies 32 loci associated with stroke and stroke subtypes. Nat. Genet. *50*, 524–537. https://doi.org/10.1038/s41588-018-0058-3.
33. Demontis, D., Walters, R.K., Martin, J., Mattheisen, M., Als, T.D., Agerbo, E., Baldursson, G., Belliveau, R., Bybjerg-Grauholm, J., Bækvad-Hansen, M., et al. (2019). Discovery of the first genome-wide significant risk loci for attention deficit/hyperactivity disorder. Nat. Genet. *51*, 63–75. https://doi.org/10.1038/s41588-018-0269-7.
34. Grove, J., Ripke, S., Als, T.D., Mattheisen, M., Walters, R.K., Won, H., Pallesen, J., Agerbo, E., Andreassen, O.A., Anney, R., et al. (2019). Identification of common genetic risk variants for autism spectrum disorder. Nat. Genet. *51*, 431–444. https://doi.org/10.1038/s41588-019-0344-8.
35. Stahl, E.A., Breen, G., Forstner, A.J., McQuillin, A., Ripke, S., Trubetskoy, V., Mattheisen, M., Wang, Y., Coleman, J.R.I., Gaspar, H.A., et al. (2019). Genome-wide association study identifies 30 loci associated with bipolar disorder. Nat. Genet. *51*, 793–803. https://doi.org/10.1038/s41588-019-0397-8.
36. Wray, N.R., Ripke, S., Mattheisen, M., Trzaskowski, M., Byrne, E.M., Abdellaoui, A., Adams, M.J., Agerbo, E., Air, T.M., Andlauer, T.M.F., et al. (2018). Genome-wide association analyses identify 44 risk variants and refine the genetic architecture of major depression. Nat. Genet. *50*, 668–681. https://doi.org/10.1038/s41588-018-0090-3.
37. Trubetskoy, V., Pardiñas, A.F., Qi, T., Panagiotaropoulou, G., Awasthi, S., Bigdeli, T.B., Bryois, J., Chen, C.Y., Dennison, C.A., Hall, L.S., et al. (2022). Mapping genomic loci implicates genes and synaptic biology in schizophrenia. Nature *604*, 502–508. https://doi.org/10.1038/s41586-022-04434-5.
38. Lam, M., Awasthi, S., Watson, H.J., Goldstein, J., Panagiotaropoulou, G., Trubetskoy, V., Karlsson, R., Frei, O., Fan, C.C., De Witte, W., et al. (2020). RICOPILI: rapid imputation for COnsortias PIpeLIne. Bioinformatics *36*, 930–933. https://doi.org/10.1093/bioinformatics/btz633.
39. Zeller, J.A., Frahm, K., Baron, R., Stingele, R., and Deuschl, G. (2004). Platelet-leukocyte interaction and platelet activation in migraine: a link to ischemic stroke? J. Neurol. Neurosurg. Psychiatry *75*, 984–987. https://doi.org/10.1136/jnnp.2003.019638.
40. Prat, A., Biernacki, K., Lavoie, J.F., Poirier, J., Duquette, P., and Antel, J.P. (2002). Migration of multiple sclerosis lymphocytes through brain endothelium. Arch. Neurol. *59*, 391–397. https://doi.org/10.1001/archneur.59.3.391.
41. Lim, Z.W., Elwood, E., Naveed, H., and Galea, I. (2016). Lymphopenia in treatment-naive relapsing multiple sclerosis. Neurol. Neuroimmunol. Neuroinflamm. *3*, e275. https://doi.org/10.1212/NXI.0000000000000275.
42. Drexhage, R.C., Hoogenboezem, T.A., Cohen, D., Versnel, M.A., Nolen, W.A., van Beveren, N.J.M., and Drexhage, H.A. (2011). An activated set point of T-cell and monocyte inflammatory networks in recent-onset schizophrenia patients involves both pro- and anti-inflammatory forces. Int. J. Neuropsychopharmacol. *14*, 746–755. https://doi.org/10.1017/S1461145710001653.
43. Liu, M., Jiang, Y., Wedow, R., Li, Y., Brazel, D.M., Chen, F., Datta, G., Davila-Velderrain, J., McGuire, D., Tian, C., et al. (2019). Association studies of up to 1.2 million individuals yield new insights into the genetic etiology of tobacco and alcohol use. Nat. Genet. *51*, 237–244. https://doi.org/10.1038/s41588-018-0307-5.
44. Okbay, A., Wu, Y., Wang, N., Jayashankar, H., Bennett, M., Nehzati, S.M., Sidorenko, J., Kweon, H., Goldman, G., Gjorgjieva, T., et al. (2022). Polygenic prediction of educational attainment within and between families from genome-wide association analyses in 3 million individuals. Nat. Genet. *54*, 437–449. https://doi.org/10.1038/s41588-022-01016-z.
45. Hill, W.D., Davies, N.M., Ritchie, S.J., Skene, N.G., Bryois, J., Bell, S., Di Angelantonio, E., Roberts, D.J., Xueyi, S., Davies, G., et al. (2019). Genome-wide analysis identifies molecular systems and 149 genetic loci associated with income. Nat. Commun. *10*, 5741. https://doi.org/10.1038/s41467-019-13585-5.
46. Allen, M., Kachadoorian, M., Quicksall, Z., Zou, F., Chai, H.S., Younkin, C., Crook, J.E., Pankratz, V.S., Carrasquillo, M.M., Krishnan, S., et al. (2014). Association of MAPT haplotypes with Alzheimer's disease risk and MAPT brain gene expression levels. Alzheimer's Res. Ther. *6*, 39. https://doi.org/10.1186/alzrt268.
47. Ghetti, B., Oblak, A.L., Boeve, B.F., Johnson, K.A., Dickerson, B.C., and Goedert, M. (2015). Invited review: frontotemporal dementia caused by microtubule-associated protein tau gene (MAPT) mutations: a chameleon for neuropathology and neuroimaging. Neuropathol. Appl. Neurobiol. *41*, 24–46. https://doi.org/10.1111/nan.12213.
48. Lloyd-Jones, L.R., Zeng, J., Sidorenko, J., Yengo, L., Moser, G., Kemper, K.E., Wang, H., Zheng, Z., Magi, R., Esko, T., et al. (2019). Improved polygenic prediction by Bayesian multiple regression on summary statistics. Nat. Commun. *10*, 5086. https://doi.org/10.1038/s41467-019-12653-0.
49. Burgess, S., and Thompson, S.G. (2015). Multivariable Mendelian randomization: the use of pleiotropic genetic variants to estimate causal effects. Am. J. Epidemiol. *181*, 251–260. https://doi.org/10.1093/aje/kwu283.
50. Võsa, U., Claringbould, A., Westra, H.-J., Bonder, M.J., Deelen, P., Zeng, B., Kirsten, H., Saha, A., Kreuzhuber, R., Kasela, S., et al. (2018). Unraveling the polygenic architecture of complex traits using blood eQTL metaanalysis. Preprint at bioRxiv. https://doi.org/10.1101/447367.
51. Kammers, K., Taub, M.A., Rodriguez, B., Yanek, L.R., Ruczinski, I., Martin, J., Kanchan, K., Battle, A., Cheng, L., Wang, Z.Z., et al. (2021).

Transcriptional profile of platelets and iPSC-derived megakaryocytes from whole-genome and RNA sequencing. Blood *137*, 959–968. https://doi.org/10.1182/blood.2020006115.

52. McRae, A.F., Marioni, R.E., Shah, S., Yang, J., Powell, J.E., Harris, S.E., Gibson, J., Henders, A.K., Bowdler, L., Painter, J.N., et al. (2018). Identification of 55, 000 replicated DNA methylation QTL. Sci. Rep. *8*, 17605. https://doi.org/10.1038/s41598-018-35871-w.
53. Qi, T., Wu, Y., Zeng, J., Zhang, F., Xue, A., Jiang, L., Zhu, Z., Kemper, K., Yengo, L., Zheng, Z., et al. (2018). Identifying gene targets for brain-related traits using transcriptomic and methylomic data from blood. Nat. Commun. *9*, 2282. https://doi.org/10.1038/s41467-018-04558-1.
54. Ge, S.X., Jung, D., and Yao, R. (2020). ShinyGO: a graphical gene-set enrichment tool for animals and plants. Bioinformatics *36*, 2628–2629. https://doi.org/10.1093/bioinformatics/btz931.
55. Kerr, D., Krishnan, C., Pucak, M.L., and Carmen, J. (2005). The immune system and neuropsychiatric diseases. Int. Rev. Psychiatry *17*, 443–449. https://doi.org/10.1080/0264830500381435.
56. Khan, S.Z., Dosluoglu, H.H., Pourafkari, L., Rivero, M., and Nader, N.D. (2020). High plateletcrit is associated with early loss of patency after open and endovascular interventions for chronic limb ischemia. J. Vasc. Surg. *71*, 2089–2097. https://doi.org/10.1016/j.jvs.2019.08.258.
57. Marto, J.P., Lambrou, D., Eskandari, A., Nannoni, S., Strambo, D., Saliou, G., Maeder, P., Sirimarco, G., and Michel, P. (2019). Associated factors and long-term prognosis of 24-hour worsening of arterial patency after ischemic stroke. Stroke *50*, 2752–2760. https://doi.org/10.1161/STROKEAHA.119.025787.
58. Tirozzi, A., Izzi, B., Noro, F., Marotta, A., Gianfagna, F., Hoylaerts, M.F., Cerletti, C., Donati, M.B., de Gaetano, G., Iacoviello, L., and Gialluisi, A. (2020). Assessing genetic overlap between platelet parameters and neurodegenerative disorders. Front. Immunol. *11*, 02127. https://doi.org/10.3389/fimmu.2020.02127.
59. Koupenova, M., Clancy, L., Corkrey, H.A., and Freedman, J.E. (2018). Circulating platelets as mediators of immunity, inflammation, and thrombosis. Circ. Res. *122*, 337–351. https://doi.org/10.1161/CIRCRESAHA.117.310795.
60. Morrell, C.N., Aggrey, A.A., Chapman, L.M., and Modjeski, K.L. (2014). Emerging roles for platelets as immune and inflammatory cells. Blood *123*, 2759–2767. https://doi.org/10.1182/blood-2013-11-462432.
61. Leiter, O., and Walker, T.L. (2020). Platelets in neurodegenerative conditions-friend or foe? Front. Immunol. *11*, 747. https://doi.org/10.3389/fimmu.2020.00747.
62. Rawish, E., Nording, H., Münte, T., and Langer, H.F. (2020). Platelets as mediators of neuroinflammation and thrombosis. Front. Immunol. *11*, 548631. https://doi.org/10.3389/fimmu.2020.548631.
63. Hirsch, E.C., and Hunot, S. (2009). Neuroinflammation in Parkinson's disease: a target for neuroprotection? Lancet Neurol. *8*, 382–397. https://doi.org/10.1016/S1474-4422(09)70062-6.
64. Wang, Q., Liu, Y., and Zhou, J. (2015). Neuroinflammation in Parkinson's disease and its potential as therapeutic target. Transl. Neurodegener. *4*, 19. https://doi.org/10.1186/s40035-015-0042-0.
65. San Luciano, M., Tanner, C.M., Meng, C., Marras, C., Goldman, S.M., Lang, A.E., Tolosa, E., Schüle, B., Langston, J.W., Brice, A., et al. (2020). Nonsteroidal anti-inflammatory use and LRRK2 Parkinson's disease penetrance. Mov. Disord. *35*, 1755–1764. https://doi.org/10.1002/mds.28189.
66. Ligthart, S., Vaez, A., Võsa, U., Stathopoulou, M.G., de Vries, P.S., Prins, B.P., Van der Most, P.J., Tanaka, T., Naderi, E., Rose, L.M., et al. (2018). Genome analyses of >200, 000 individuals identify 58 loci for chronic inflammation and highlight pathways that link inflammation and complex disorders. Am. J. Hum. Genet. *103*, 691–706. https://doi.org/10.1016/j.ajhg.2018.09.009.
67. Park, S.M., Jung, H.Y., Kim, H.O., Rhim, H., Paik, S.R., Chung, K.C., Park, J.H., and Kim, J. (2002). Evidence that alpha-synuclein functions as a negative regulator of Ca(++)-dependent alpha-granule release from human platelets. Blood *100*, 2506–2514. https://doi.org/10.1182/blood.V100.7.2506.
68. Siewert, K.M., Klarin, D., Damrauer, S.M., Chang, K.M., Tsao, P.S., Assimes, T.L., Davey Smith, G., and Voight, B.F.; The International Headache Genetics Consortium (2020). Cross-trait analyses with migraine reveal widespread pleiotropy and suggest a vascular component to migraine headache. Int. J. Epidemiol. *49*, 1022–1031. https://doi.org/10.1093/ije/dyaa050.
69. Jooss, N.J., De Simone, I., Provenzale, I., Fernández, D.I., Brouns, S.L.N., Farndale, R.W., Henskens, Y.M.C., Kuijpers, M.J.E., Ten Cate, H., van der Meijden, P.E.J., et al. (2019). Role of platelet glycoprotein VI and tyrosine kinase syk in thrombus formation on collagen-like surfaces. Int. J. Mol. Sci. *20*, 2788. https://doi.org/10.3390/ijms20112788.
70. Kumari, S., and Dash, D. (2013). Regulation of beta-catenin stabilization in human platelets. Biochimie *95*, 1252–1257. https://doi.org/10.1016/j.biochi.2013.01.021.
71. Huigsloot, M., Nijtmans, L.G., Szklarczyk, R., Baars, M.J.H., van den Brand, M.A.M., Hendriksfranssen, M.G.M., van den Heuvel, L.P., Smeitink, J.A.M., Huynen, M.A., and Rodenburg, R.J.T. (2011). A mutation in C2orf64 causes impaired cytochrome c oxidase assembly and mitochondrial cardiomyopathy. Am. J. Hum. Genet. *88*, 488–493. https://doi.org/10.1016/j.ajhg.2011.03.002.
72. Schapira, A.H., Cooper, J.M., Dexter, D., Jenner, P., Clark, J.B., and Marsden, C.D. (1989). Mitochondrial complex I deficiency in Parkinson's disease. Lancet *1*, 1269. https://doi.org/10.1016/s0140-6736(89)92366-0.
73. Boudreau, L.H., Duchez, A.C., Cloutier, N., Soulet, D., Martin, N., Bollinger, J., Paré, A., Rousseau, M., Naika, G.S., Lévesque, T., et al. (2014). Platelets release mitochondria serving as substrate for bactericidal group IIA-secreted phospholipase A2 to promote inflammation. Blood *124*, 2173–2183. https://doi.org/10.1182/blood-2014-05-573543.
74. Torchy, M.P., Hamiche, A., and Klaholz, B.P. (2015). Structure and function insights into the NuRD chromatin remodeling complex. Cell. Mol. Life Sci. *72*, 2491–2507. https://doi.org/10.1007/s00018-015-1880-8.
75. Torretta, S., Rampino, A., Basso, M., Pergola, G., Di Carlo, P., Shin, J.H., Kleinman, J.E., Hyde, T.M., Weinberger, D.R., Masellis, R., et al. (2020). NURR1 and ERR1 modulate the expression of genes of a DRD2 coexpression network enriched for schizophrenia risk. J. Neurosci. *40*, 932–941. https://doi.org/10.1523/JNEUROSCI.0786-19.2019.
76. Liu, H., Sun, Y., Zhang, X., Li, S., Hu, D., Xiao, L., Chen, Y., He, L., and Wang, D.W. (2020). Integrated analysis of summary statistics to identify pleiotropic genes and pathways for the comorbidity of schizophrenia and cardiometabolic disease. Front. Psychiatry *11*, 256. https://doi.org/10.3389/fpsyt.2020.00256.
77. Ma, C., Gu, C., Huo, Y., Li, X., and Luo, X.J. (2018). The integrated landscape of causal genes and pathways in schizophrenia. Transl. Psychiatry *8*, 67. https://doi.org/10.1038/s41398-018-0114-x.
78. Gregory, G.D., Miccio, A., Bersenev, A., Wang, Y., Hong, W., Zhang, Z., Poncz, M., Tong, W., and Blobel, G.A. (2010). FOG1 requires NuRD to promote hematopoiesis and maintain lineage fidelity within the megakaryocytic-erythroid compartment. Blood *115*, 2156–2166. https://doi.org/10.1182/blood-2009-10-251280.
79. Hauberg, M.E., Zhang, W., Giambartolomei, C., Franzén, O., Morris, D.L., Vyse, T.J., Ruusalepp, A., CommonMind Consortium; Sklar, P., Schadt, E.E., et al. (2017). Large-scale identification of common trait and disease variants affecting gene expression. Am. J. Hum. Genet. *101*, 157. https://doi.org/10.1016/j.ajhg.2017.06.003.
80. Siskind, D., McCartney, L., Goldschlager, R., and Kisely, S. (2016). Clozapine v. first- and second-generation antipsychotics in treatment-refractory schizophrenia: systematic review and meta-analysis. Br. J. Psychiatry *209*, 385–392. https://doi.org/10.1192/bjp.bp.115.177261.
81. Myles, N., Myles, H., Xia, S., Large, M., Kisely, S., Galletly, C., Bird, R., and Siskind, D. (2018). Meta-analysis examining the epidemiology of

clozapine-associated neutropenia. Acta Psychiatr. Scand. *138*, 101–109. https://doi.org/10.1111/acps.12898.

82. Yu, H., Cheng, W., Zhang, X., Wang, X., and Yue, W. (2020). Integration analysis of methylation quantitative trait loci and GWAS identify three schizophrenia risk variants. Neuropsychopharmacology *45*, 1179–1187. https://doi.org/10.1038/s41386-020-0605-3.
83. Pouget, J.G., Schizophrenia Working Group of the Psychiatric Genomics Consortium; Han, B., Wu, Y., Mignot, E., Ollila, H.M., Barker, J., Spain, S., Dand, N., Trembath, R., et al. (2019). Cross-disorder analysis of schizophrenia and 19 immune-mediated diseases identifies shared genetic risk. Hum. Mol. Genet. *28*, 3498–3513. https://doi.org/10.1093/hmg/ddz145.
84. Deutsch, S.I., Rosse, R.B., and Lakshman, R.M. (2006). Dysregulation of tau phosphorylation is a hypothesized point of convergence in the pathogenesis of Alzheimer's disease, frontotemporal dementia and schizophrenia with therapeutic implications. Prog. Neuro-Psychopharmacol. Biol. Psychiatry *30*, 1369–1380. https://doi.org/10.1016/j.pnpbp.2006.04.007.
85. Majerova, P., Zilkova, M., Kazmerova, Z., Kovac, A., Paholikova, K., Kovacech, B., Zilka, N., and Novak, M. (2014). Microglia display modest phagocytic capacity for extracellular tau oligomers. J. Neuroinflammation *11*, 161. https://doi.org/10.1186/s12974-014-0161-z.
86. Burgess, S., Davies, N.M., and Thompson, S.G. (2016). Bias due to participant overlap in two-sample Mendelian randomization. Genet. Epidemiol. *40*, 597–608. https://doi.org/10.1002/gepi.21998.
87. Bulik-Sullivan, B.K., Loh, P.R., Finucane, H.K., Ripke, S., Yang, J., Schizophrenia Working Group of the Psychiatric Genomics; C., Patterson, N., Daly, M.J., Price, A.L., and Neale, B.M. (2015). LD Score regression distinguishes confounding from polygenicity in genome-wide association studies. Nat. Genet. *47*, 291–295. https://doi.org/10.1038/ng.3211.
88. Bulik-Sullivan, B., Finucane, H.K., Anttila, V., Gusev, A., Day, F.R., Loh, P.R., ReproGen Consortium; Psychiatric Genomics Consortium; Genetic Consortium for Anorexia Nervosa of the Wellcome Trust Case Control Consortium 3; and Duncan, L., et al. (2015). An atlas of genetic correlations across human diseases and traits. Nat. Genet. *47*, 1236–1241. https://doi.org/10.1038/ng.3406.
89. GTEx Consortium (2013). The genotype-tissue expression (GTEx) project. Nat. Genet. *45*, 580–585. https://doi.org/10.1038/ng.2653.
90. Fromer, M., Roussos, P., Sieberts, S.K., Johnson, J.S., Kavanagh, D.H., Perumal, T.M., Ruderfer, D.M., Oh, E.C., Topol, A., Shah, H.R., et al. (2016). Gene expression elucidates functional impact of polygenic risk for schizophrenia. Nat. Neurosci. *19*, 1442–1453. https://doi.org/10.1038/nn.4399.
91. Ng, B., White, C.C., Klein, H.U., Sieberts, S.K., McCabe, C., Patrick, E., Xu, J., Yu, L., Gaiteri, C., Bennett, D.A., et al. (2017). An xQTL map integrates the genetic architecture of the human brain's transcriptome and epigenome. Nat. Neurosci. *20*, 1418–1426. https://doi.org/10.1038/nn.4632.
92. Hannon, E., Spiers, H., Viana, J., Pidsley, R., Burrage, J., Murphy, T.M., Troakes, C., Turecki, G., O'Donovan, M.C., Schalkwyk, L.C., et al. (2016). Methylation QTLs in the developing brain and their enrichment in schizophrenia risk loci. Nat. Neurosci. *19*, 48–54. https://doi.org/10.1038/nn.4182.
93. Jaffe, A.E., Gao, Y., Deep-Soboslay, A., Tao, R., Hyde, T.M., Weinberger, D.R., and Kleinman, J.E. (2016). Mapping DNA methylation across development, genotype and schizophrenia in the human frontal cortex. Nat. Neurosci. *19*, 40–47. https://doi.org/10.1038/nn.4181.
94. 1000 Genomes Project Consortium (2012). An integrated map of genetic variation from 1, 092 human genomes. Nature *491*, 56–65. https://doi.org/10.1038/nature11632.
95. Carter, A.R., Harrison, S., Gill, D., Davey Smith, G., Taylor, A.E., Howe, L.D., and Davies, N.M. (2022). Educational attainment as a modifier for the effect of polygenic scores for cardiovascular risk factors: cross-sectional and prospective analysis of UK Biobank. Int. J. Epidemiol. *51*, 885–897. https://doi.org/10.1093/ije/dyac002.
96. Pollitt, R.A., Kaufman, J.S., Rose, K.M., Diez-Roux, A.V., Zeng, D., and Heiss, G. (2007). Early-life and adult socioeconomic status and inflammatory risk markers in adulthood. Eur. J. Epidemiol. *22*, 55–66. https://doi.org/10.1007/s10654-006-9082-1.
97. Hahad, O., Daiber, A., Michal, M., Kuntic, M., Lieb, K., Beutel, M., and Münzel, T. (2021). Smoking and neuropsychiatric disease-associations and underlying mechanisms. Int. J. Mol. Sci. *22*, 7272. https://doi.org/10.3390/ijms22147272.
98. Bates, M.E., Barry, D., Labouvie, E.W., Fals-Stewart, W., Voelbel, G., and Buckman, J.F. (2004). Risk factors and neuropsychological recovery in clients with alcohol use disorders who were exposed to different treatments. J. Consult. Clin. Psychol. *72*, 1073–1080. https://doi.org/10.1037/0022-006X.72.6.1073.
99. Comes, A.L., Senner, F., Budde, M., Adorjan, K., Anderson-Schmidt, H., Andlauer, T.F.M., Gade, K., Hake, M., Heilbronner, U., Kalman, J.L., et al. (2019). The genetic relationship between educational attainment and cognitive performance in major psychiatric disorders. Transl. Psychiatry *9*, 210. https://doi.org/10.1038/s41398-019-0547-x.
100. Dohrenwend, B.P., Levav, I., Shrout, P.E., Schwartz, S., Naveh, G., Link, B.G., Skodol, A.E., and Stueve, A. (1992). Socioeconomic status and psychiatric disorders: the causation-selection issue. Science *255*, 946–952. https://doi.org/10.1126/science.1546291.
101. Berisa, T., and Pickrell, J.K. (2016). Approximately independent linkage disequilibrium blocks in human populations. Bioinformatics *32*, 283–285. https://doi.org/10.1093/bioinformatics/btv546.
102. Byrne, E.M., Zhu, Z., Qi, T., Skene, N.G., Bryois, J., Pardinas, A.F., Stahl, E., Smoller, J.W., Rietschel, M., et al.; Bipolar Working Group of the Psychiatric Genomics Consortium; Major Depressive Disorder Working Group of the Psychiatric Genomics Consortium (2021). Conditional GWAS analysis to identify disorder-specific SNPs for psychiatric disorders. Mol. Psychiatr *26*, 2070–2081. https://doi.org/10.1038/s41380-020-0705-9.
103. Burgess, S., Bowden, J., Fall, T., Ingelsson, E., and Thompson, S.G. (2017). Sensitivity analyses for robust causal inference from mendelian randomization analyses with multiple genetic variants. Epidemiology *28*, 30–42. https://doi.org/10.1097/EDE.0000000000000559.

STAR★METHODS

KEY RESOURCES TABLE

REAGENT or RESOURCE	SOURCE	IDENTIFIER
Deposited data		
GWAS summary statistics for BCTs	Vuckovic et al.[26]	http://ftp.ebi.ac.uk/pub/databases/gwas/summary_statistics/GCST90002001-GCST90003000
GWAS summary statistics for AD	Jansen et al.[27]	https://ctg.cncr.nl/software/summary_statistics
GWAS summary statistics for ALS	Nicolas et al.[28]	http://ftp.ebi.ac.uk/pub/databases/gwas/summary_statistics/GCST005001-GCST006000/GCST005647/
GWAS summary statistics for migraine	Gormlet et al.[29]	http://www.headachegenetics.org/content/datasets-and-cohorts
GWAS summary statistics for MS	IMSGC[30]	https://imsgc.net/?page_id=31
GWAS summary statistics for PD	Nalls et al.[31]	https://research.23andme.com/collaborate/#publication
GWAS summary statistics for stroke	Malik et al.[32]	https://www.megastroke.org/download.html
GWAS summary statistics for psychiatric disorders	PGC	https://www.med.unc.edu/pgc/download-results/
GWAS summary statistics for cigarettes per day	Liu et al.[43]	https://conservancy.umn.edu/handle/11299/201564
GWAS summary statistics for drinks per week	Liu et al.[43]	https://conservancy.umn.edu/handle/11299/201564
GWAS summary statistics for education attainment	Okbay et al.[44]	http://www.thessgac.org/data
GWAS summary statistics for household income	Hill et al.[45]	http://ftp.ebi.ac.uk/pub/databases/gwas/summary_statistics/GCST009001-GCST010000/GCST009523/
Blood-based *cis*-eQTL	eQTLGen[50]	https://www.eqtlgen.org/cis-eqtls.html
Platelet *cis*-eQTL	GeneSTAR[51]	https://www.biostat.jhsph.edu/~kkammers/GeneSTAR/
Brain-based *cis*-eQTL	GTEx[53]	https://cnsgenomics.com/software/smr/#DataResource
Blood-based mQTL	BSGS and LBC[52]	https://cnsgenomics.com/software/smr/#DataResource
Brain-based mQTL	Qi et al.[53]	https://cnsgenomics.com/software/smr/#DataResource
Individual-level data from UK Biobank	UK Biobank	https://biobank.ndph.ox.ac.uk/showcase/
Software and algorithms		
R 4.0.5	R Core Team	https://www.r-project.org/
HDL 1.3.8	Ning et al.[16]	https://github.com/zhenin/HDL
LDSC 1.0.1	Bulik-Sullivan et al.[87,88]	https://github.com/bulik/ldsc
ρ-HESS 0.5.4	Shi et al.[17]	https://huwenboshi.github.io/hess/
CAUSE 1.2.0	Morrison et al.[18]	https://jean997.github.io/cause/
TwoSampleMR 0.5.6	Hemani et al.[32]	https://mrcieu.github.io/TwoSampleMR/
GSMR 1.0.9	Zhu et al.[23]	https://yanglab.westlake.edu.cn/software/gsmr/
LCV	O'Connor et al.[24]	https://github.com/lukejoconnor/LCV
MVMR via TwoSampleMR 0.5.6	Hemani et al.[32]	https://mrcieu.github.io/TwoSampleMR/
mtCOJO 1.9.3.2 beta	Zhu et al.[23]	https://yanglab.westlake.edu.cn/software/gcta/#mtCOJO
SMR 1.03	Zhu et al.[25]	https://yanglab.westlake.edu.cn/software/smr/
PLINK 1.9	PLINK Working Group	https://www.cog-genomics.org/plink/1.9/
ShinyGo 0.76	Ge et al.[54]	http://bioinformatics.sdstate.edu/go/
Ricopili 1118b	Lam et al.[38]	https://sites.google.com/a/broadinstitute.org/ricopili/

RESOURCE AVAILABILITY

Lead contact

Further information and requests for resources and reagents should be directed to and will be fulfilled by the lead contact, Yuanhao Yang (yuanhao.yang@mater.uq.edu.au).

Materials availability

This study did not generate new unique reagents.

Data and code availability

- GWAS summary statistics for MS are available by application from https://imsgc.net/?page_id=31. GWAS summary statistics for migraine are available from the International Headache Genetics Consortium (IHGC, http://www.headachegenetics.org/content/datasets-and-cohorts) by request to Professor Dale Nyholt (d.nyholt@qut.edu.au). All other data are publicly available and listed in the key resources table.
- This study did not generate any unique datasets or code.
- Any additional information required to reanalyze the data reported in this paper is available from the lead contact upon request.

METHOD DETAILS

GWAS summary data

We obtained publicly available European-ancestry GWAS summary data for 29 BCTs,[26] including measures of red cells (e.g., hematocrit, hemoglobin), platelets (e.g., PCT, PDW), and white cells (e.g., BASO#, LYMPH#), and 11 common NPDs, including AD,[27] ADHD,[33] ALS,[28] ASD,[34] bipolar disorder (BIP),[35] MDD,[36] migraine,[29] MS,[30] PD,[31] SCZ[37] and stroke[32] (Tables 1 and 2). BCTs reported by Vuckovic et al.[26] were extracted from the main hematological indices of clinic-based blood samples from 408,112 European participants in the UKB. The authors implemented linear mixed regression to generate BCT GWAS summary statistics for the transformed and inversely normalized BCT residuals (i.e., regressing out effects from sex, age, age-squared, principal components, and recruitment center). GWAS of common NPDs were performed based on large-scale European samples, with the number of individuals ranging from ~40K for MS to >1.45M for PD. Among 11 NPDs, eight (ADHD, AD, ALS, ASD, BIP, MS, SCZ and stroke) involved analysis of cases diagnosed by clinicians or physicians (or with an equivalent clinical diagnosis), and three (MDD, migraine, PD) involved a combination clinical and self-reported cases. Each GWAS summary dataset comprised ~6-10M common SNPs after filtering out SNPs with MAF <1% (Tables 1 and 2).

cis-eQTL and mQTL summary data

We used summary data for blood- and brain-based *cis*-eQTL and mQTL for SMR analyses (see below). Blood-based *cis*-eQTL and mQTL data were obtained from the eQTLGen consortium (n_{sample} = 31,684; n_{probe} = 19,250)[50] and the BSGS and LBC (1921 and 1936; n_{sample} = 1,980; n_{probe} = 94,338),[52] respectively. We also obtained platelet *cis*-eQTL data (n_{sample} = 180; n_{probe} = 4,555) from the GeneSTAR Research Study.[51] Brain-based *cis*-eQTL data ($n_{effect\ sample}$ = 1,194; n_{probe} = 28,538)[53] were based on a meta-analysis of 10 Genotype-Tissue Expression (GTEx v6)[89] brain regions, the CommonMind Consortium (CMC)[90] and Religious Orders Study and Memory and Aging Project (ROSMAP)[91]; and the brain-based mQTL data ($n_{effect\ sample}$ = 1,160; n_{probe} = 436,077)[53] were based on a meta-analysis of three datasets: ROSMAP,[91] Hannon et al.[92] and Jaffe et al.[93] All these multi-omics data were publicly available and of European descent, with imputation based on the 1000 Genomes European reference panel (hg19 genome build).[94]

Estimation of genetic correlations using high-definition likelihood (HDL)

We used the HDL[16] method to estimate the genetic correlation for each pair of BCTs and NPDs, using GWAS summary statistics. HDL is a recently developed extension of bivariate LDSC,[87] which makes use of LD across the entire autosomal genome with exclusion of the MHC region (chromosome 6: 28,477,797-33,448,354 bp) via fitting an additional variance-covariance LD matrix to achieve significant reductions in variance of r_g estimates, thereby improving power. Here, HDL was applied to 319 pairs of BCTs and NPDs, with the method implemented using the default UKB reference with ~1M imputed HapMap3 autosomal SNPs, after excluding strand-ambiguous SNPs (i.e., A/T, C/G). We defined significant HDL r_g estimates as those surpassing the Bonferroni corrected threshold ($p < 1.57 \times 10^{-4}$, i.e., $\frac{0.05}{29\times11}$).

Estimation of genetic correlations using LD score regression (LDSC)

We also conducted bivariate LDSC[87,88] for each pair of traits as a sensitivity analysis. Bivariate LDSC estimates the r_g between traits using the slope from the regression of the product of the single trait GWAS test statistics (*Z* scores) on LD score. We applied bivariate LDSC to 319 pairs of BCTs and NPDs using the default LD scores of the 1000 Genomes European reference, again excluding SNPs if they were strand-ambiguous or located within the MHC region. As with HDL, we defined significant LDSC-based r_g estimates as those surpassing the Bonferroni corrected threshold ($p < 1.57 \times 10^{-4}$).

Investigating potential confounding factors mediating the shared genetics underlying pairs of traits with significant genetic correlations

For BCT-NPD trait pairs with Bonferroni-corrected or FDR significant genome-wide r_g (from HDL or LDSC), we investigated whether their shared genetics were driven by potential confounding factors, including smoking, drinking, educational attainment, and socioeconomic status that have been reported to be commonly associated with BCTs[7,95,96] and NPDs.[97–100] We investigated the roles of these potential confounding factors using a conditional approach. First, we utilised mtCOJO[23] to condition GWAS summary data of BCTs and NPDs on the GWAS of cigarettes per day,[43] drinks per week,[43] educational attainment,[44] and household income,[45]

respectively. We used genotype data from unrelated Europeans in the UK Biobank as a reference. We then re-estimated the genetic correlations between specific pairs of BCTs and NPDs on the basis of their conditional GWAS summary statistics, using HDL.

Estimation of local genetic correlations using ρ-HESS

Pairs of BCTs and NPDs may share genetic variance in small genomic regions even in the absence of a significant genome-wide genetic correlation. Moreover, the pattern of local genetic correlations in trait-associated regions can indicate potential causal relationships between traits. To investigate these possibilities, we used ρ-HESS[17] to estimate local genetic correlations between 319 BCT-NPD pairs in 1,693 approximately independent LD regions (average width ≈1.5Mb,[101] based on the hg19-based 1000 Genomes European reference), excluding those in the MHC region. We defined significant local genetic correlations as those surpassing the Bonferroni corrected threshold ($p < 9.26 \times 10^{-8}$; i.e., $\frac{0.05}{1693\times29\times11}$).

We then followed the approach proposed by Shi et al.[17] and classified the local genetic correlations into four groups for each pair of traits: (i) regions harboring only NPD-specific SNPs, (ii) regions harboring only BCT-specific SNPs, (iii) regions harboring SNPs shared by both members of the BCT-NPD trait pair ("Intersection"), and (iv) other regions ("Neither"). We defined trait-specific SNPs (used to classify genomic regions into each of the four groups) as those with $p < 1 \times 10^{-5}$, and compared these results to four other p value cut-offs ($p < 5 \times 10^{-8}$, $p < 1 \times 10^{-6}$, $p < 1 \times 10^{-4}$, and $p < 1 \times 10^{-3}$), as a means of accommodating differential GWAS power between BCTs and NPDs. We also performed a further sensitivity analysis using a Bayesian-based approach (SBayesR)[48] to define trait-specific SNPs. SBayesR implements a Bayesian likelihood multiple regression procedure to refine the estimated effect sizes of trait-associated SNPs by updating the 'prior' SNP effects of GWAS summary statistics to 'posterior' SNP effects. We used a sparse LD correlation matrix generated from Europeans in the UK Biobank as a reference for SBayesR. Genomic regions were excluded if the estimated local genetic correlation was missing (e.g., because the local estimated single-trait heritability was negative), less than −1 or greater than 1 (e.g., because at least one of the local estimated single-trait heritability estimates was close to zero). For each group that comprised ≥5 local genetic correlation estimates, we calculated the mean and SE of the local genetic correlations within the group. A causal effect of BCT on NPD was suggested if the average local genetic correlation in regions harboring BCT-specific SNPs was Bonferroni significantly non-zero ($p < 1.57 \times 10^{-4}$, for 319 pairs) and Bonferroni significantly different from that in "Intersection" regions, "Neither" regions, and regions harboring NPD-specific SNPs ($p < 1.57 \times 10^{-4}$ based on a two-tailed *Z*-test). We used an equivalent strategy to identify patterns of local genetic correlations consistent with a potential causal effect of NPD on BCT.

Mendelian randomization analyses

We used multiple MR methods to evaluate evidence for causality of BCTs on risk for NPDs, and vice versa. We focused on a total of 70 trait pairs with nominally significant ($p < 0.05$) genome-wide r_g (from HDL or LDSC), recognizing that a causal relationship is unlikely to exist in the absence of a global genetic correlation between highly polygenic traits like the BCTs and NPDs used in our study.

We first utilized the Bayesian multivariate linear model-based MR method CAUSE,[18] that assumes the genetic effect of the exposure on the outcome is comprised of a causal effect (β), correlated pleiotropy (η; defined as instruments with horizontal effects on both exposure and outcome through a shared pathway), and uncorrelated pleiotropy (q; defined as instruments with horizontal effects on the exposure and outcome via separate mechanisms or pathways). This approach enables CAUSE to distinguish a causal effect from correlated pleiotropy by quantifying the joint distribution of instrumental SNP effects, under the assumption that all instrumental SNPs are influenced by a causal effect, whereas only a subset are influenced by correlated pleiotropy. The CAUSE method utilizes more (approximately independent; LD $r^2 < 0.10$ based on the 1000 Genomes European reference) instrumental SNPs (with an arbitrary $p < 1 \times 10^{-3}$) than many other MR methods that rely solely on genome-wide significant SNPs, which is purported to increase power.[18] CAUSE also implements an approach called expected log pointwise posterior density (ELPD) to compare the overall model fit between the null model (no causal or pleiotropy effect), sharing model (the existence of a pleiotropic effect but no causal effect), and causal model (the existence of both causal and pleiotropic effects). We applied CAUSE using the R package '*cause*', excluding SNPs in the MHC region. We considered a relationship to be putatively causal if the causal effect estimated by the causal model surpassed the Bonferroni corrected significance threshold ($p < 3.57 \times 10^{-4}$, i.e., $\frac{0.05}{70\times2}$), and the overall fitness of the causal model was significantly ($p < 0.05$) better than the sharing model or null model.

To strengthen evidence of causality from the CAUSE analysis, we performed sensitivity analyses using six alternative MR methods with different assumptions on pleiotropy, including inverse variance weighting (IVW),[19] MR-Egger,[20] WMo,[21] WMe,[22] and GSMR.[23] Among the six alternative models, IVW[19] is the basic approach that assumes no correlated pleiotropy and the presence of uncorrelated pleiotropy (with mean zero), thereby adding noise to the random-effects meta-analysis of SNP effects. MR-Egger[20] is an extension of IVW that assumes no correlated pleiotropy but non-zero uncorrelated pleiotropy, which adds an extra intercept to the IVW to account for such uncorrelated pleiotropy. GSMR[23] has the same assumptions as MR-Egger and utilizes the HEIDI approach to identify and exclude confounding SNPs due to uncorrelated pleiotropy. Both WMe[22] and WMo[21] are capable of removing partial correlated and uncorrelated pleiotropy. WMe[22] is implemented using the weighted median but not weighted mean of the SNP ratio, and thus is capable of identifying true causality if the proportion of invalid instrumental SNPs of correlated and uncorrelated pleiotropy is ≤50%. WMo[21] estimates the causal effect merely from the largest subset of SNPs with consistent effects. While WMo drops some instrumental SNPs and likely has reduced power, it has the ability to identify true causality, particularly when a majority of instrumental SNPs are invalid. Furthermore, we inferred putative causal relationships between BCTs and NPDs using the LCV (latent causal

variable) model.[24] The LCV model assumes that the genetic correlation between two traits is mediated by a latent variable, which has a causal effect on each trait and can be quantified by estimating the GCP (genetic causality proportion) using the mixed fourth moments of marginal SNP effect sizes for each trait. GCP estimates vary between 0 (no causal relationship) to 1 (fully causal relationship), with higher values implying a stronger partially causal relationship.

We considered causal relationships that were consistently identified ($p < 0.05$) by all alternative methods as unlikely to be false positives. We applied these alternative methods using the R packages '*TwoSampleMR*', '*gsmr*', and '*LCV*', with exclusion of SNPs within the MHC region. Independent SNPs (LD clumping $r^2 < 0.05$ within 1,000Kb windows based on the 1000 Genomes European reference) with $p < 5 \times 10^{-8}$ were selected as instrumental variables for all these alternative MR methods except LCV, for which all SNPs were used. For MR effect size estimates for binary exposures (i.e., NPDs), we converted the MR effects from logit-scale to liability-scale using the method of Byrne et al.[102] All MR effects were then transformed into ORs for concise interpretation. The interpretation of the OR for "BCT → NPD" is that, as an example, if the estimated OR is 1.2, the NPD risk is increased by 1.2-fold for each SD increase in the BCT. Similarly, the interpretation of the OR for "NPD → BCT" at 1.2 (as an example) is that the level of BCT is increased by 1.2-fold per SD increase in NPD liability.

To evaluate the reliability of our MR results, we implemented several additional sensitivity analyses to evaluate the validity of instrumental SNPs for pairs of traits with consistent evidence for a causal relationship across all MR models.[103] The sensitivity analyses included: (i) checking whether the intercept term in MR-Egger regression is significantly different from zero; (ii) checking for heterogeneity among instrumental SNPs using Cochran's *Q* and I^2; and (iii) performing leave-one-out analyses using each of the four two-sample MR models to evaluate if single instrumental SNPs may be responsible for the inferred causal relationship(s). MR results satisfying all three sensitivity analyses were considered robust.

Finally, we investigated the contribution of four potential confounding factors (i.e., cigarettes per day,[43] drinks per week,[43] educational attainment,[44] household income[45]) on estimates of inferred causality between specific pairs of BCTs and NPDs, using two approaches. First, we re-estimated the causal effects for each pair of traits with consistent evidence for a causal relationship by applying the same MR methods (and LCV) to their conditional GWAS summary statistics, generated using mtCOJO. Second, we applied MVMR[49] analysis to each BCT-NPD trait pair with consistent evidence for a causal relationship. The MVMR method is capable of estimating causal effects between an exposure and outcome whilst adjusting for the potential pleiotropic effects of multiple outcome-related confounding factors concurrently.

Multi-omics analysis of putatively functional mechanisms underlying shared genetic loci for BCTs and neurological and psychiatric disorders

Next, we utilized SMR[25] to identify putatively functional genes and regulatory elements shared by pairs of BCTs and NPDs. SMR is an MR-equivalent analysis method that utilizes GWAS summary statistics to test for an association between gene expression (i.e., exposure) and a target phenotype (i.e., outcome), using genome-wide significant SNPs as instrumental variables. In our analyses, we used SMR to test for (i) association of gene expression (exposure) with pairs of BCTs and NPDs (outcomes), (ii) association of DNA methylation (exposure) with gene expression (outcome), and (iii) association of DNA methylation (exposure) with pairs of BCTs and NPDs (outcome). We also implemented the HEIDI test to distinguish linkage from a causal effect or pleiotropy, given a significant SMR association could be explained by different causal SNPs in high LD having effects on the exposure and outcome separately (i.e., linkage), rather than by a causal variant affecting outcome via changes in the exposure (i.e., causal effect) or the causal variant having a shared effect on both exposure and outcome (i.e., pleiotropy). Here, we performed SMR analyses across 70 pairs of BCTs and NPDs with evidence for a nominally significant ($p < 0.05$) r_g (by HDL or LDSC) and/or a causal relationship on the basis of MR analyses.

We first tested for an association of blood-based gene expression (exposure) with BCT-NPD pairs (outcome traits) using blood-based *cis*-eQTLs from eQTLGen,[50] reporting genes surpassing Bonferroni correction ($p_{SMR} < 3.18 \times 10^{-6}$, based on correction for testing of 15,743 probes with *cis*-eQTL $p < 5 \times 10^{-8}$) and also the HEIDI test ($p_{HEIDI} > 0.01$ with $\geq$10 SNPs). With respect to pairs of platelet parameters and related NPDs (e.g., PCT-stroke and PDW-PD), we further carried out SMR using platelet *cis*-eQTLs from GeneSTAR[51] (Bonferroni-corrected $p_{SMR} < 6.31 \times 10^{-5}$, i.e., $\frac{0.05}{793\ qualified\ eQTL\ probes}$, $p_{HEIDI} > 0.01$ with $\geq$10 SNPs). For all Bonferroni-significant genes, we then used SMR to test for an association of blood-based DNA methylation (exposure) with gene expression (outcome), using mQTL summary data from BSGS and LBC and *cis*-eQTL data from eQTLGen, respectively. DNA methylation-gene expression associations were declared significant if they had a Bonferroni corrected $p_{SMR} < 5.37 \times 10^{-7}$ (correction for testing of 93,122 probes with mQTL $p < 5 \times 10^{-8}$) and surpassed the HEIDI test ($p_{HEIDI} > 0.01$ with $\geq$10 SNPs). For all Bonferroni-significant DNA methylation probes, we then performed SMR using DNA methylation as exposure and BCT-NPD pairs as outcome, to determine if DNA methylation was also directly associated (Bonferroni corrected $p_{SMR} < 5.37 \times 10^{-7}$; and $p_{HEIDI} > 0.01$ with $\geq$10 SNPs) with the same pairs of BCTs and NPDs. We considered genes and regulatory elements with consistent evidence for significant associations across all SMR analyses to be noteworthy. Additionally, we applied the same three types of SMR analyses in regions of Bonferroni-significant local genetic correlation ($p < 9.23 \times 10^{-8}$), focusing on the subset of BCT-NPD pairs that also had negligible ($p > 0.05$) genome-wide r_g.

We also conducted parallel SMR analyses using brain-based *cis*-eQTL[53] and mQTL summary data[53] as sensitivity analyses, using the same analytic process as described above (but limited to the specific NPDs instead of pairs of BCTs and NPDs). We concentrated on functional genes and regulatory elements that were identified with consistent evidence for significant blood-based associations across the three types of SMR analyses. We considered brain-based SMR associations to be significant if they surpassed both a

Bonferroni-corrected SMR p value threshold ($p_{SMR} < 6.63 \times 10^{-6}$, i.e., $\frac{0.05}{7538\ qualified\ cis-eQTL\ probes}$, using *cis*-eQTL as exposure and GWAS of NPD as outcome; $<5.28 \times 10^{-7}$, i.e., $\frac{0.05}{94679\ qualified\ mQTL\ probes}$, using mQTL as exposure and *cis*-eQTL as outcome, and when using mQTL as exposure and GWAS of NPD as outcome) and the HEIDI test ($p_{HEIDI} > 0.01$ with ≥ 10 SNPs).

All SMR analyses were restricted to expression (or DNA methylation) probes with a *cis*-eQTL (or mQTL) $p < 5 \times 10^{-8}$, and probes located in the MHC region were excluded. LD was adjusted according to the 1000 Genomes European ref. [94]. For SMR analysis using mQTL as exposure and GWAS as outcome, genes were matched to each DNA methylation site if they were located within a 500Kb window. For multiple DNA methylation sites associated with the same gene with consistent direction of effect, we calculated the correlations between each pair of DNA methylation sites by measuring the correlations between SMR effects of their common genes. We filtered out DNA methylation sites if they were less significant and correlated ($R > 0.05$) with other DNA methylation sites.

Gene set enrichment analysis (GSEA)

Finally, we performed GSEA to identify biological pathways shared by specific pairs of BCTs and NPDs. We used the ShinyGO tool[54] based on the Gene Ontology (GO) annotation resource, comprising a hierarchy of biological processes, cellular components and molecular functions. To maintain power and sensitivity, we applied ShinyGO to candidate gene sets comprising five or more genes whose expression levels were Bonferroni-significant for both members of specific pairs of BCTs and NPDs, based on SMR analysis of blood-based and/or brain-based *cis*-eQTLs (Table S50). We defined significantly enriched pathways as those with ≥ 2 pathway-specific genes and an FDR <5%.

QUANTIFICATION AND STATISTICAL ANALYSIS

Statistical analyses were performed using R 4.0.5, HDL 1.3.8, LDSC 1.0.1, ρ-HESS 0.5.4, LCV, mtCOJO 1.9.3.2 beta, SMR 1.03, PLINK 1.9, ShinyGo 0.76 and Ricopili 1118b. All methodological details can be found in the STAR Methods, and all statistical tests are named as they are used. All statistical tests are two-sided, with the exception of the heterogeneity test among instrumental SNPs in the MR sensitivity analyses, which were one-sided.

Cell Genomics, Volume *3*

Supplemental information

The shared genetic landscape of blood cell traits and risk of neurological and psychiatric disorders

Yuanhao Yang, Yuan Zhou, Dale R. Nyholt, Chloe X. Yap, Rudolph K. Tannenberg, Ying Wang, Yang Wu, Zhihong Zhu, Bruce V. Taylor, and Jacob Gratten

Supplemental Figures

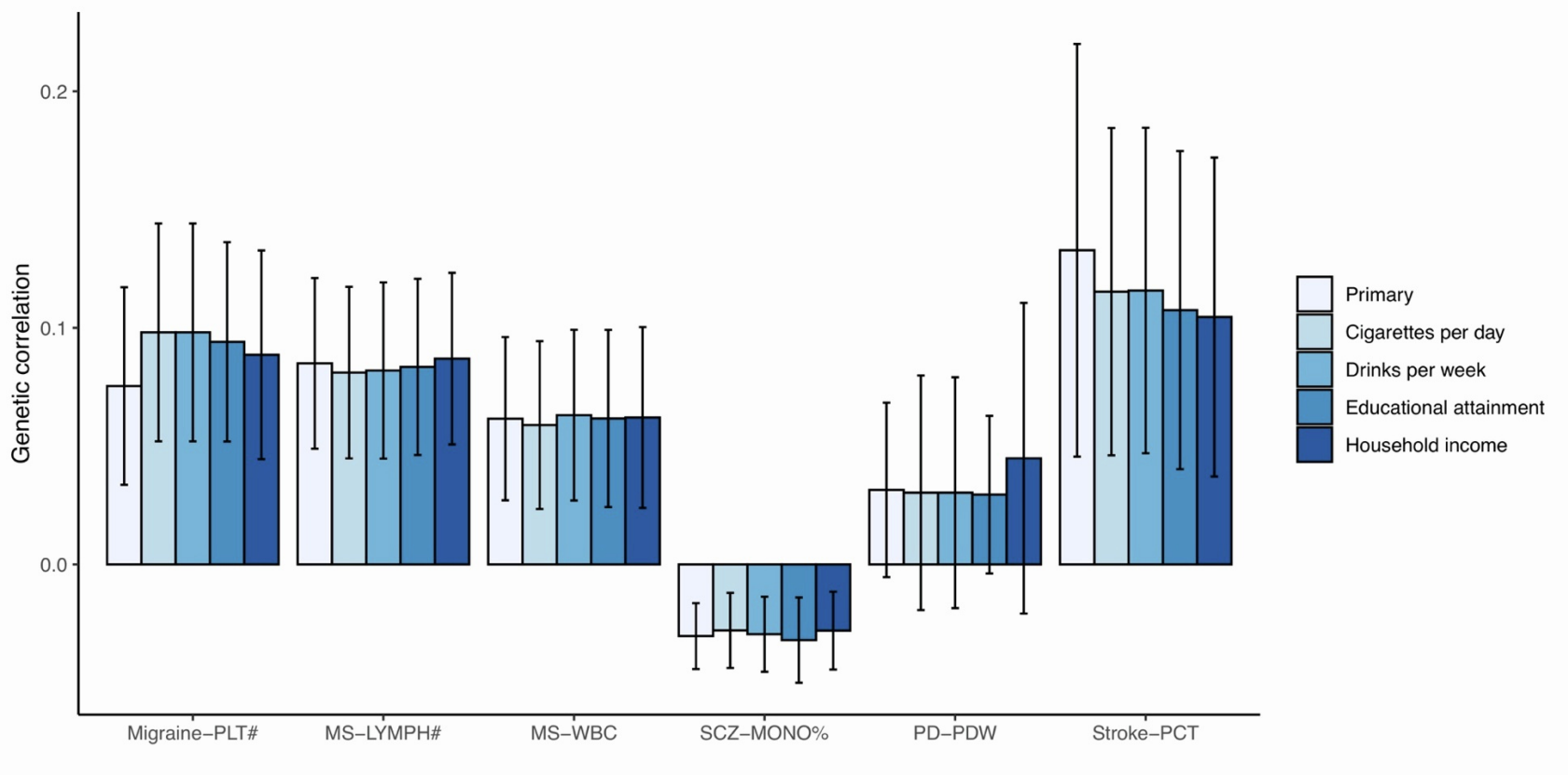

Figure S1. Summary of genetic correlations for specific BCT–NPD pairs estimated by primary HDL and HDL after conditioning GWAS summary data of specific BCTs and NPDs on the GWAS of cigarettes per day, drinks per week, educational attainment, and household income, respectively; related to Figure 2 and STAR Methods. BCT–NPD pairs were included if they had a Bonferroni- or FDR-significant genetic correlation (i.e., MS and LYMPH#, MS and WBC, SCZ and MONO%, migraine and PLT#) or a putative causal relationship (i.e., stroke and PCT, PD and PDW). Error bars represent the 95% CIs for the estimated genetic correlations.

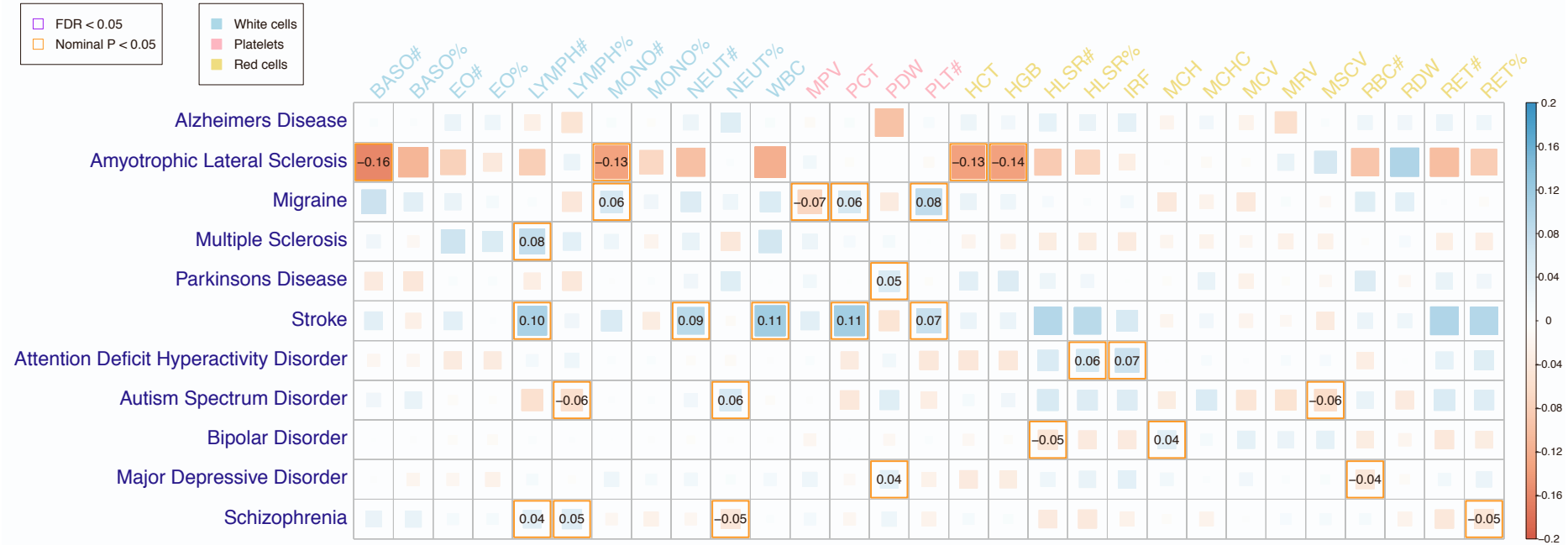

Figure S2. Estimated genetic correlations between BCTs and NPDs using the LDSC model, related to Figure 2 and STAR Methods. Significant genetic correlations (with estimates provided) are highlighted by red, purple, or orange boxes if they were Bonferroni-significant, FDR-significant, or nominally significant, respectively.

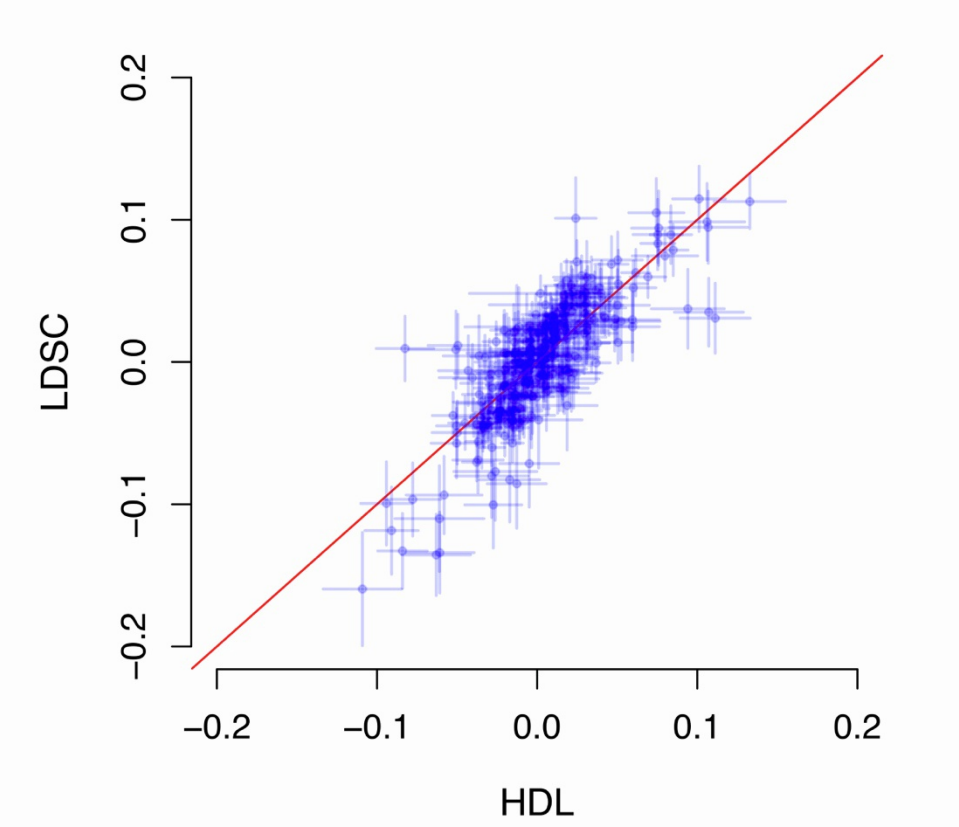

Figure S3. Comparison of genetic correlations estimated by HDL and LDSC, related to Figure 2 and STAR Methods. The estimated correlation = 0.81 (95% CI = 0.76-0.84) between genetic correlations for BCT–NPD pairs estimated by HDL and LDSC.

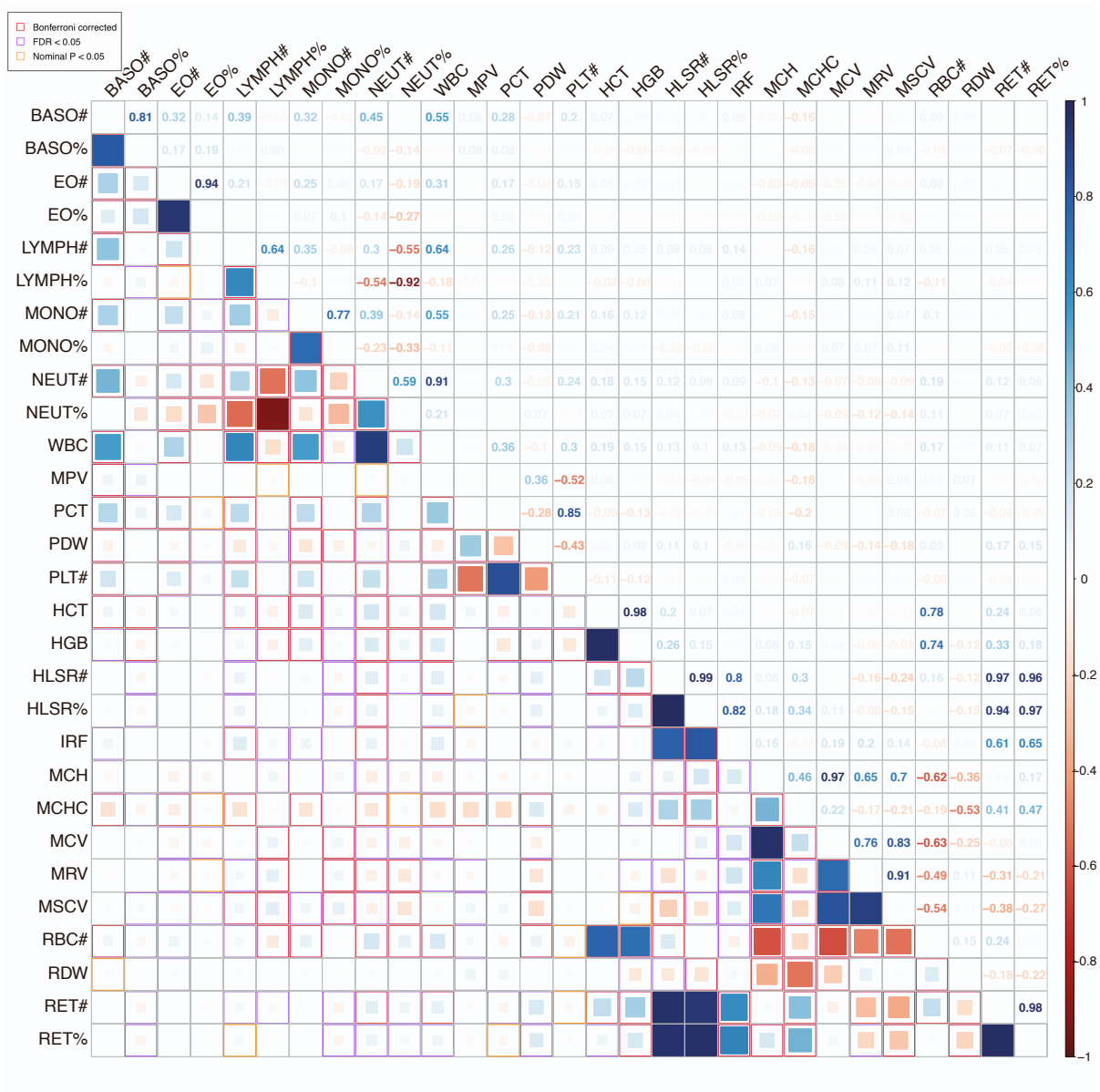

Figure S4. Estimated genetic correlations among BCTs using the HDL model, related to STAR Methods. Significant genetic correlations (in lower triangular heatmap) are highlighted by red, purple, or orange boxes if they were Bonferroni-significant, FDR-significant, or nominally significant, respectively. Estimated genetic correlations are shown in the upper triangular heatmap.

Figure S5. Estimated genetic correlations among BCTs using the LDSC model, related to STAR Methods. Significant genetic correlations (in lower triangular heatmap) are highlighted by red, purple, or orange boxes if they were Bonferroni-significant, FDR-significant, or nominally significant, respectively. Estimated genetic correlations are shown in the upper triangular heatmap.

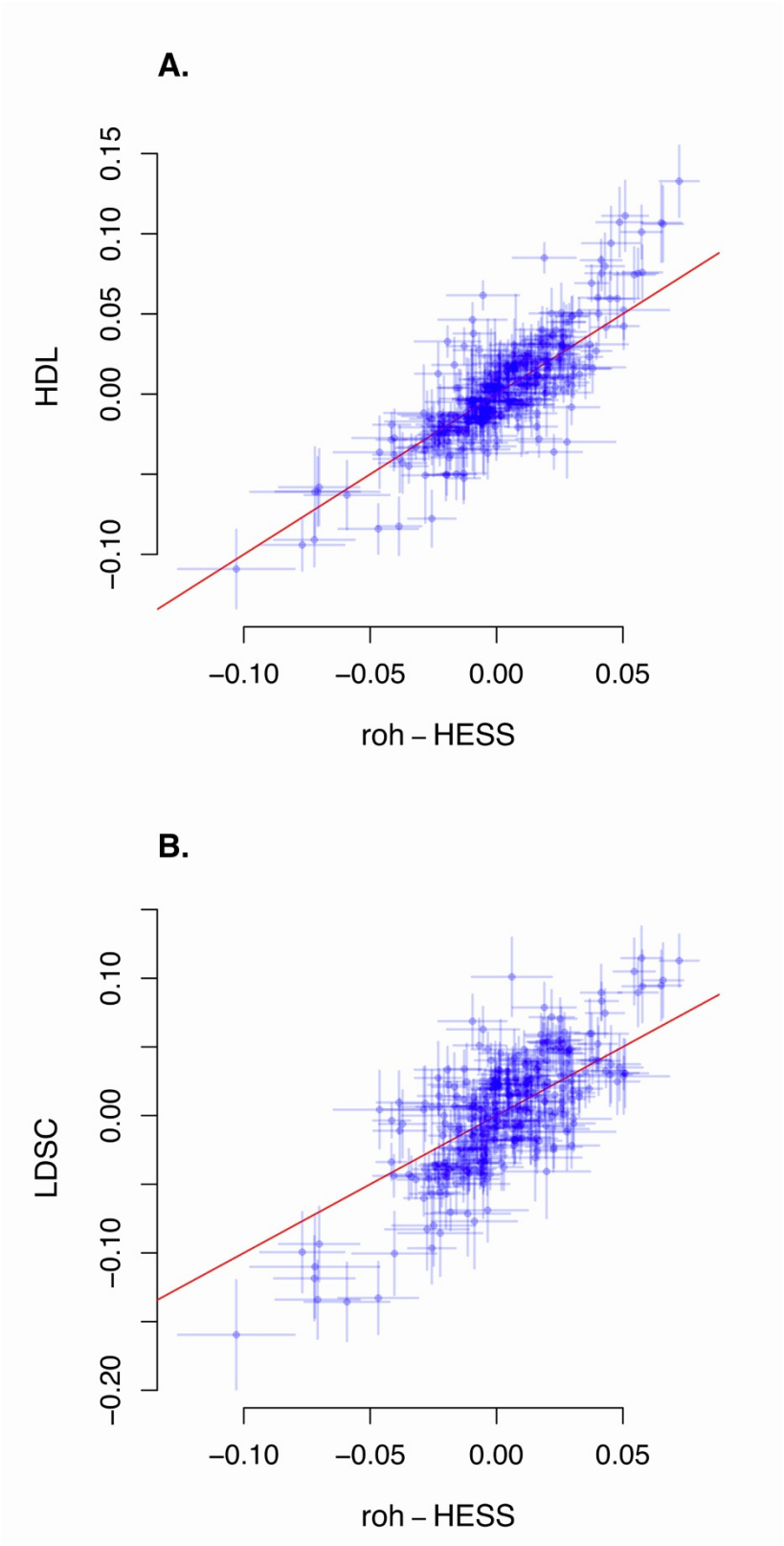

Figure S6. Comparison of genetic correlations for BCT–NPD pairs estimated by ρ-HESS and HDL (A) or LDSC (B), related to Figure 2 and STAR Methods. The estimated correlation = 0.83 (95% CI = 0.79-0.86) for ρ-HESS and HDL; and 0.74 (95% CI = 0.68-0.79) for ρ-HESS and LDSC.

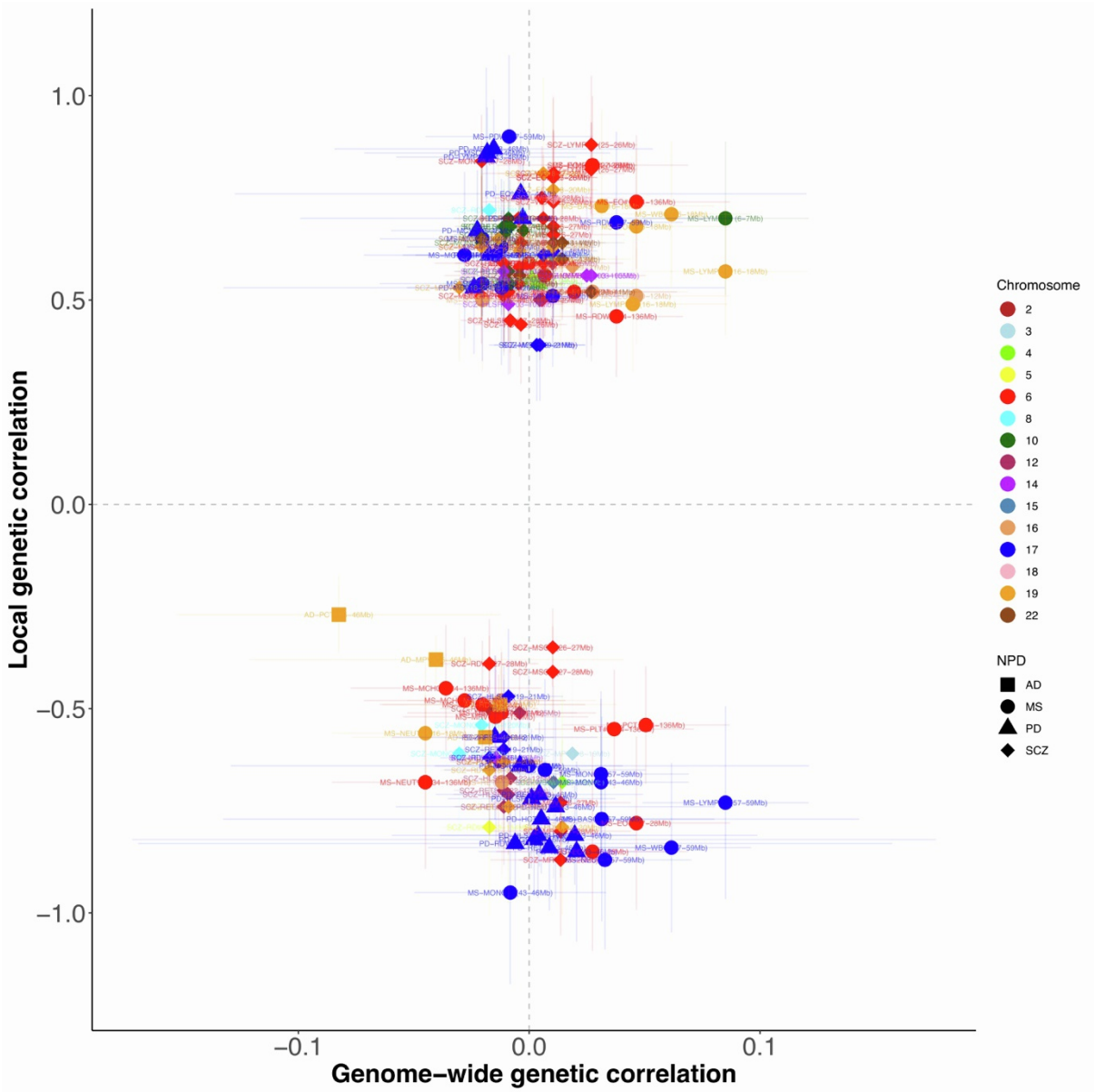

Figure S7. Comparison of genome-wide genetic correlations estimated by HDL (x-axis) and local genetic correlations estimated by ρ-HESS (y-axis) for specific pairs of BCTs and NPDs with Bonferroni-significant local heritability and local genetic correlations, related to STAR Methods. Error bars represent the 95% CIs for the estimated (local) genetic correlations.

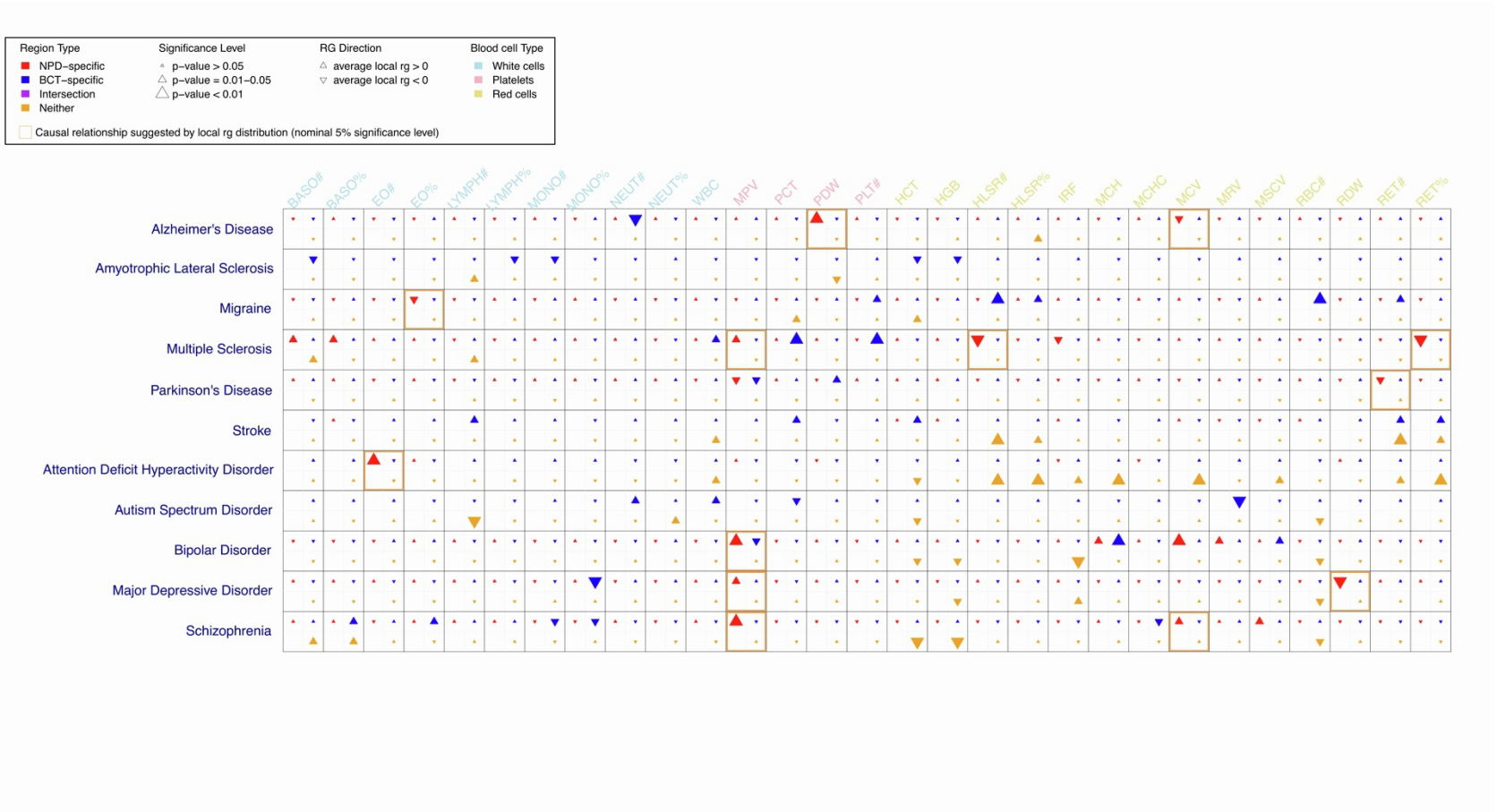

Figure S8. Summary of average local genetic correlations between BCTs and NPDs across trait-specific regions using ρ-HESS, related to STAR Methods. Trait-specific SNPs with GWAS p-value < 5×10^{-8} were used for classifying trait-associated genomic regions and to investigate differences in average local genetic correlation between traits. Significant associations are bordered by orange boxes if (i) the average local genetic correlation in regions harbouring BCT-specific SNPs was significantly different from that in "Intersection" regions, "Neither" regions, and regions harbouring the NPD-specific SNPs; and (ii) at least one of the average local genetic correlations estimated from regions harbouring either BCT- or NPD-specific SNPs was significantly non-zero ($p < 0.05$). See Table S19 for complete details of the ρ-HESS estimates.

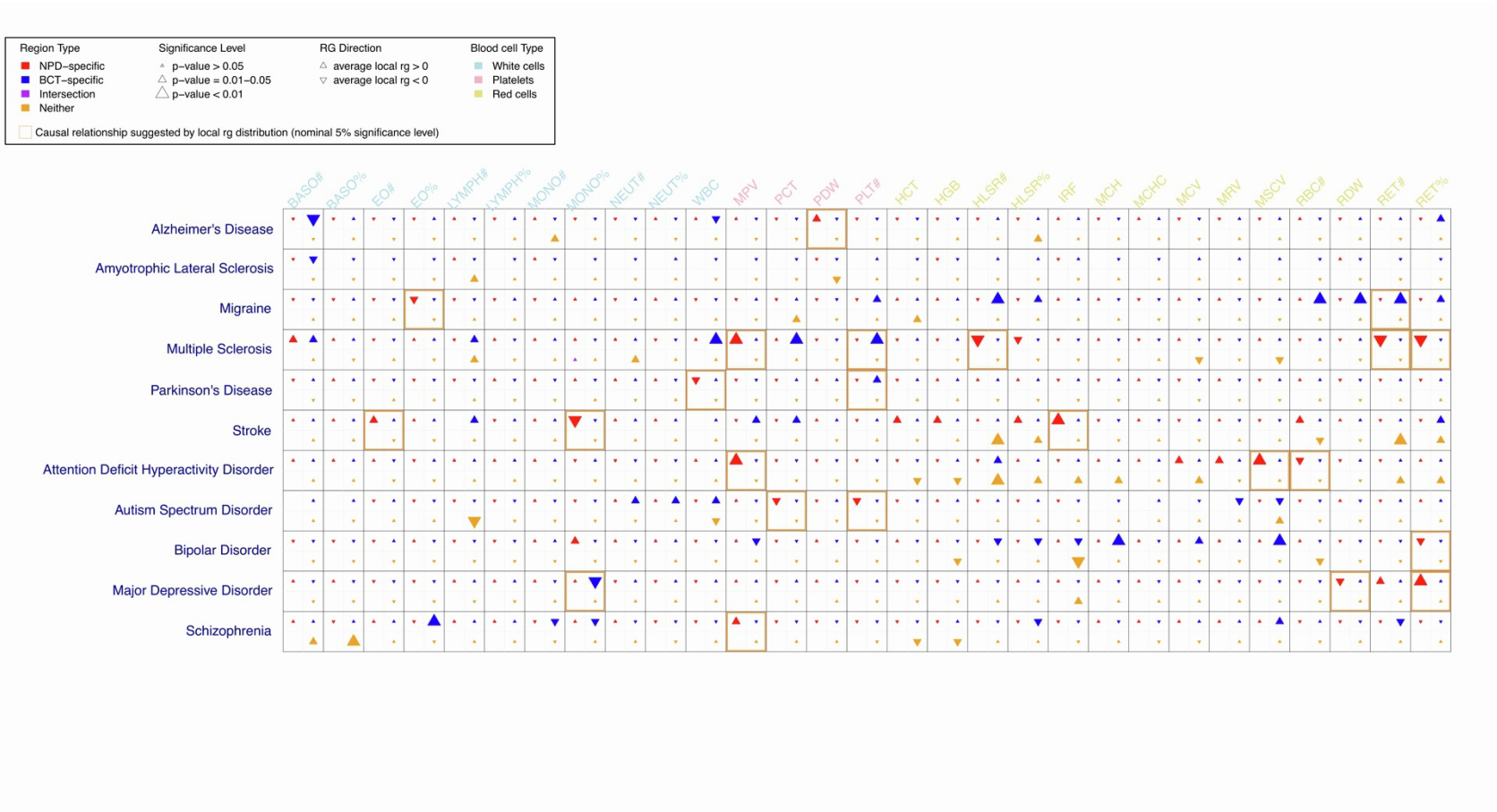

Figure S9. Summary of average local genetic correlations between BCTs and NPDs across trait-specific regions using ρ-HESS, related to STAR Methods. Trait-specific SNPs with GWAS p-value < 1×10^{-6} were used for classifying trait-associated genomic regions and to investigate differences in average local genetic correlation between traits. Significant associations are bordered by orange boxes if (i) the average local genetic correlation in regions harbouring BCT-specific SNPs was significantly different from that in "Intersection" regions, "Neither" regions, and regions harbouring the NPD-specific SNPs; and (ii) at least one of the average local genetic correlations estimated from regions harbouring either BCT- or NPD-specific SNPs was significantly non-zero ($p < 0.05$). See Table S20 for complete details of the ρ-HESS estimates.

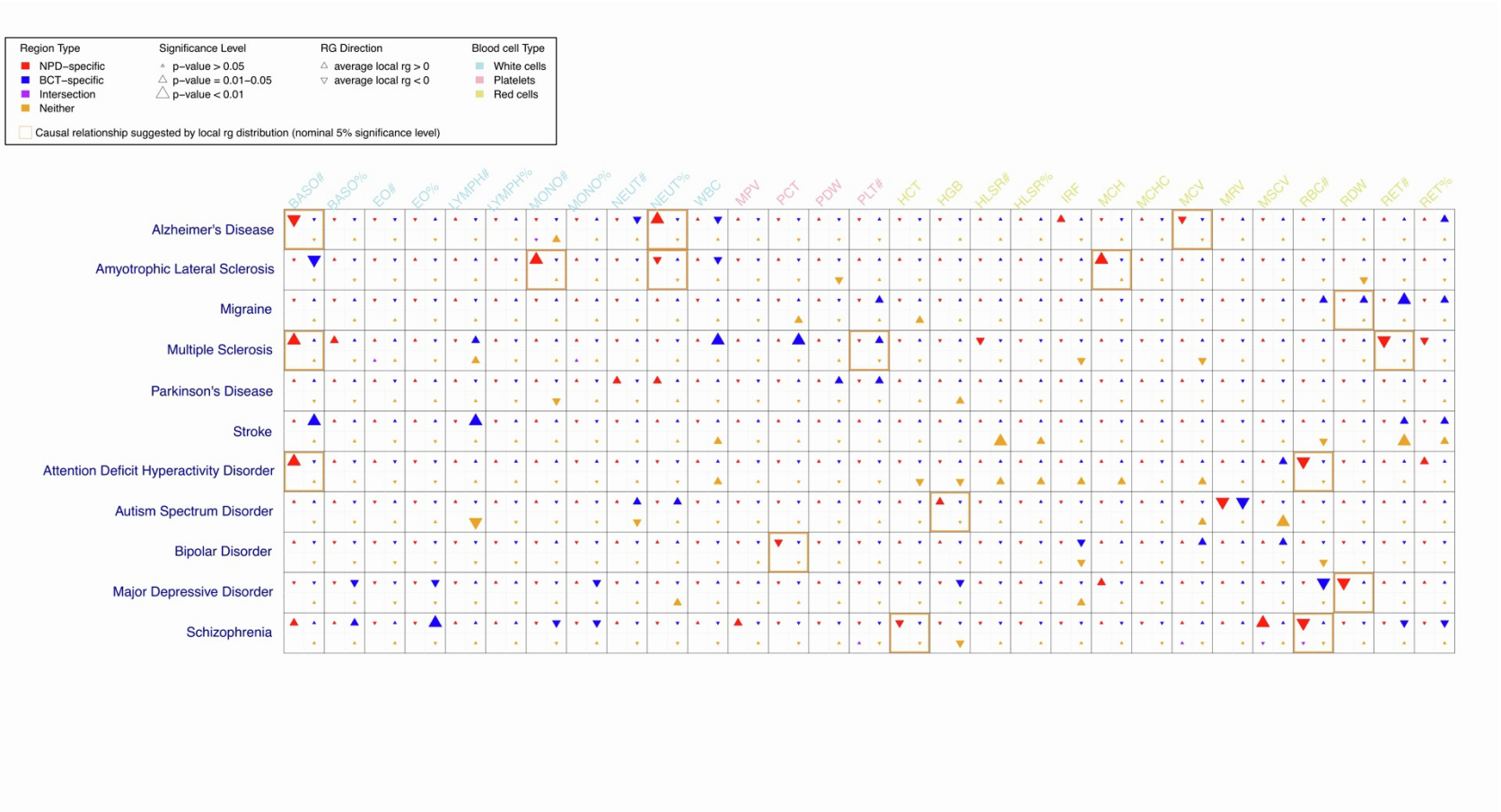

Figure S10. Summary of average local genetic correlations between BCTs and NPDs across trait-specific regions using ρ-HESS, related to STAR Methods. Trait-specific SNPs with GWAS p-value < 1×10^{-5} were used for classifying trait-associated genomic regions and to investigate differences in average local genetic correlation between traits. Significant associations are bordered by orange boxes if (i) the average local genetic correlation in regions harbouring BCT-specific SNPs was significantly different from that in "Intersection" regions, "Neither" regions, and regions harbouring the NPD-specific SNPs; and (ii) at least one of the average local genetic correlations estimated from regions harbouring either BCT- or NPD-specific SNPs was significantly non-zero ($p < 0.05$). See Table S21 for complete details of the ρ-HESS estimates.

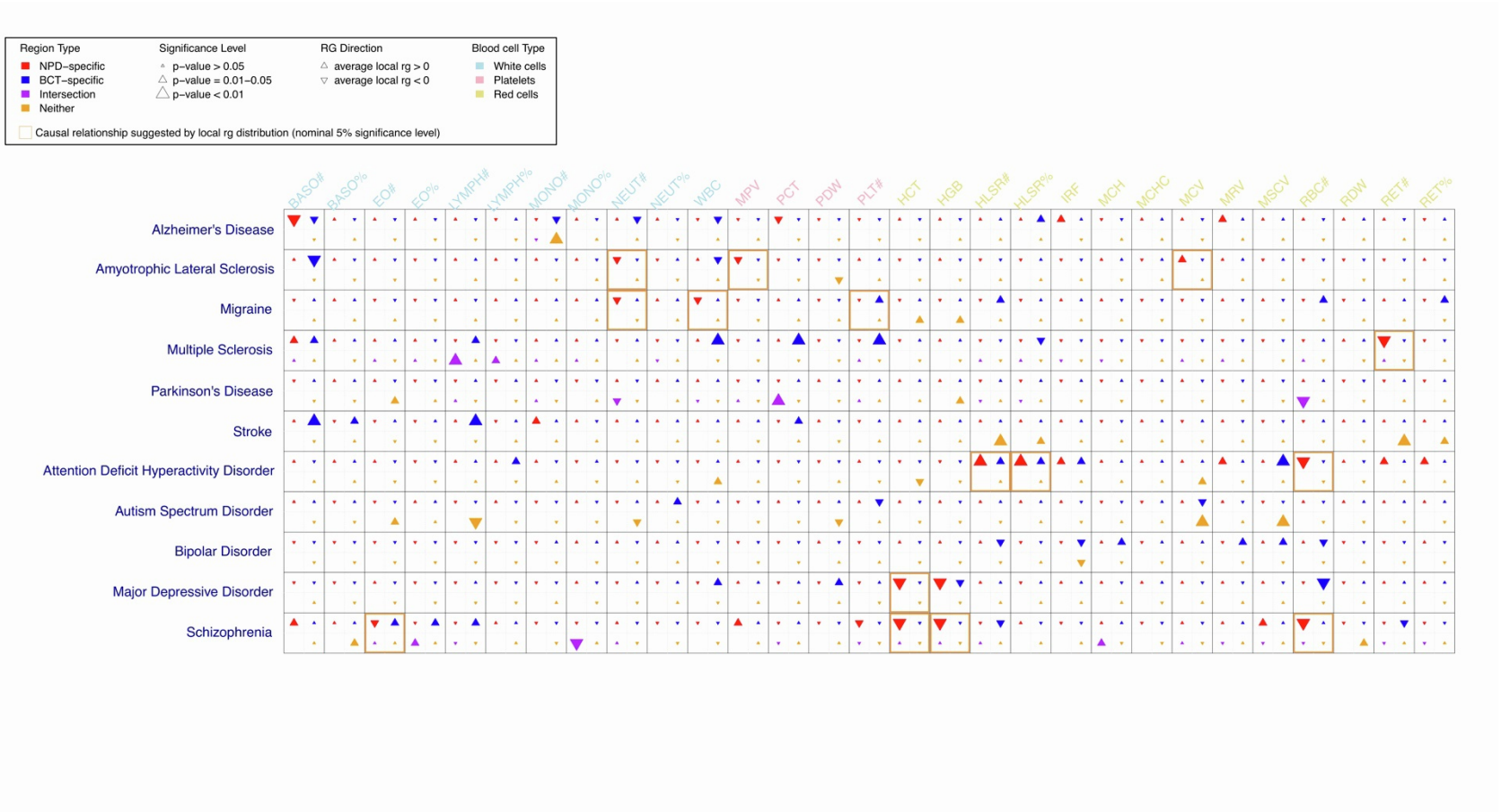

Figure S11. Summary of average local genetic correlations between BCTs and NPDs across trait-specific regions using ρ-HESS, related to STAR Methods. Trait-specific SNPs with GWAS p-value < 1×10^{-4} were used for classifying trait-associated genomic regions and to investigate differences in average local genetic correlation between traits. Significant associations are bordered by orange boxes if (i) the average local genetic correlation in regions harbouring BCT-specific SNPs was significantly different from that in "Intersection" regions, "Neither" regions, and regions harbouring the NPD-specific SNPs; and (ii) at least one of the average local genetic correlations estimated from regions harbouring either BCT- or NPD-specific SNPs was significantly non-zero ($p < 0.05$). See Table S22 for complete details of the ρ-HESS estimates.

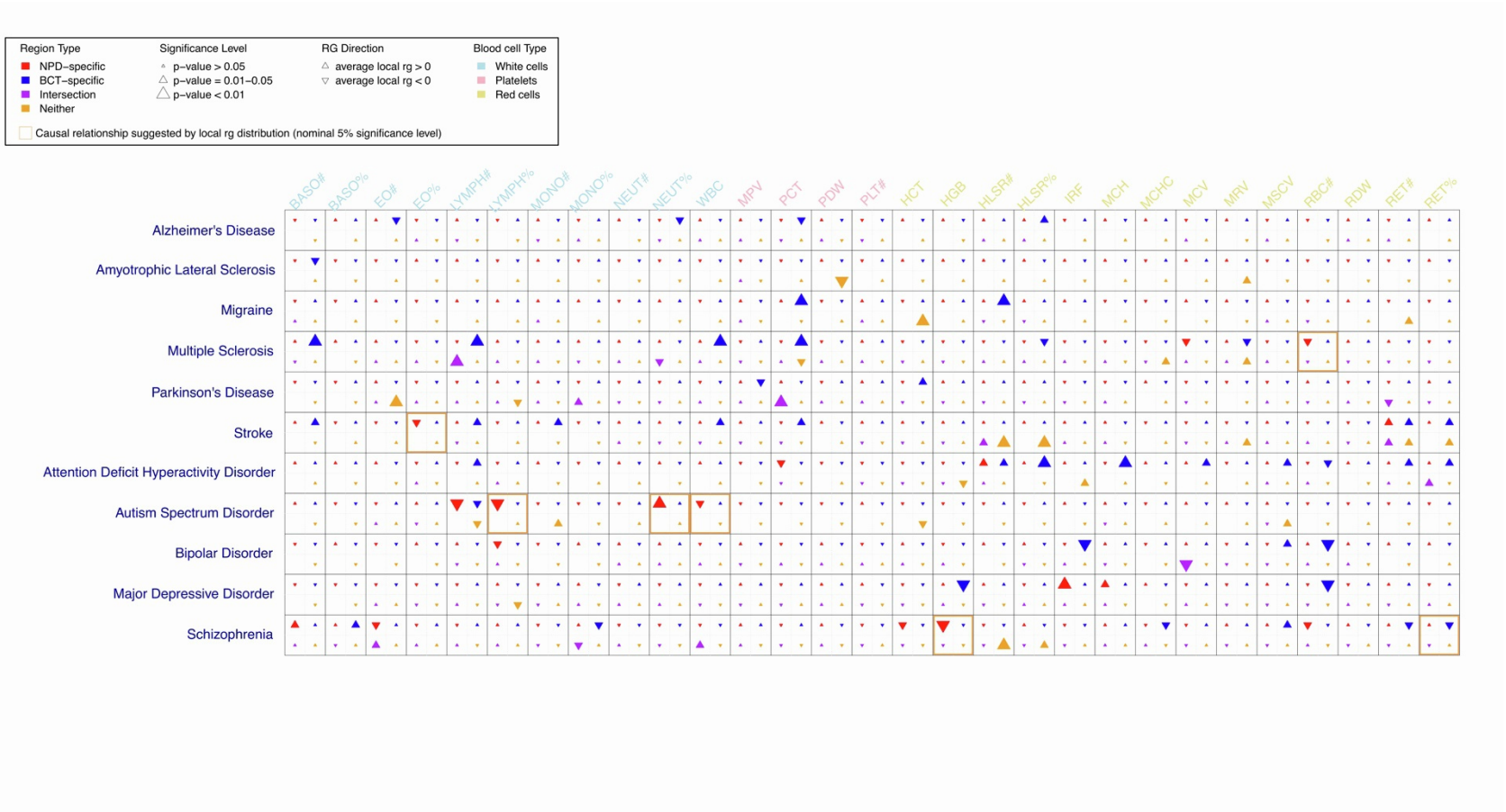

Figure S12. Summary of average local genetic correlations between BCTs and NPDs across trait-specific regions using ρ-HESS, related to STAR Methods. Trait-specific SNPs with GWAS p-value < 1×10^{-3} were used for classifying trait-associated genomic regions and to investigate differences in average local genetic correlation between traits. Significant associations are bordered by orange boxes if (i) the average local genetic correlation in regions harbouring BCT-specific SNPs was significantly different from that in "Intersection" regions, "Neither" regions, and regions harbouring the NPD-specific SNPs; and (ii) at least one of the average local genetic correlations estimated from regions harbouring either BCT- or NPD-specific SNPs was significantly non-zero ($p < 0.05$). See Table S23 for complete details of the ρ-HESS estimates.

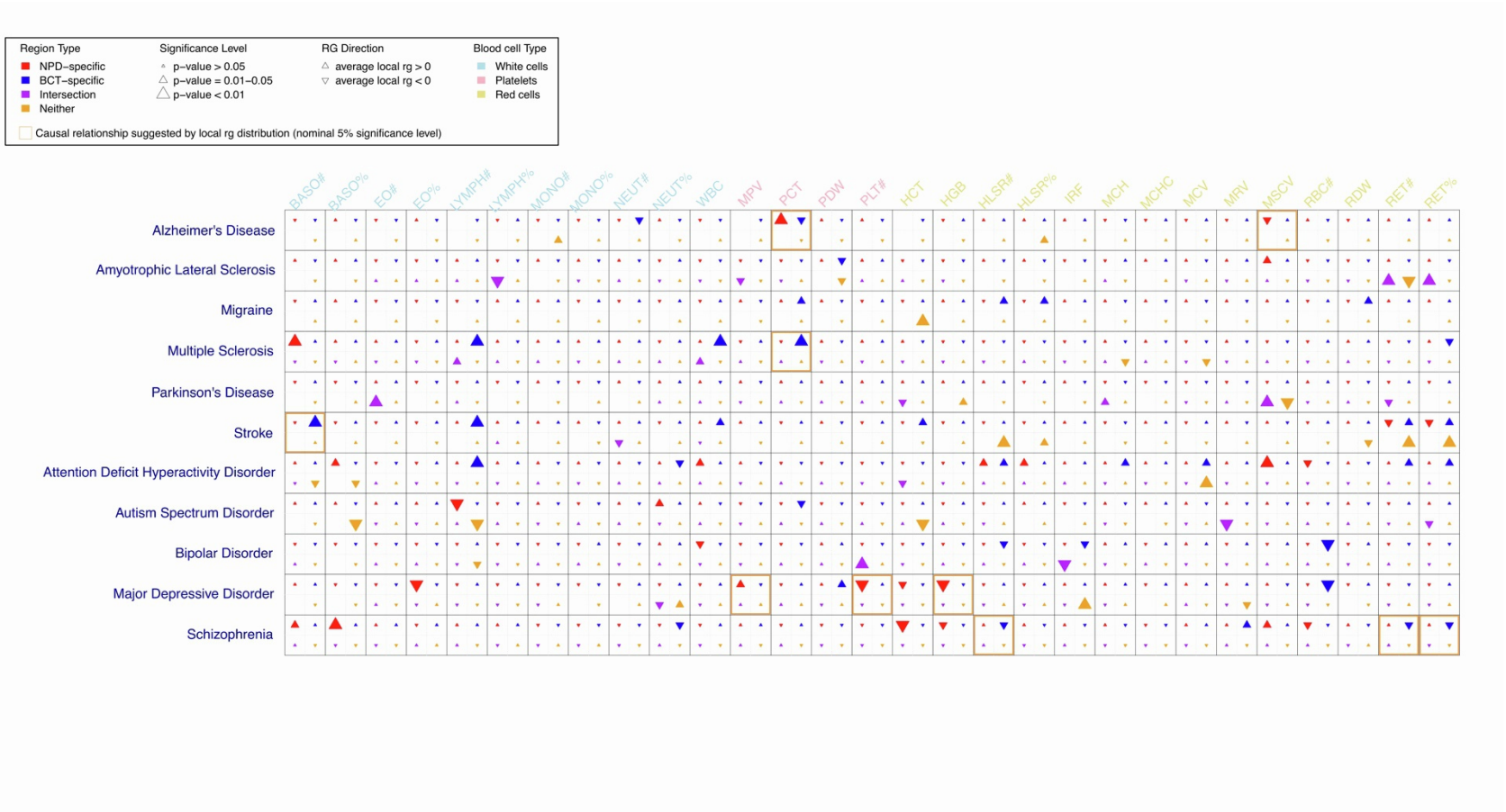

Figure S13. Summary of average local genetic correlations between BCTs and NPDs across trait-specific regions using ρ-HESS, related to STAR Methods. Specific SNPs were selected using the SBayesR method[1] and used for classifying trait-associated genomic regions and to investigate differences in average local genetic correlation between traits. Significant associations are bordered by orange boxes if (i) the average local genetic correlation in regions harbouring BCT-specific SNPs was significantly different from that in "Intersection" regions, "Neither" regions, and regions harbouring the NPD-specific SNPs; and (ii) at least one of the average local genetic correlations estimated from regions harbouring either BCT- or NPD-specific SNPs was significantly non-zero ($p < 0.05$). See Table S24 for complete details of the ρ-HESS estimates.

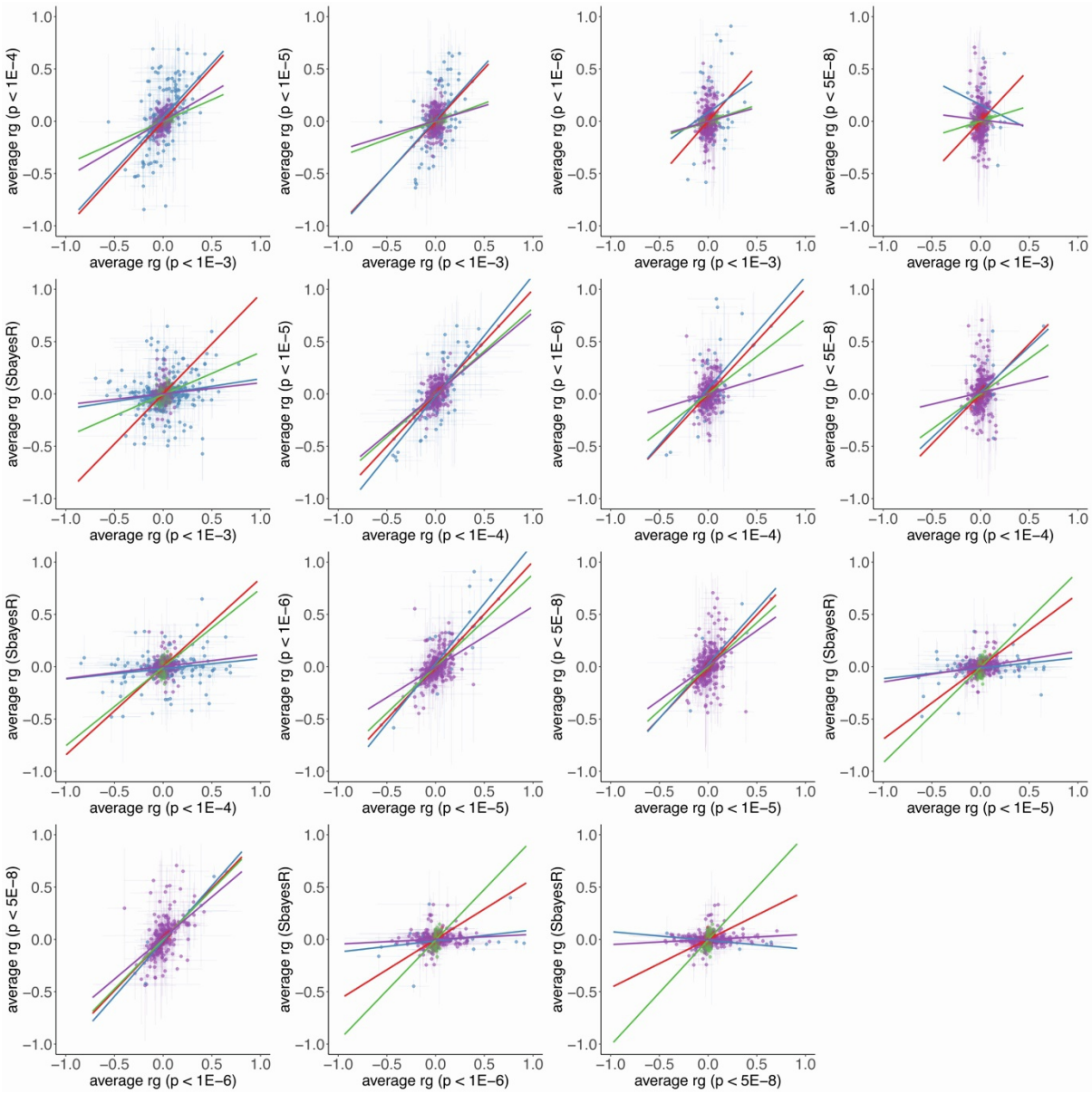

Figure S14. Comparison of average local genetic correlations between n = 319 BCT-NPD trait pairs from analyses performed using different p-value thresholds to define trait-specific regions, related to STAR Methods. Dots in red, green, purple and blue represent the estimated average local genetic correlations from the "BCT-specific" regions, "Neither" regions, "NPD-specific" regions, and "Intersection" regions, respectively, with estimated regression lines displayed in the corresponding colours. Error bars represent the standard errors of the estimated average local genetic correlations.

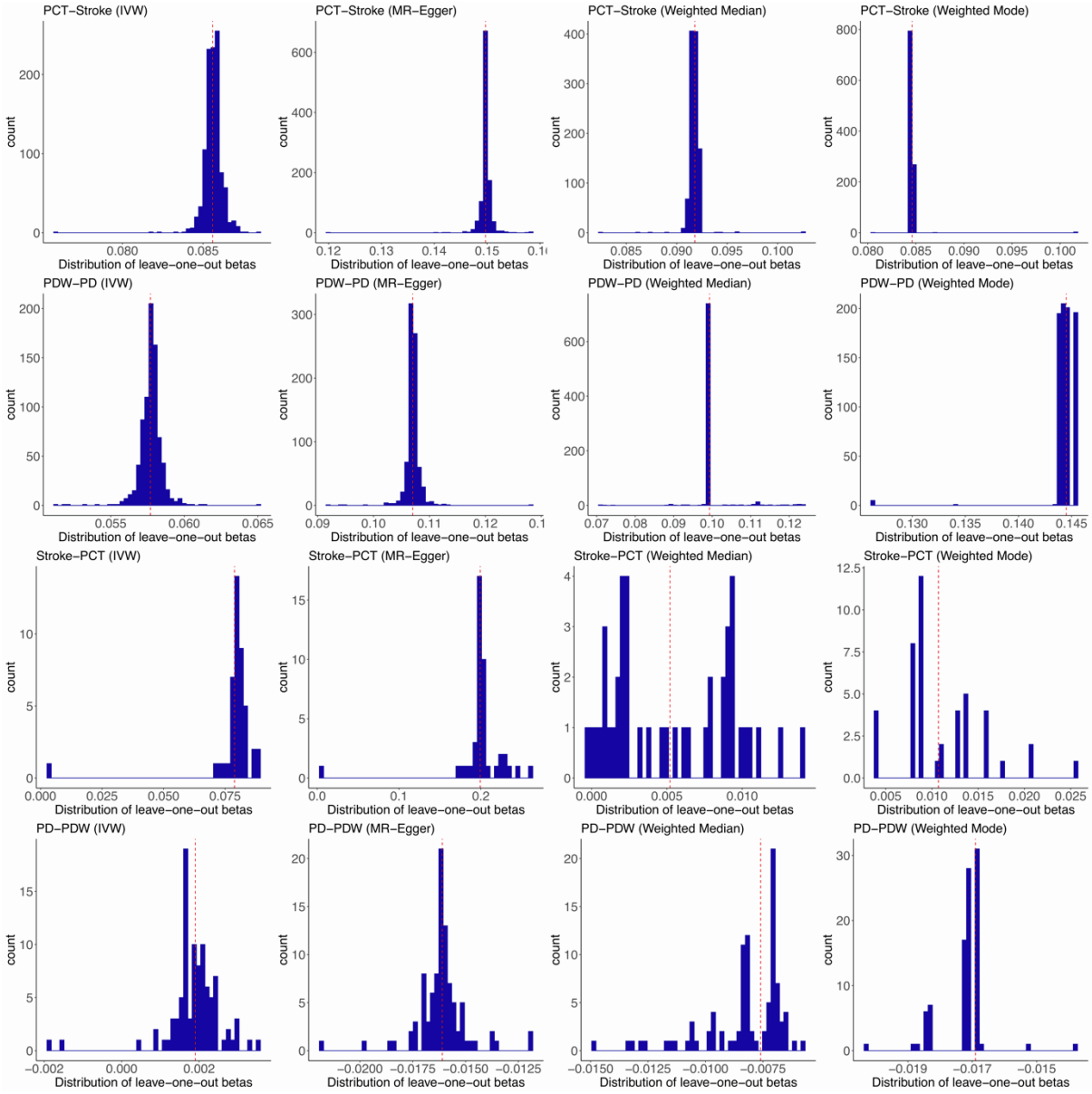

Figure S15. Histograms for estimated beta values from leave-one-out analyses assessing the impact of each instrumental SNP on the putative causal relationships between PCT-stroke and PDW-PD, using IVW, MR-Egger, weighted median, and weighted mode models, respectively, related to Figure 3 and STAR Methods. Plots are also shown for the reverse analyses (i.e., stroke-PCT and PD-PDW). Red dashed lines represent the estimated beta values from the original analyses based on all instrumental SNPs.

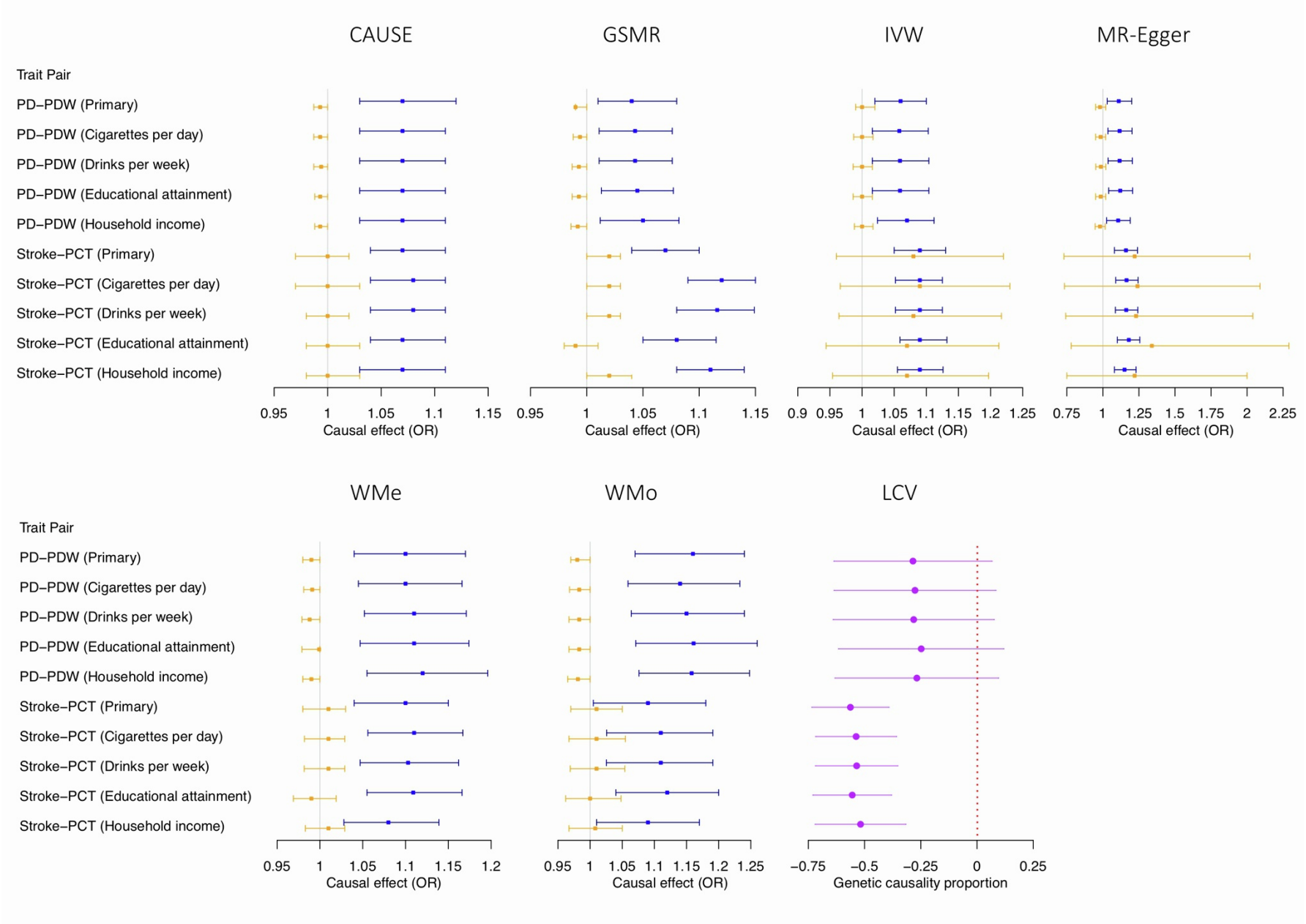
CAUSE
GSMR
IVW
MR-Egger
Trait Pair
PD–PDW (Primary)
PD–PDW (Cigarettes per day)
PD–PDW (Drinks per week)
PD–PDW (Educational attainment)
PD–PDW (Household income)
Stroke–PCT (Primary)
Stroke–PCT (Cigarettes per day)
Stroke–PCT (Drinks per week)
Stroke–PCT (Educational attainment)
Stroke–PCT (Household income)
0.95 1 1.05 1.1 1.15
0.95 1 1.05 1.1 1.15
0.9 0.95 1 1.05 1.1 1.15 1.2 1.25
0.75 1 1.25 1.5 1.75 2 2.25
Causal effect (OR)
WMe
WMo
LCV
Trait Pair
PD–PDW (Primary)
PD–PDW (Cigarettes per day)
PD–PDW (Drinks per week)
PD–PDW (Educational attainment)
PD–PDW (Household income)
Stroke–PCT (Primary)
Stroke–PCT (Cigarettes per day)
Stroke–PCT (Drinks per week)
Stroke–PCT (Educational attainment)
Stroke–PCT (Household income)
0.95 1 1.05 1.1 1.15 1.2
0.95 1 1.05 1.1 1.15 1.2 1.25
−0.75 −0.5 −0.25 0 0.25
Causal effect (OR)
Genetic causality proportion

Figure S16. Summary of the putative causal relationships between PDW and PD as well as between PCT and stroke after adjusting for the effects of cigarettes per day, drinks per week, educational attainment and household income, respectively, related to Figure 3 and STAR Methods. Results coloured in blue represent the estimated causal effect of BCTs on NPDs, while results coloured in orange represent the estimated causal effect of NPDs on BCTs. Error bars for MR methods represent 95% CIs and those for LCV-based GCP point estimates represent standard errors. For LCV, a negative GCP indicates a causal effect of BCT on NPD, and *vice versa*. See Table S34 for complete details of the estimates.

Supplemental Tables

Table S2. Summary of HDL-based genetic correlations adjusted by smoking, drinking, educational attainment and household income individually, related to Figure 2 and STAR Methods.

Risk factor	Trait 1 (NPD)	Trait 2 (BCT)	h^2 (Trait 1)	h^2 se (Trait 1)	h^2 (Trait 2)	h^2 se (Trait 2)	genetic covariance	r_g	r_g se	p-value (r_g)
Cigarettes per day	Migraine	Platelet count	0.0299	0.0022	0.3169	0.0249	0.0096	0.0981	0.0235	3.01×10^{-5}
	Multiple sclerosis	Lymphocyte count	0.3398	0.0227	0.2411	0.0168	0.0232	0.0811	0.0185	1.17×10^{-5}
	Multiple sclerosis	White blood cell count	0.3398	0.0227	0.2317	0.0152	0.0165	0.0589	0.0181	1.11×10^{-3}
	Parkinson's disease	Platelet distribution width	0.0159	0.0016	0.2214	0.0201	0.0018	0.0303	0.0253	0.23
	Schizophrenia	Monocyte percentage of white cells	0.3666	0.0096	0.2451	0.0258	-0.0084	-0.0279	0.0081	5.50×10^{-4}
	Stroke	Plateletcrit	0.0128	0.0021	0.2748	0.0258	0.0068	0.1153	0.0353	1.10×10^{-3}
Drinks per week	Migraine	Platelet count	0.0290	0.0021	0.3166	0.0248	0.0094	0.0981	0.0235	2.93×10^{-5}
	Multiple sclerosis	Lymphocyte count	0.3400	0.0226	0.2404	0.0168	0.0235	0.0820	0.0190	1.55×10^{-5}
	Multiple sclerosis	White blood cell count	0.3400	0.0226	0.2320	0.0152	0.0177	0.0631	0.0184	6.09×10^{-4}
	Parkinson's disease	Platelet distribution width	0.0159	0.0015	0.2215	0.0200	0.0018	0.0303	0.0249	0.22
	Schizophrenia	Monocyte percentage of white cells	0.3803	0.0097	0.2449	0.0258	-0.0090	-0.0295	0.0081	2.69×10^{-4}
	Stroke	Plateletcrit	0.0131	0.0021	0.2748	0.0257	0.0070	0.1158	0.0351	9.64×10^{-4}
Educational attainment	Migraine	Platelet count	0.0329	0.0022	0.3184	0.0246	0.0096	0.0941	0.0215	1.26×10^{-5}
	Multiple sclerosis	Lymphocyte count	0.3396	0.0216	0.2363	0.0153	0.0236	0.0835	0.0190	1.17×10^{-5}
	Multiple sclerosis	White blood cell count	0.3396	0.0216	0.2242	0.0139	0.0170	0.0617	0.0191	1.24×10^{-3}
	Parkinson's disease	Platelet distribution width	0.0167	0.0016	0.2258	0.0200	0.0018	0.0295	0.0170	0.082
	Schizophrenia	Monocyte percentage of white cells	0.3718	0.0098	0.2373	0.0254	-0.0095	-0.0320	0.0092	4.78×10^{-4}
	Stroke	Plateletcrit	0.0129	0.0020	0.2792	0.0261	0.0065	0.1075	0.0343	1.72×10^{-3}
Household income	Migraine	Platelet count	0.0304	0.0022	0.3138	0.0245	0.0087	0.0886	0.0225	8.13×10^{-5}
	Multiple sclerosis	Lymphocyte count	0.3416	0.0225	0.2358	0.0162	0.0247	0.0870	0.0185	2.46×10^{-6}
	Multiple sclerosis	White blood cell count	0.3416	0.0225	0.2215	0.0145	0.0171	0.0621	0.0195	1.42×10^{-3}
	Parkinson's disease	Platelet distribution width	0.0156	0.0015	0.2223	0.0201	0.0026	0.0449	0.0335	0.18
	Schizophrenia	Monocyte percentage of white cells	0.3361	0.0090	0.2395	0.0251	-0.0080	-0.0280	0.0084	9.03×10^{-4}
	Stroke	Plateletcrit	0.0129	0.0020	0.2747	0.0258	0.0062	0.1046	0.0344	2.35×10^{-3}

BCT: blood cell trait. NPD: neurological and psychiatric disorder. h^2: heritability. r_g: genetic correlation. se: standard error. HDL: high-definition likelihood.

Table S25. Comparison of average local genetic correlation between BCTs and NPDs per trait-specific region among different SNP sets for classification of trait-associated regions, related to STAR Methods.

Comparison	Group	Correlation (95% CI)	*p*-value
$p < 1\times10^{-3}$ vs $p < 1\times10^{-4}$	NPD-specific	0.38 (0.28,0.47)	3.02×10^{-12}
$p < 1\times10^{-3}$ vs $p < 1\times10^{-4}$	BCT-specific	0.88 (0.85,0.90)	3.82×10^{-105}
$p < 1\times10^{-3}$ vs $p < 1\times10^{-4}$	Neither	0.67 (0.60,0.73)	7.80×10^{-43}
$p < 1\times10^{-3}$ vs $p < 1\times10^{-4}$	Intersection	0.55 (0.42,0.65)	2.33×10^{-12}
$p < 1\times10^{-3}$ vs $p < 1\times10^{-5}$	NPD-specific	0.13 (0.02,0.24)	0.017
$p < 1\times10^{-3}$ vs $p < 1\times10^{-5}$	BCT-specific	0.79 (0.74,0.82)	4.19×10^{-68}
$p < 1\times10^{-3}$ vs $p < 1\times10^{-5}$	Neither	0.61 (0.54,0.68)	2.52×10^{-34}
$p < 1\times10^{-3}$ vs $p < 1\times10^{-5}$	Intersection	0.52 (0.32,0.67)	4.12×10^{-6}
$p < 1\times10^{-3}$ vs $p < 1\times10^{-6}$	NPD-specific	0.09 (-0.02,0.20)	0.091
$p < 1\times10^{-3}$ vs $p < 1\times10^{-6}$	BCT-specific	0.76 (0.71,0.80)	4.76×10^{-61}
$p < 1\times10^{-3}$ vs $p < 1\times10^{-6}$	Neither	0.60 (0.52,0.66)	3.94×10^{-32}
$p < 1\times10^{-3}$ vs $p < 1\times10^{-6}$	Intersection	0.23 (-0.14,0.54)	0.22
$p < 1\times10^{-3}$ vs $p < 5\times10^{-8}$	NPD-specific	-0.03 (-0.15,0.09)	0.63
$p < 1\times10^{-3}$ vs $p < 5\times10^{-8}$	BCT-specific	0.66 (0.59,0.72)	4.53×10^{-41}
$p < 1\times10^{-3}$ vs $p < 5\times10^{-8}$	Neither	0.57 (0.50,0.64)	2.48×10^{-29}
$p < 1\times10^{-3}$ vs $p < 5\times10^{-8}$	Intersection	-0.18 (-0.67,0.41)	0.55
$p < 1\times10^{-4}$ vs $p < 1\times10^{-5}$	NPD-specific	0.52 (0.44,0.60)	1.43×10^{-23}
$p < 1\times10^{-4}$ vs $p < 1\times10^{-5}$	BCT-specific	0.90 (0.88,0.92)	3.40×10^{-118}
$p < 1\times10^{-4}$ vs $p < 1\times10^{-5}$	Neither	0.90 (0.88,0.92)	3.55×10^{-118}
$p < 1\times10^{-4}$ vs $p < 1\times10^{-5}$	Intersection	0.82 (0.73,0.89)	1.92×10^{-18}
$p < 1\times10^{-4}$ vs $p < 1\times10^{-6}$	NPD-specific	0.15 (0.04,0.25)	9.31×10^{-3}
$p < 1\times10^{-4}$ vs $p < 1\times10^{-6}$	BCT-specific	0.83 (0.79,0.86)	4.89×10^{-83}
$p < 1\times10^{-4}$ vs $p < 1\times10^{-6}$	Neither	0.85 (0.82,0.88)	1.08×10^{-90}
$p < 1\times10^{-4}$ vs $p < 1\times10^{-6}$	Intersection	0.64 (0.37,0.81)	1.13×10^{-4}
$p < 1\times10^{-4}$ vs $p < 5\times10^{-8}$	NPD-specific	0.08 (-0.04,0.20)	0.18
$p < 1\times10^{-4}$ vs $p < 5\times10^{-8}$	BCT-specific	0.73 (0.68,0.78)	2.81×10^{-55}
$p < 1\times10^{-4}$ vs $p < 5\times10^{-8}$	Neither	0.82 (0.78,0.85)	5.49×10^{-78}
$p < 1\times10^{-4}$ vs $p < 5\times10^{-8}$	Intersection	0.51 (-0.06,0.83)	0.076
$p < 1\times10^{-5}$ vs $p < 1\times10^{-6}$	NPD-specific	0.44 (0.35,0.53)	8.25×10^{-17}
$p < 1\times10^{-5}$ vs $p < 1\times10^{-6}$	BCT-specific	0.92 (0.90,0.93)	1.84×10^{-129}
$p < 1\times10^{-5}$ vs $p < 1\times10^{-6}$	Neither	0.96 (0.95,0.96)	6.83×10^{-171}
$p < 1\times10^{-5}$ vs $p < 1\times10^{-6}$	Intersection	0.90 (0.80,0.95)	4.50×10^{-12}
$p < 1\times10^{-5}$ vs $p < 5\times10^{-8}$	NPD-specific	0.34 (0.23,0.44)	7.77×10^{-9}
$p < 1\times10^{-5}$ vs $p < 5\times10^{-8}$	BCT-specific	0.84 (0.80,0.87)	7.12×10^{-86}
$p < 1\times10^{-5}$ vs $p < 5\times10^{-8}$	Neither	0.93 (0.91,0.94)	7.69×10^{-136}
$p < 1\times10^{-5}$ vs $p < 5\times10^{-8}$	Intersection	0.88 (0.64,0.96)	6.89×10^{-5}
$p < 1\times10^{-6}$ vs $p < 5\times10^{-8}$	NPD-specific	0.50 (0.41,0.59)	2.22×10^{-19}
$p < 1\times10^{-6}$ vs $p < 5\times10^{-8}$	BCT-specific	0.91 (0.89,0.92)	5.84×10^{-121}
$p < 1\times10^{-6}$ vs $p < 5\times10^{-8}$	Neither	0.97 (0.96,0.97)	1.41×10^{-190}
$p < 1\times10^{-6}$ vs $p < 5\times10^{-8}$	Intersection	0.96 (0.87,0.99)	1.86×10^{-7}
$p < 1\times10^{-3}$ vs $p <$ SbayesR	NPD-specific	0.07 (-0.04,0.18)	0.19
$p < 1\times10^{-3}$ vs $p <$ SbayesR	BCT-specific	0.81 (0.77,0.85)	1.46×10^{-76}
$p < 1\times10^{-3}$ vs $p <$ SbayesR	Neither	0.40 (0.30,0.48)	1.98×10^{-13}
$p < 1\times10^{-3}$ vs $p <$ SbayesR	Intersection	0.17 (0.05,0.29)	7.84×10^{-3}
$p < 1\times10^{-4}$ vs $p <$ SbayesR	NPD-specific	0.12 (0.01,0.22)	0.038
$p < 1\times10^{-4}$ vs $p <$ SbayesR	BCT-specific	0.83 (0.79,0.86)	4.87×10^{-83}
$p < 1\times10^{-4}$ vs $p <$ SbayesR	Neither	0.45 (0.36,0.54)	1.72×10^{-17}
$p < 1\times10^{-4}$ vs $p <$ SbayesR	Intersection	0.18 (0.01,0.35)	0.041
$p < 1\times10^{-5}$ vs $p <$ SbayesR	NPD-specific	0.22 (0.12,0.33)	5.75×10^{-5}
$p < 1\times10^{-5}$ vs $p <$ SbayesR	BCT-specific	0.76 (0.70,0.80)	2.45×10^{-60}
$p < 1\times10^{-5}$ vs $p <$ SbayesR	Neither	0.50 (0.41,0.58)	1.14×10^{-21}
$p < 1\times10^{-5}$ vs $p <$ SbayesR	Intersection	0.25 (-0.01,0.48)	0.060
$p < 1\times10^{-6}$ vs $p <$ SbayesR	NPD-specific	0.09 (-0.02,0.20)	0.099

$p < 1\times10^{-6}$ vs $p <$ SbayesR	BCT-specific	0.69 (0.63,0.74)	1.59×10^{-46}
$p < 1\times10^{-6}$ vs $p <$ SbayesR	Neither	0.49 (0.40,0.57)	1.18×10^{-20}
$p < 1\times10^{-6}$ vs $p <$ SbayesR	Intersection	0.29 (-0.14,0.62)	0.19
$p < 5\times10^{-8}$ vs $p <$ SbayesR	NPD-specific	0.13 (0.01,0.24)	0.033
$p < 5\times10^{-8}$ vs $p <$ SbayesR	BCT-specific	0.59 (0.52,0.66)	1.17×10^{-31}
$p < 5\times10^{-8}$ vs $p <$ SbayesR	Neither	0.50 (0.41,0.58)	1.33×10^{-21}
$p < 5\times10^{-8}$ vs $p <$ SbayesR	Intersection	-0.54 (-0.92,0.35)	0.21

BCT: blood cell trait. NPD: neurological and psychiatric disorder. SNP: single nucleotide polymorphism. CI: confidence interval.

Table S27. Summary of MR sensitivity analyses, related to Figure 3 and STAR Methods.					
LCV					
Trait 1	Trait 2	n of SNPs	GCP*	GCP se	*p*-value
Autism spectrum disorder	Mean spheric corpuscular volume	1149387	-0.07	0.32	0.46
Multiple sclerosis	Lymphocyte count	1162211	-0.19	0.13	0.25
Multiple sclerosis	Plateletcrit	1162184	0.01	0.58	0.98
Multiple sclerosis	White blood cell count	1162194	0.08	0.37	0.99
Parkinson's disease	Platelet distribution width	1056850	-0.35	0.43	0.17
Stroke	Plateletcrit	1145599	-0.69	0.21	4.43×10^{-23}
GSMR					
Exposure	Outcome	n of SNPs (n after HEIDI-outlier test)	Beta (95% CI)	OR	*p*-value
Autism spectrum disorder**	Mean spheric corpuscular volume	34 (30)	-0.01 (-0.0222, 0.0002)	0.99	0.054
Mean spheric corpuscular volume	Autism spectrum disorder	1172 (1104)	-0.07 (-0.1073, -0.0299)	0.93	5.17×10^{-4}
Multiple sclerosis	Lymphocyte count	70 (29)	0.01 (0.0007, 0.0146)	1.01	0.030
Lymphocyte count	Multiple sclerosis	790 (635)	0.07 (-0.0084, 0.1411)	1.07	0.082
Multiple sclerosis	Plateletcrit	70 (44)	0.00 (-0.0081, 0.0031)	1.00	0.38
Plateletcrit	Multiple sclerosis	1003 (867)	0.11 (0.05600, 0.1669)	1.12	8.19×10^{-5}
Multiple sclerosis	White blood cell count	70 (41)	0.01 (0.0058, 0.0176)	1.01	1.01×10^{-4}
White blood cell count	Multiple sclerosis	802 (662)	0.11 (0.0396, 0.1828)	1.12	2.33×10^{-3}
Parkinson's disease	Platelet distribution width	95 (84)	-0.01 (-0.0123, -0.0004)	0.99	0.036
Platelet distribution width	Parkinson's disease	804 (719)	0.04 (0.0114, 0.0732)	1.04	7.26×10^{-3}
Stroke**	Plateletcrit	44 (32)	0.02 (0.0007, 0.0327)	1.02	0.041
Plateletcrit	Stroke	1067 (984)	0.07 (0.0385, 0.0972)	1.07	5.83×10^{-6}
IVW					
Exposure	Outcome	n of SNPs	Beta (95% CI)	OR	*p*-value
Autism spectrum disorder**	Mean spheric corpuscular volume	34	-0.04 (-0.0812, 0.0093)	0.96	0.12
Mean spheric corpuscular volume	Autism spectrum disorder	1172	-0.08 (-0.1190, -0.0354)	0.93	2.94×10^{-4}
Multiple sclerosis	Lymphocyte count	70	0.02 (-0.0112, 0.0448)	1.02	0.24
Lymphocyte count	Multiple sclerosis	790	0.25 (0.1413, 0.3612)	1.29	7.45×10^{-6}
Multiple sclerosis	Plateletcrit	70	-0.01 (-0.0363, 0.0086)	0.99	0.23
Plateletcrit	Multiple sclerosis	1003	0.09 (0.0080, 0.1702)	1.09	0.031
Multiple sclerosis	White blood cell count	70	0.00 (-0.0177, 0.0214)	1.00	0.85
White blood cell count	Multiple sclerosis	802	0.12 (0.0181, 0.2279)	1.13	0.022
Parkinson's disease	Platelet distribution width	95	0.00 (-0.0128, 0.0165)	1.00	0.80
Platelet distribution width	Parkinson's disease	804	0.06 (0.0164, 0.0990)	1.06	6.13×10^{-3}
Stroke**	Plateletcrit	44	0.08 (-0.0380, 0.1956)	1.08	0.19

Plateletcrit	Stroke	1067	0.09 (0.0519, 0.1193)	1.09	6.32×10^{-7}
MR-Egger					
Exposure	Outcome	n of SNPs	Beta (95% CI)	OR	*p*-value
Autism spectrum disorder**	Mean spheric corpuscular volume	34	-0.06 (-0.3282, 0.2110)	0.94	0.67
Mean spheric corpuscular volume	Autism spectrum disorder	1172	-0.06 (-0.1375, 0.0170)	0.94	0.13
Multiple sclerosis	Lymphocyte count	70	-0.04 (-0.1713, 0.0909)	0.96	0.55
Lymphocyte count	Multiple sclerosis	790	0.59 (0.3429, 0.8434)	1.81	3.97×10^{-6}
Multiple sclerosis	Plateletcrit	70	-0.04 (-0.1456, 0.0660)	0.96	0.46
Plateletcrit	Multiple sclerosis	1003	0.21 (0.0425, 0.3773)	1.23	0.014
Multiple sclerosis	White blood cell count	70	-0.01 (-0.1038, 0.0805)	0.99	0.81
White blood cell count	Multiple sclerosis	802	0.08 (-0.1726, 0.3365)	1.09	0.53
Parkinson's disease	Platelet distribution width	95	-0.02 (-0.0513, 0.0191)	0.98	0.37
Platelet distribution width	Parkinson's disease	804	0.11 (0.0321, 0.1819)	1.11	5.23×10^{-3}
Stroke**	Plateletcrit	44	0.20 (-0.3047, 0.7034)	1.22	0.44
Plateletcrit	Stroke	1067	0.15 (0.0813, 0.2181)	1.16	1.96×10^{-5}
Weighted Median					
Exposure	Outcome	n of SNPs	Beta (95% CI)	OR	*p*-value
Autism spectrum disorder**	Mean spheric corpuscular volume	34	-0.01 (-0.0261, 0.0068)	0.99	0.25
Mean spheric corpuscular volume	Autism spectrum disorder	1172	-0.05 (-0.1262, 0.0177)	0.95	0.14
Multiple sclerosis	Lymphocyte count	70	-0.01 (-0.0191, 0.0027)	0.99	0.14
Lymphocyte count	Multiple sclerosis	790	0.33 (0.2056, 0.4519)	1.39	1.69×10^{-7}
Multiple sclerosis	Plateletcrit	70	0.00 (-0.0126, 0.0055)	1.00	0.44
Plateletcrit	Multiple sclerosis	1003	0.10 (-0.0113, 0.2041)	1.10	0.079
Multiple sclerosis	White blood cell count	70	0.01 (-0.0015, 0.0176)	1.01	0.099
White blood cell count	Multiple sclerosis	802	0.15 (0.0302, 0.2730)	1.16	0.014
Parkinson's disease	Platelet distribution width	95	-0.01 (-0.0175, 0.0023)	0.99	0.12
Platelet distribution width	Parkinson's disease	804	0.10 (0.0426, 0.1560)	1.10	7.08×10^{-4}
Stroke**	Plateletcrit	44	0.01 (-0.0187, 0.0292)	1.01	0.68
Plateletcrit	Stroke	1067	0.09 (0.0406, 0.1429)	1.10	5.28×10^{-4}
Weighted Mode					
Exposure	Outcome	n of SNPs	Beta (95% CI)	OR	*p*-value
Autism spectrum disorder**	Mean spheric corpuscular volume	34	0.00 (-0.0359, 0.0275)	1.00	0.80
Mean spheric corpuscular volume	Autism spectrum disorder	1172	-0.08 (-0.1749, 0.0118)	0.92	0.087
Multiple sclerosis	Lymphocyte count	70	-0.02 (-0.0346, -0.0002)	0.98	0.051
Lymphocyte count	Multiple sclerosis	790	0.71 (0.4183, 1.0041)	2.04	2.31×10^{-6}
Multiple sclerosis	Plateletcrit	70	0.00 (-0.0180, 0.0087)	1.00	0.50
Plateletcrit	Multiple sclerosis	1003	0.13 (-0.0234, 0.2895)	1.14	0.096

Multiple sclerosis	White blood cell count	70	0.00 (-0.0115, 0.0215)	1.00	0.56
White blood cell count	Multiple sclerosis	802	0.13 (-0.1263, 0.3828)	1.14	0.32
Parkinson's disease	Platelet distribution width	95	-0.02 (-0.0320, -0.0018)	0.98	0.020
Platelet distribution width	Parkinson's disease	804	0.14 (0.0641, 0.2250)	1.16	1.87×10^{-4}
Stroke**	Plateletcrit	44	0.01 (-0.0310, 0.0523)	1.01	0.64
Plateletcrit	Stroke	1067	0.08 (0.0045, 0.1646)	1.09	0.049

*Positive GCP suggests the causal effect of NPD on BCT, and *vice versa*. **MR models utilised instrumental SNPs with $p < 1\times10^{-5}$. BCT: blood cell trait. NPD: neurological and psychiatric disorder. OR: odds ratio. SNP: single nucleotide polymorphism. MR: Mendelian randomisation. LCV: latent causal variable model. GSMR: generalised summary-data-based Mendelian randomisation. IVW: inverse variance weighting. GCP: genetic causal proportion. se: standard error.

Table S28. Phenotypic correlations between LYMPH# and MS, PCT and stroke, and PDW and PD in the UK Biobank, related to Figure 3 and STAR Methods.

Neurological and psychiatric disorder UK Biobank code (field code)		Trait Pair		
		LYMPH# - MS	PCT - Stroke	PDW - PD
		MS (41270 [G35])	Stroke (42007+42009+41270 [I64]; exclude self-report only)	PD (41270 [G20])
Full sample	Sample size (MS/Stroke/PD cases)	347898 (1238)	347898 (5288)	347898 (1323)
	Correlation	-0.0010	0.0042	0.0057
	p-value	0.55	0.014	8.44×10^{-4}
proportion of cases at 1%	Sample size (MS/Stroke/PD cases)	123800 (1238)	-	132300 (1323)
	Correlation	-0.0016	-	0.0055
	p-value	0.57	-	0.071
proportion of cases at 2%	Sample size (MS/Stroke/PD cases)	61900 (1238)	-	66150 (1323)
	Correlation	-0.0025	-	0.0077
	p-value	0.54	-	0.051
proportion of cases at 5%	Sample size (MS/Stroke/PD cases)	24760 (1238)	105760 (5288)	26460 (1323)
	Correlation	-0.0021	0.0131	0.0123
	p-value	0.75	2.86×10^{-5}	0.049
proportion of cases at 10%	Sample size (MS/Stroke/PD cases)	-	52880 (5288)	-
	Correlation	-	0.0097	-
	p-value	-	0.029	-

Controls randomly selected from the 'control' individuals (matched by age [+/- 2 year] and sex per case) to match the proportion of cases (i.e., 1%, 2%, 5% and 10%). More details are provided in the Supplementary Note. LYMPH#: lymphocyte count. MS: multiple sclerosis. PCT: plateletcrit. PDW: platelet distribution width. PD: Parkinson's disease.

Table S29. Summary of intercept term tests (in MR-Egger regression) and heterogeneity analyses (in IVW and MR-Egger regression), related to Figure 3 and STAR Methods.

MR-Egger Intercept test				
Exposure	Outcome	Intercept	Intercept se	*p*-value
Plateletcrit	Stroke	-0.0018	0.0008	0.035
Stroke	Plateletcrit	-0.0069	0.0142	0.63
Platelet distribution width	Parkinson's disease	-0.0017	0.0011	0.12
Parkinson's disease	Platelet distribution width	0.0018	0.0016	0.27
Heterogeneity analysis (IVW)				
Exposure	Outcome	Cochran's *Q*	Cochran's I^2	Cochran's *Q* *p*-value
Plateletcrit	Stroke	1550.99	0.31	1.15×10^{-20}
Stroke	Plateletcrit	3292.04	0.99	0.00
Platelet distribution width	Parkinson's disease	1542.76	0.48	3.58×10^{-49}
Parkinson's disease	Platelet distribution width	607.26	0.85	4.51×10^{-76}
Heterogeneity analysis (IVW, removal of pleiotropic SNPs identified by GSMR)				
Exposure	Outcome	Cochran's *Q*	Cochran's I^2	Cochran's *Q* *p*-value
Plateletcrit	Stroke	855.88	0.00	1
Stroke	Plateletcrit	39.52	0.22	0.14
Platelet distribution width	Parkinson's disease	732.97	0.03	0.29
Parkinson's disease	Platelet distribution width	109.41	0.27	0.016
Heterogeneity analysis (MR-Egger)				
Exposure	Outcome	Cochran's *Q*	Cochran's I^2	Cochran's *Q* *p*-value
Plateletcrit	Stroke	1544.56	0.31	2.62×10^{-20}
Stroke	Plateletcrit	3273.92	0.99	0
Platelet distribution width	Parkinson's disease	1538.18	0.48	7.76×10^{-49}
Parkinson's disease	Platelet distribution width	599.43	0.84	4.88×10^{-75}
Heterogeneity analysis (MR-Egger, removal of pleiotropic SNPs identified by GSMR)				
Exposure	Outcome	Cochran's *Q*	Cochran's I^2	Cochran's *Q* *p*-value
Plateletcrit	Stroke	854.92	0.00	1
Stroke	Plateletcrit	38.19	0.21	0.15
Platelet distribution width	Parkinson's disease	728.55	0.02	0.32
Parkinson's disease	Platelet distribution width	106.18	0.26	0.022
Estimated causal effects using IVW after the removal of pleiotropic SNPs identified by GSMR				
Exposure	Outcome	Beta	Beta se	*p*-value
Plateletcrit	Stroke	0.0687	0.0150	4.38×10^{-6}
Stroke	Plateletcrit	0.0167	0.0092	0.069

Platelet distribution width	Parkinson's disease	0.0455	0.0161	4.85×10^{-3}
Parkinson's disease	Platelet distribution width	-0.0065	0.0037	0.083
Estimated causal effects using MR-Egger after the removal of pleiotropic SNPs identified by GSMR				
Exposure	Outcome	Beta	Beta se	*p*-value
Plateletcrit	Stroke	0.0951	0.0308	2.06×10^{-3}
Stroke	Plateletcrit	-0.0179	0.0352	0.61
Platelet distribution width	Parkinson's disease	0.0956	0.0290	1.03×10^{-3}
Parkinson's disease	Platelet distribution width	-0.0198	0.0094	0.038
Estimated causal effects using Weighted Median after the removal of pleiotropic SNPs identified by GSMR				
Exposure	Outcome	Beta	Beta se	*p*-value
Plateletcrit	Stroke	0.0788	0.0260	2.42×10^{-3}
Stroke	Plateletcrit	0.0177	0.0117	0.13
Platelet distribution width	Parkinson's disease	0.0729	0.0296	0.014
Parkinson's disease	Platelet distribution width	-0.0156	0.0050	1.91×10^{-3}
Estimated causal effects using Weighted Mode after the removal of pleiotropic SNPs identified by GSMR				
Exposure	Outcome	Beta	Beta se	*p*-value
Plateletcrit	Stroke	0.0865	0.0423	0.041
Stroke	Plateletcrit	-0.0071	0.0266	0.79
Platelet distribution width	Parkinson's disease	0.1382	0.0384	3.47×10^{-4}
Parkinson's disease	Platelet distribution width	-0.0209	0.0084	0.014

MR: Mendelian randomisation. IVW: inverse variance weighting. SNP: single nucleotide polymorphism. GSMR: generalised summary-data-based Mendelian randomisation. se: standard error.

Table S30. Summary of the leave-one-out analysis for the causal effect of PD on PDW, related to Figure 3 and STAR Methods.

Exposure	Outcome	SNP	IVW			MR-Egger			Weighted Median			Weighted Mode		
			Beta	Beta se	*p*-value	Beta	Beta se	*p*-value	Beta	Beta se	*p*-value	Beta	Beta se	*p*-value
PD	PDW	rs10134885	0.0023	0.0075	0.76	-0.0165	0.0180	0.36	-0.0071	0.0052	0.17	-0.0168	0.0077	0.03
		rs10495249	0.0030	0.0075	0.69	-0.0160	0.0178	0.37	-0.0070	0.0052	0.18	-0.0183	0.0077	0.02
		rs10502915	0.0018	0.0075	0.81	-0.0161	0.0181	0.38	-0.0083	0.0051	0.11	-0.0172	0.0080	0.03
		rs10513789	0.0011	0.0076	0.88	-0.0185	0.0183	0.31	-0.0132	0.0049	7.03×10^{-3}	-0.0171	0.0074	0.02
		rs10516850	0.0023	0.0076	0.76	-0.0153	0.0185	0.41	-0.0065	0.0052	0.21	-0.0169	0.0083	0.04
		rs10810834	0.0021	0.0076	0.78	-0.0160	0.0180	0.38	-0.0069	0.0050	0.17	-0.0169	0.0083	0.05
		rs10878247	0.0013	0.0075	0.86	-0.0161	0.0180	0.37	-0.0096	0.0051	0.06	-0.0171	0.0074	0.02
		rs10913578	0.0004	0.0073	0.95	-0.0138	0.0175	0.43	-0.0079	0.0051	0.12	-0.0171	0.0080	0.03
		rs11060180	0.0009	0.0076	0.90	-0.0173	0.0180	0.34	-0.0127	0.0052	0.01	-0.0171	0.0079	0.03
		rs11150601	0.0026	0.0076	0.73	-0.0157	0.0180	0.38	-0.0067	0.0052	0.19	-0.0168	0.0079	0.04
		rs11174631	0.0019	0.0076	0.80	-0.0163	0.0183	0.38	-0.0106	0.0051	0.04	-0.0172	0.0082	0.04
		rs11175655	0.0024	0.0076	0.75	-0.0152	0.0181	0.40	-0.0068	0.0050	0.17	-0.0169	0.0085	0.05
		rs11683001	0.0021	0.0075	0.78	-0.0164	0.0180	0.37	-0.0070	0.0051	0.17	-0.0169	0.0079	0.03
		rs11726508	0.0017	0.0076	0.83	-0.0166	0.0181	0.36	-0.0106	0.0052	0.04	-0.0172	0.0080	0.03
		rs11950533	0.0021	0.0075	0.78	-0.0160	0.0180	0.38	-0.0071	0.0048	0.13	-0.0169	0.0077	0.03
		rs12147950	0.0015	0.0075	0.84	-0.0152	0.0181	0.40	-0.0081	0.0050	0.11	-0.0171	0.0078	0.03
		rs12287601	0.0020	0.0075	0.79	-0.0164	0.0181	0.37	-0.0070	0.0051	0.17	-0.0184	0.0076	0.02
		rs12497850	0.0015	0.0075	0.84	-0.0156	0.0180	0.39	-0.0083	0.0050	0.09	-0.0171	0.0082	0.04
		rs12503997	0.0016	0.0075	0.84	-0.0161	0.0180	0.37	-0.0085	0.0052	0.10	-0.0171	0.0079	0.03
		rs12505194	0.0016	0.0075	0.83	-0.0158	0.0181	0.38	-0.0088	0.0051	0.09	-0.0171	0.0079	0.03
		rs12505231	0.0023	0.0075	0.76	-0.0148	0.0181	0.41	-0.0071	0.0048	0.14	-0.0183	0.0080	0.02
		rs12726330	0.0016	0.0077	0.83	-0.0219	0.0202	0.28	-0.0149	0.0053	4.99×10^{-3}	-0.0203	0.0080	0.01
		rs1293298	-0.0015	0.0069	0.83	-0.0184	0.0164	0.27	-0.0081	0.0051	0.12	-0.0171	0.0082	0.04
		rs12942703	0.0019	0.0075	0.80	-0.0161	0.0180	0.37	-0.0083	0.0049	0.09	-0.0172	0.0078	0.03
		rs13078687	0.0021	0.0075	0.78	-0.0161	0.0180	0.37	-0.0072	0.0050	0.15	-0.0168	0.0084	0.05
		rs13294100	0.0021	0.0076	0.78	-0.0160	0.0180	0.38	-0.0068	0.0049	0.17	-0.0169	0.0081	0.04
		rs1441904	0.0021	0.0076	0.78	-0.0160	0.0180	0.38	-0.0068	0.0052	0.19	-0.0169	0.0083	0.05
		rs1450522	0.0017	0.0075	0.82	-0.0159	0.0181	0.38	-0.0084	0.0050	0.09	-0.0171	0.0079	0.03
		rs1461809	0.0017	0.0075	0.82	-0.0159	0.0181	0.38	-0.0083	0.0051	0.11	-0.0171	0.0079	0.03
		rs1530297	0.0017	0.0075	0.82	-0.0158	0.0181	0.39	-0.0081	0.0050	0.10	-0.0171	0.0077	0.03
		rs1624451	0.0022	0.0076	0.77	-0.0158	0.0181	0.39	-0.0066	0.0051	0.20	-0.0184	0.0081	0.02
		rs16857578	0.0015	0.0076	0.85	-0.0168	0.0181	0.36	-0.0099	0.0051	0.05	-0.0171	0.0083	0.04
		rs17015738	0.0020	0.0075	0.79	-0.0164	0.0181	0.37	-0.0070	0.0050	0.16	-0.0169	0.0078	0.03
		rs17201246	0.0015	0.0075	0.84	-0.0162	0.0180	0.37	-0.0084	0.0051	0.10	-0.0171	0.0074	0.02
		rs17698151	0.0029	0.0074	0.70	-0.0162	0.0177	0.36	-0.0073	0.0050	0.14	-0.0183	0.0078	0.02
		rs17810668	0.0021	0.0076	0.78	-0.0156	0.0182	0.39	-0.0069	0.0051	0.18	-0.0169	0.0081	0.04
		rs1801274	0.0024	0.0075	0.75	-0.0170	0.0180	0.35	-0.0070	0.0051	0.17	-0.0168	0.0081	0.04
		rs1866996	0.0016	0.0076	0.83	-0.0174	0.0182	0.34	-0.0096	0.0050	0.06	-0.0172	0.0080	0.03
		rs199449	0.0035	0.0077	0.65	-0.0120	0.0192	0.53	-0.0058	0.0051	0.25	-0.0138	0.0090	0.13
		rs2243453	0.0016	0.0076	0.84	-0.0167	0.0181	0.36	-0.0107	0.0051	0.04	-0.0172	0.0072	0.02
		rs2245801	0.0030	0.0077	0.69	-0.0135	0.0189	0.48	-0.0061	0.0053	0.26	-0.0153	0.0087	0.08
		rs2269905	0.0020	0.0075	0.79	-0.0165	0.0181	0.36	-0.0071	0.0052	0.17	-0.0169	0.0078	0.03

		rs2280104	0.0020	0.0075	0.79	-0.0167	0.0181	0.36	-0.0071	0.0050	0.16	-0.0169	0.0076	0.03
		rs2295545	0.0022	0.0075	0.77	-0.0169	0.0180	0.35	-0.0071	0.0050	0.16	-0.0168	0.0086	0.05
		rs2320431	0.0019	0.0075	0.81	-0.0161	0.0180	0.37	-0.0084	0.0052	0.10	-0.0172	0.0081	0.04
		rs26434	0.0013	0.0075	0.86	-0.0151	0.0180	0.40	-0.0081	0.0050	0.11	-0.0171	0.0078	0.03
		rs2835763	0.0033	0.0074	0.65	-0.0174	0.0175	0.32	-0.0072	0.0048	0.13	-0.0183	0.0082	0.03
		rs298616	0.0016	0.0075	0.83	-0.0156	0.0181	0.39	-0.0081	0.0049	0.10	-0.0171	0.0077	0.03
		rs3104767	0.0024	0.0075	0.75	-0.0169	0.0180	0.35	-0.0070	0.0050	0.16	-0.0168	0.0083	0.05
		rs34869253	0.0022	0.0075	0.77	-0.0169	0.0180	0.35	-0.0071	0.0051	0.16	-0.0168	0.0082	0.04
		rs35643925	0.0019	0.0076	0.81	-0.0175	0.0187	0.35	-0.0129	0.0049	8.49×10^{-3}	-0.0188	0.0077	0.02
		rs35902694	0.0020	0.0075	0.79	-0.0166	0.0181	0.36	-0.0071	0.0048	0.14	-0.0169	0.0080	0.04
		rs3744434	0.0019	0.0075	0.80	-0.0161	0.0180	0.37	-0.0084	0.0049	0.09	-0.0184	0.0086	0.04
		rs3768408	0.0024	0.0075	0.74	-0.0161	0.0179	0.37	-0.0072	0.0049	0.14	-0.0183	0.0076	0.02
		rs3802920	0.0019	0.0076	0.81	-0.0161	0.0181	0.37	-0.0113	0.0051	0.03	-0.0172	0.0080	0.03
		rs3857047	0.0019	0.0076	0.80	-0.0161	0.0181	0.38	-0.0097	0.0051	0.05	-0.0172	0.0078	0.03
		rs4122861	0.0023	0.0076	0.76	-0.0151	0.0186	0.42	-0.0066	0.0050	0.18	-0.0169	0.0080	0.04
		rs4130047	0.0020	0.0076	0.79	-0.0160	0.0181	0.38	-0.0117	0.0051	0.02	-0.0187	0.0083	0.03
		rs4690326	0.0021	0.0076	0.78	-0.0159	0.0182	0.38	-0.0133	0.0053	0.01	-0.0184	0.0089	0.04
		rs4698412	0.0024	0.0076	0.75	-0.0155	0.0181	0.39	-0.0065	0.0049	0.18	-0.0169	0.0081	0.04
		rs4771267	0.0017	0.0075	0.83	-0.0158	0.0181	0.38	-0.0081	0.0051	0.12	-0.0171	0.0078	0.03
		rs4785224	0.0021	0.0075	0.78	-0.0169	0.0181	0.35	-0.0071	0.0049	0.15	-0.0169	0.0079	0.04
		rs535283	0.0014	0.0075	0.85	-0.0161	0.0180	0.37	-0.0098	0.0051	0.05	-0.0171	0.0084	0.04
		rs544169	0.0020	0.0075	0.79	-0.0165	0.0181	0.36	-0.0071	0.0050	0.15	-0.0169	0.0078	0.03
		rs5910	-0.0019	0.0062	0.76	-0.0120	0.0149	0.42	-0.0078	0.0048	0.11	-0.0173	0.0077	0.03
		rs6076910	0.0021	0.0075	0.78	-0.0162	0.0180	0.37	-0.0072	0.0050	0.15	-0.0168	0.0077	0.03
		rs6676110	0.0017	0.0075	0.83	-0.0159	0.0181	0.38	-0.0083	0.0049	0.09	-0.0171	0.0080	0.03
		rs6734966	0.0019	0.0075	0.80	-0.0162	0.0180	0.37	-0.0074	0.0049	0.13	-0.0184	0.0079	0.02
		rs6803771	0.0009	0.0075	0.90	-0.0146	0.0179	0.42	-0.0081	0.0050	0.10	-0.0171	0.0083	0.04
		rs6812193	0.0016	0.0076	0.84	-0.0163	0.0180	0.37	-0.0115	0.0052	0.03	-0.0172	0.0081	0.04
		rs6828371	0.0022	0.0076	0.78	-0.0155	0.0182	0.40	-0.0069	0.0051	0.17	-0.0169	0.0077	0.03
		rs6857404	0.0022	0.0075	0.77	-0.0169	0.0180	0.35	-0.0071	0.0050	0.16	-0.0168	0.0084	0.05
		rs6963	0.0012	0.0075	0.87	-0.0151	0.0180	0.40	-0.0081	0.0050	0.11	-0.0171	0.0080	0.04
		rs7075684	0.0019	0.0075	0.80	-0.0163	0.0181	0.37	-0.0082	0.0051	0.10	-0.0172	0.0078	0.03
		rs721579	0.0015	0.0075	0.85	-0.0160	0.0180	0.38	-0.0093	0.0049	0.06	-0.0171	0.0079	0.03
		rs7562413	0.0018	0.0075	0.81	-0.0161	0.0181	0.38	-0.0081	0.0051	0.11	-0.0172	0.0079	0.03
		rs7749147	0.0016	0.0075	0.83	-0.0161	0.0180	0.37	-0.0081	0.0050	0.10	-0.0171	0.0079	0.03
		rs7938782	0.0018	0.0075	0.82	-0.0161	0.0180	0.37	-0.0083	0.0051	0.10	-0.0172	0.0077	0.03
		rs7991335	0.0016	0.0075	0.83	-0.0157	0.0181	0.39	-0.0081	0.0049	0.10	-0.0171	0.0078	0.03
		rs8012377	0.0019	0.0075	0.80	-0.0165	0.0181	0.37	-0.0083	0.0050	0.10	-0.0184	0.0081	0.03
		rs8018800	0.0017	0.0076	0.83	-0.0161	0.0180	0.37	-0.0104	0.0049	0.03	-0.0172	0.0077	0.03
		rs8045689	0.0023	0.0075	0.76	-0.0170	0.0180	0.35	-0.0071	0.0050	0.16	-0.0168	0.0078	0.03
		rs823114	0.0028	0.0076	0.71	-0.0149	0.0180	0.41	-0.0065	0.0052	0.21	-0.0168	0.0077	0.03
		rs823136	0.0020	0.0075	0.79	-0.0158	0.0181	0.39	-0.0071	0.0052	0.17	-0.0169	0.0080	0.04
		rs8327	0.0016	0.0076	0.83	-0.0161	0.0180	0.37	-0.0096	0.0051	0.06	-0.0172	0.0076	0.03
		rs8946	0.0022	0.0075	0.77	-0.0164	0.0180	0.37	-0.0069	0.0048	0.15	-0.0169	0.0077	0.03
		rs896435	0.0016	0.0076	0.83	-0.0160	0.0180	0.38	-0.0093	0.0049	0.06	-0.0171	0.0075	0.03
		rs9217	0.0030	0.0074	0.68	-0.0197	0.0176	0.26	-0.0074	0.0050	0.14	-0.0167	0.0082	0.04

		rs9295746	0.0017	0.0076	0.82	-0.0161	0.0180	0.38	-0.0090	0.0051	0.07	-0.0172	0.0076	0.03
		rs940634	0.0024	0.0075	0.75	-0.0159	0.0180	0.38	-0.0070	0.0050	0.16	-0.0183	0.0082	0.03
		rs9442714	0.0024	0.0075	0.75	-0.0169	0.0180	0.35	-0.0071	0.0049	0.15	-0.0183	0.0077	0.02
		rs970668	0.0013	0.0075	0.87	-0.0163	0.0179	0.37	-0.0080	0.0048	0.10	-0.0171	0.0084	0.04
		rs976080	0.0014	0.0076	0.85	-0.0175	0.0181	0.34	-0.0106	0.0050	0.03	-0.0171	0.0079	0.03
		rs979812	0.0014	0.0075	0.85	-0.0154	0.0181	0.40	-0.0085	0.0049	0.08	-0.0171	0.0083	0.04
		rs9917256	0.0028	0.0076	0.71	-0.0137	0.0183	0.45	-0.0065	0.0050	0.19	-0.0168	0.0076	0.03
		All	0.0019	0.0075	0.80	-0.0161	0.0180	0.37	-0.0076	0.0049	0.12	-0.0169	0.0071	0.02

PDW: platelet distribution width. PD: Parkinson's disease. IVW: inverse variance weighting. SNP: single nucleotide polymorphism. se: standard error.

Table S32. Summary of the leave-one-out analysis for the causal effect of stroke on PCT, related to Figure 3 and STAR Methods.

Exposure	Outcome	SNP	IVW			MR-Egger			Weighted Median			Weighted Mode		
			Beta	Beta se	*p*-value	Beta	Beta se	*p*-value	Beta	Beta se	*p*-value	Beta	Beta se	*p*-value
Stroke	PCT	rs1052053	0.0879	0.0613	0.15	0.2372	0.2630	0.37	0.0125	0.0123	0.31	0.0080	0.0183	0.66
		rs10778417	0.0789	0.0608	0.19	0.2034	0.2644	0.45	0.0022	0.0125	0.86	0.0089	0.0203	0.66
		rs11105439	0.0802	0.0610	0.19	0.1985	0.2603	0.45	0.0010	0.0126	0.94	0.0112	0.0203	0.59
		rs11952498	0.0792	0.0609	0.19	0.2007	0.2632	0.45	0.0018	0.0126	0.89	0.0088	0.0199	0.66
		rs12361415	0.0828	0.0607	0.17	0.1879	0.2610	0.48	0.0078	0.0121	0.52	0.0080	0.0209	0.70
		rs12445022	0.0802	0.0610	0.19	0.1986	0.2603	0.45	0.0006	0.0122	0.96	0.0088	0.0224	0.70
		rs12562305	0.0813	0.0609	0.18	0.2252	0.2676	0.40	0.0093	0.0126	0.46	0.0128	0.0220	0.56
		rs12635936	0.0813	0.0608	0.18	0.2305	0.2696	0.40	0.0088	0.0120	0.46	0.0128	0.0219	0.56
		rs1471859	0.0798	0.0608	0.19	0.1980	0.2634	0.46	0.0018	0.0128	0.89	0.0088	0.0214	0.68
		rs1537375	0.0839	0.0610	0.17	0.1961	0.2597	0.45	0.0101	0.0122	0.41	0.0080	0.0203	0.69
		rs1563788	0.0871	0.0600	0.15	0.1705	0.2588	0.51	0.0061	0.0120	0.61	0.0078	0.0210	0.71
		rs17021459	0.0798	0.0610	0.19	0.2618	0.3031	0.39	0.0009	0.0124	0.94	0.0040	0.0218	0.86
		rs17260983	0.0820	0.0611	0.18	0.2233	0.2665	0.41	0.0110	0.0123	0.37	0.0208	0.0217	0.34
		rs1939214	0.0811	0.0608	0.18	0.2021	0.2602	0.44	0.0090	0.0129	0.49	0.0128	0.0219	0.56
		rs2284665	0.0810	0.0610	0.18	0.2039	0.2608	0.44	0.0104	0.0125	0.41	0.0208	0.0207	0.32
		rs2526619	0.0804	0.0612	0.19	0.2195	0.2698	0.42	-0.0002	0.0124	0.99	0.0040	0.0229	0.86
		rs2585193	0.0806	0.0610	0.19	0.1975	0.2604	0.45	0.0098	0.0125	0.43	0.0160	0.0219	0.47
		rs2723334	0.0832	0.0616	0.18	0.2434	0.2742	0.38	0.0141	0.0130	0.28	0.0256	0.0229	0.27
		rs2742313	0.0886	0.0601	0.14	0.1776	0.2577	0.49	0.0065	0.0122	0.60	0.0080	0.0209	0.70
		rs3176326	0.0779	0.0609	0.20	0.1990	0.2603	0.45	0.0023	0.0119	0.85	0.0137	0.0220	0.54
		rs3790604	0.0784	0.0609	0.20	0.2009	0.2651	0.45	0.0022	0.0119	0.85	0.0089	0.0205	0.67
		rs4132234	0.0796	0.0610	0.19	0.1990	0.2603	0.45	0.0009	0.0125	0.94	0.0040	0.0220	0.86
		rs42039	0.0736	0.0609	0.23	0.1934	0.2596	0.46	0.0033	0.0125	0.79	0.0137	0.0216	0.53
		rs4783296	0.0791	0.0610	0.19	0.1994	0.2603	0.45	0.0013	0.0119	0.92	0.0088	0.0199	0.66
		rs4793588	0.0785	0.0609	0.20	0.1995	0.2603	0.45	0.0021	0.0124	0.87	0.0089	0.0211	0.68
		rs4886564	0.0805	0.0609	0.19	0.2060	0.2616	0.44	0.0092	0.0125	0.46	0.0160	0.0207	0.45
		rs4903725	0.0791	0.0608	0.19	0.1999	0.2605	0.45	0.0022	0.0123	0.86	0.0088	0.0212	0.68
		rs4950915	0.0801	0.0608	0.19	0.1964	0.2634	0.46	0.0054	0.0127	0.67	0.0112	0.0208	0.59
		rs495828	0.0744	0.0607	0.22	0.2011	0.2594	0.44	0.0039	0.0130	0.76	0.0137	0.0209	0.51
		rs564018	0.0797	0.0611	0.19	0.2086	0.2653	0.44	0.0004	0.0123	0.97	0.0040	0.0230	0.86
		rs653178	0.0036	0.0220	0.87	0.0062	0.0938	0.95	0.0051	0.0122	0.68	0.0104	0.0210	0.62
		rs6544653	0.0709	0.0603	0.24	0.2300	0.2588	0.38	0.0046	0.0125	0.72	0.0137	0.0218	0.53
		rs6561321	0.0789	0.0612	0.20	0.2007	0.2619	0.45	-0.0001	0.0128	0.99	0.0089	0.0209	0.67
		rs6584579	0.0770	0.0610	0.21	0.2030	0.2606	0.44	0.0020	0.0125	0.87	0.0137	0.0193	0.48
		rs6596445	0.0789	0.0609	0.19	0.1994	0.2604	0.45	0.0019	0.0117	0.87	0.0089	0.0219	0.69
		rs6825454	0.0828	0.0609	0.17	0.1997	0.2597	0.45	0.0093	0.0121	0.44	0.0080	0.0217	0.71
		rs6838973	0.0828	0.0607	0.17	0.1821	0.2632	0.49	0.0079	0.0121	0.52	0.0080	0.0227	0.73
		rs6872625	0.0807	0.0608	0.18	0.1977	0.2603	0.45	0.0091	0.0123	0.46	0.0160	0.0208	0.45
		rs7488386	0.0792	0.0608	0.19	0.2016	0.2644	0.45	0.0021	0.0126	0.87	0.0088	0.0195	0.65
		rs8064211	0.0812	0.0609	0.18	0.1929	0.2621	0.47	0.0093	0.0124	0.46	0.0176	0.0204	0.39
		rs879324	0.0816	0.0608	0.18	0.2019	0.2600	0.44	0.0087	0.0119	0.46	0.0128	0.0214	0.55
		rs880315	0.0871	0.0606	0.15	0.1953	0.2582	0.45	0.0077	0.0124	0.53	0.0080	0.0214	0.71

		rs9112	0.0788	0.0610	0.20	0.2008	0.2615	0.45	0.0015	0.0123	0.90	0.0089	0.0199	0.66
		rs9305020	0.0809	0.0608	0.18	0.2010	0.2602	0.44	0.0091	0.0125	0.47	0.0160	0.0214	0.46
		All	0.0788	0.0596	0.19	0.1993	0.2572	0.44	0.0052	0.0128	0.68	0.0107	0.0224	0.64

PCT: plateletcrit. IVW: inverse variance weighting. SNP: single nucleotide polymorphism. se: standard error.

Table S35. Summary of MVMR sensitivity analyses adjusting for smoking, drinking, educational attainment and household income concurrently, related to Figure 3 and STAR Methods.

Exposure	Outcome	n of SNPs	OR (95% CI)	*p*-value
Parkinson's disease	Platelet distribution width	87	1.00 (0.98, 1.02)	0.97
Platelet distribution width	Parkinson's disease	798	1.05 (1.01, 1.10)	0.011
Stroke*	Plateletcrit	40	1.12 (0.98, 1.27)	0.093
Plateletcrit	Stroke	1027	1.09 (1.05, 1.13)	3.79×10^{-7}

*MR models utilised instrumental SNPs with stroke GWAS $p < 1\times10^{-5}$. MVMR: multivariate Mendelian randomisation. SNP: single nucleotide polymorphism. OR: odds ratio. CI: confidence interval.

Table S37. FDR-significant (FDR < 0.05) SMR associations between platelet-based gene expression and BCT-NPD trait pairs with evidence for a putative causal relationship, related to Figure 4 and STAR Methods.

Gene	*RHD*		*FXYD5*		*MAP1LC3A*		*SRSF6*	
Probe ID	ENSG00000187010		ENSG00000089327		ENSG00000101460		ENSG00000124193	
Chromosome	1		19		20		20	
Probe position (hg19)	24579435		34629498		32139351		41087450	
top SNP	rs72660908		rs1633915		rs2295444		rs3746532	
Top SNP chromosome	1		19		20		20	
Top SNP position (hg19)	25583610		35649324		33173883		42099331	
effect allele	G		C		T		C	
non-effect allele	C		G		C		A	
effect allele frequency	0.38		0.21		0.49		0.27	
Trait	PD	PDW	PD	PDW	PD	PDW	PD	PDW
Beta (GWAS)	0.05	0.02	-0.04	-0.04	0.03	0.01	-0.04	0.01
Beta se (GWAS)	0.01	0.00	0.01	0.00	0.01	0.00	0.01	0.00
p-value (GWAS)	1.34×10^{-4}	1.30×10^{-27}	5.12×10^{-4}	1.70×10^{-48}	6.05×10^{-4}	8.90×10^{-4}	8.71×10^{-4}	5.60×10^{-3}
Beta (*cis*-eQTL)	0.54	0.54	-0.35	-0.35	-0.19	-0.19	-0.31	-0.31
Beta se (*cis*-eQTL)	0.05	0.05	0.04	0.04	0.02	0.02	0.03	0.03
p-value (*cis*-eQTL)	4.53×10^{-28}	4.53×10^{-28}	1.73×10^{-15}	1.73×10^{-15}	1.63×10^{-15}	1.63×10^{-15}	1.09×10^{-27}	1.09×10^{-27}
Beta (SMR)	0.09	0.04	0.12	0.12	-0.17	-0.04	0.13	-0.02
Beta se (SMR)	0.02	0.01	0.04	0.02	0.05	0.01	0.04	0.01
p-value (SMR)	3.17×10^{-4}	1.06×10^{-14}	1.46×10^{-3}	2.71×10^{-12}	1.58×10^{-3}	2.16×10^{-3}	1.45×10^{-3}	7.28×10^{-3}
FDR (SMR)	0.015	1.05×10^{-12}	0.047	$1.79\text{E}\times10^{-10}$	0.049	0.011	0.047	0.029
p-value (HEIDI)	0.11	0.057	0.078	0.15	0.17	0.062	0.43	0.12
n of SNPs after HEIDI	18	20	10	15	20	20	20	20

BCT: blood cell trait. NPD: neurological and psychiatric disorder. PD: Parkinson's disease. PDW: platelet distribution width. SNP: single nucleotide polymorphism. se: standard error. GWAS: genome-wide association study. *cis*-eQTL: *cis*-expression quantitative trait loci. SMR: Summary-data-based Mendelian randomisation. HEIDI: HEterogeneity In Dependent Instruments. FDR: Benjamini-Hochberg false discovery rate.

Table S38. FDR-significant (FDR < 0.05) SMR associations between brain-based gene expression and Parkinson's disease or stroke (for genes presented in Tables S36-37), related to Figure 4 and STAR Methods.

Gene	*RHD*	*DNAJB4*	*UBXN2A*	*SFXN5*	*GGCX*	*COA5*	*ARL8B*
probe ID	ENSG00000187010	ENSG00000162616	ENSG00000173960	ENSG00000144040	ENSG00000115486	ENSG00000183513	ENSG00000134108
Chromosome	1	1	2	2	2	2	3
Probe position (hg19)	25627910	78464253	24188967	73235956	85781706	99220375	5193250
top SNP	rs72660908	rs7514180	rs12621152	rs73945731	rs6714157	rs72823796	rs6787725
Top SNP chromosome	1	1	2	2	2	2	3
Top SNP position (hg19)	25583610	78460935	24257682	73252335	85763274	99227812	5201054
effect allele	G	G	C	C	G	T	G
non-effect allele	C	A	T	T	A	C	A
effect allele frequency	0.39	0.79	0.83	0.94	0.50	0.27	0.67
Trait	Parkinson's disease	Parkinson's disease	Parkinson's disease	Parkinson's disease	Parkinson's disease	Parkinson's disease	Parkinson's disease
Beta (GWAS)	0.05	-0.05	0.05	0.06	-0.03	0.03	-0.04
Beta se (GWAS)	0.01	0.01	0.01	0.02	0.01	0.01	0.01
p-value (GWAS)	1.34×10^{-4}	8.08×10^{-5}	2.15×10^{-4}	1.79×10^{-3}	2.32×10^{-3}	2.32×10^{-3}	5.75×10^{-4}
Beta (*cis*-eQTL)	-0.93	-0.45	0.30	0.69	0.43	0.45	1.14
Beta se (*cis*-eQTL)	0.08	0.06	0.05	0.08	0.04	0.05	0.03
p-value (*cis*-eQTL)	8.48×10^{-28}	4.39×10^{-14}	2.11×10^{-9}	1.66×10^{-19}	1.88×10^{-29}	1.09×10^{-18}	2.09×10^{-291}
Beta (SMR)	-0.05	0.10	0.17	0.09	-0.07	0.07	-0.03
Beta se (SMR)	0.01	0.03	0.06	0.03	0.02	0.02	0.01
p-value (SMR)	3.20×10^{-4}	4.87×10^{-4}	1.66×10^{-3}	3.13×10^{-3}	3.31×10^{-3}	3.97×10^{-3}	6.14×10^{-4}
FDR (SMR)	6.57×10^{-3}	6.57×10^{-3}	9.98×10^{-3}	0.012	0.012	0.013	6.64×10^{-3}
p-value (HEIDI)	0.18	0.28	0.037	0.19	0.71	0.21	0.073
n of SNPs after HEIDI	16	20	20	10	20	19	20
Gene	*PPM1M*	*GLYCTK*	*PTK2*	*TSPAN4*	*PLA2G4B*	*RANBP10*	*SOX15*
probe ID	ENSG00000164088	ENSG00000168237	ENSG00000169398	ENSG00000214063	ENSG00000243708	ENSG00000141084	ENSG00000129194
Chromosome	3	3	8	11	15	16	17
Probe position (hg19)	52282227	52325188	141840157	854962	42135159	67798780	7492902
top SNP	rs353547	rs7622851	rs7815898	rs9704919	rs28708888	rs9938862	rs12938899
Top SNP chromosome	3	3	8	11	15	16	17
Top SNP position (hg19)	52268866	52333671	141876541	842682	41898885	67723801	7525546
effect allele	C	C	G	G	C	C	C
non-effect allele	T	G	C	A	A	T	T
effect allele frequency	0.58	0.48	0.43	0.67	0.38	0.04	0.82
Trait	Parkinson's disease	Parkinson's disease	Parkinson's disease	Parkinson's disease	Parkinson's disease	Parkinson's disease	Parkinson's disease
Beta (GWAS)	-0.03	-0.04	0.04	0.03	0.04	0.06	-0.04
Beta se (GWAS)	0.01	0.01	0.01	0.01	0.01	0.02	0.01
p-value (GWAS)	8.62×10^{-4}	6.92×10^{-5}	2.71×10^{-4}	1.40×10^{-3}	3.78×10^{-4}	2.34×10^{-3}	9.08×10^{-4}
Beta (*cis*-eQTL)	0.47	0.28	-0.37	-0.42	0.97	-0.84	0.38
Beta se (*cis*-eQTL)	0.04	0.05	0.05	0.05	0.03	0.11	0.06
p-value (*cis*-eQTL)	1.37×10^{-36}	5.57×10^{-9}	4.14×10^{-15}	2.73×10^{-17}	5.79×10^{-261}	1.41×10^{-15}	2.55×10^{-10}
Beta (SMR)	-0.07	-0.13	-0.10	-0.08	0.04	-0.08	-0.10
Beta se (SMR)	0.02	0.04	0.03	0.03	0.01	0.03	0.04

p-value (SMR)	1.32×10^{-3}	1.02×10^{-3}	9.26×10^{-4}	2.83×10^{-3}	3.92×10^{-4}	4.46×10^{-3}	3.42×10^{-3}
FDR (SMR)	8.94×10^{-3}	7.83×10^{-3}	7.83×10^{-3}	0.012	6.57×10^{-3}	0.013	0.012
p-value (HEIDI)	0.08	0.032	0.96	0.44	0.15	0.69	0.25
n of SNPs after HEIDI	20	20	20	20	20	20	20
Gene	*PDCD5*	*FXYD5*	*MGAT3*	*CLBA1*	*IVD*	*RMC1*	
probe ID	ENSG00000105185	ENSG00000089327	ENSG00000128268	ENSG00000140104	ENSG00000128928	ENSG00000141452	
Chromosome	19	19	22	14	15	18	
Probe position (hg19)	33075166	35653209	39870774	105464465	40712916	21097609	
top SNP	rs8182578	rs9807816	rs5750828	rs2033932	rs7165012	rs1618725	
Top SNP chromosome	19	19	22	14	15	18	
Top SNP position (hg19)	33056477	35684944	39835083	105447075	40654038	21126952	
effect allele	A	G	C	C	G	T	
non-effect allele	G	T	T	T	A	C	
effect allele frequency	0.40	0.79	0.70	0.79	0.53	0.47	
Trait	Parkinson's disease	Parkinson's disease	Parkinson's disease	Stroke	Stroke	Stroke	
Beta (GWAS)	-0.04	0.04	-0.03	-0.04	-0.03	-0.02	
Beta se (GWAS)	0.01	0.01	0.01	0.01	0.01	0.01	
p-value (GWAS)	4.73×10^{-5}	2.24×10^{-3}	3.83×10^{-3}	3.11×10^{-3}	2.59×10^{-3}	0.012	
Beta (*cis*-eQTL)	1.02	-0.42	0.33	-1.27	0.48	0.47	
Beta se (*cis*-eQTL)	0.03	0.06	0.05	0.03	0.04	0.04	
p-value (*cis*-eQTL)	1.03×10^{-288}	4.88×10^{-13}	4.45×10^{-11}	5.73×10^{-305}	6.18×10^{-40}	3.83×10^{-36}	
Beta (SMR)	-0.04	-0.09	-0.10	0.03	-0.06	-0.05	
Beta se (SMR)	0.01	0.03	0.04	0.01	0.02	0.02	
p-value (SMR)	5.06×10^{-5}	4.88×10^{-3}	8.22×10^{-3}	3.26×10^{-3}	3.44×10^{-3}	0.014	
FDR (SMR)	2.73×10^{-3}	0.014	0.019	0.012	0.012	0.031	
p-value (HEIDI)	0.94	0.65	0.11	0.75	0.13	0.68	
n of SNPs after HEIDI	20	11	18	20	20	20	

SNP: single nucleotide polymorphism. se: standard error. GWAS: genome-wide association study. *cis*-eQTL: *cis*-expression quantitative trait loci. SMR: Summary-data-based Mendelian randomisation. HEIDI: HEterogeneity In Dependent Instruments. FDR: Benjamini-Hochberg false discovery rate.

Table S45. Bonferroni-significant SMR associations between brain-based gene expression and specific NPDs shown in Tables S43-44, related to Figure 5 and STAR Methods.

Gene	*GNL3*	*AC100854.1*	*OGFOD2*	*GATAD2A*
probe ID	ENSG00000163938	ENSG00000254352	ENSG00000111325	ENSG00000167491
Chromosome	3	8	12	19
Listed table	S36	S35	S35 & S36	S35 & S36
Probe position (hg19)	52721840	79636201	123461858	19558189
top SNP	rs7646741	rs2717538	rs1727309	rs8101499
Top SNP chromosome	3	8	12	19
Top SNP position (hg19)	52785238	79633149	123658258	19476984
effect allele	A	A	G	A
non-effect allele	G	G	A	G
effect allele frequency	0.48	0.29	0.78	0.33
Trait	Schizophrenia	Multiple sclerosis	Schizophrenia	Schizophrenia
Beta (GWAS)	0.08	0.10	-0.07	0.07
Beta se (GWAS)	0.01	0.02	0.01	0.01
p-value (GWAS)	2.19×10^{-17}	1.46×10^{-8}	5.53×10^{-11}	4.57×10^{-15}
Beta (*cis*-eQTL)	0.58	-0.68	-0.38	-0.31
Beta se (*cis*-eQTL)	0.05	0.08	0.05	0.04
p-value (*cis*-eQTL)	1.70×10^{-36}	7.39×10^{-16}	4.11×10^{-13}	2.08×10^{-16}
Beta (SMR)	0.13	-0.15	0.19	-0.24
Beta se (SMR)	0.02	0.03	0.04	0.04
p-value (SMR)	2.11×10^{-12}	3.55×10^{-6}	1.10×10^{-6}	1.51×10^{-8}
p-value (HEIDI)	0.43	0.38	0.053	0.40
n of SNPs after HEIDI	20	16	20	20

NPD: neurological and psychiatric disorder. SNP: single nucleotide polymorphism. se: standard error. GWAS: genome-wide association study. *cis*-eQTL: *cis*-expression quantitative trait loci. SMR: Summary-data-based Mendelian randomisation. HEIDI: HEterogeneity In Dependent Instruments.

Table S46. Bonferroni-significant SMR associations between brain-based DNA methylation and gene expression for genes shown in Table S45, related to Figure 5 and STAR Methods.

Exp ID (mQTL)	cg14845053	cg02792780	cg07148594	cg16977858	cg17372223	cg05564831
Exp chromosome	3	3	3	3	3	3
Exp probe position (hg19)	52276132	52529341	52565909	52567510	52568218	52568323
Out ID (eQTL)	ENSG00000163938	ENSG00000163938	ENSG00000163938	ENSG00000163938	ENSG00000163938	ENSG00000163938
Out Chromosome	3	3	3	3	3	3
Out Gene	*GNL3*	*GNL3*	*GNL3*	*GNL3*	*GNL3*	*GNL3*
Out probe position (hg19)	52721840	52721840	52721840	52721840	52721840	52721840
Top SNP	rs610060	rs1570	rs4282054	rs7639267	rs12489828	rs12489828
Top SNP chromosome	3	3	3	3	3	3
Top SNP position (hg19)	52273421	52586682	52566065	52568805	52567014	52567014
effect allele	A	T	T	G	G	G
non-effect allele	G	A	C	T	T	T
effect allele frequency	0.48	0.57	0.44	0.43	0.45	0.45
Beta (*cis*-eQTL)	0.46	0.49	0.49	0.50	0.43	0.43
Beta se (*cis*-eQTL)	0.05	0.05	0.05	0.05	0.05	0.05
p-value (*cis*-eQTL)	7.02×10^{-22}	2.27×10^{-24}	7.77×10^{-25}	3.08×10^{-26}	5.48×10^{-19}	5.48×10^{-19}
Beta (mQTL)	0.40	0.36	0.59	0.37	-0.40	-0.51
Beta se (mQTL)	0.06	0.06	0.04	0.04	0.04	0.04
p-value (mQTL)	3.80×10^{-11}	7.14×10^{-9}	3.25×10^{-47}	4.05×10^{-17}	9.53×10^{-21}	2.18×10^{-35}
Beta (SMR)	1.14	1.34	0.83	1.38	-1.07	-0.83
Beta se (SMR)	0.21	0.27	0.10	0.21	0.17	0.11
p-value (SMR)	5.11×10^{-8}	4.85×10^{-7}	5.35×10^{-17}	4.45×10^{-11}	1.16×10^{-10}	4.68×10^{-13}
p-value (HEIDI)	0.12	0.26	0.019	0.091	0.040	0.019
n of SNPs after HEIDI	14	14	20	14	12	20
Exp ID (mQTL)	cg24629711	cg23815702	cg17117718	cg22694191	cg14449575	cg13364410
Exp chromosome	3	3	17	19	19	19
Exp probe position (hg19)	52869263	52869738	43663208	19373575	19373743	19373755
Out ID (eQTL)	ENSG00000163938	ENSG00000163938	ENSG00000264070	ENSG00000167491	ENSG00000167491	ENSG00000167491
Out Chromosome	3	3	17	19	19	19
Out Gene	*GNL3*	*GNL3*	*DND1P1*	*GATAD2A*	*GATAD2A*	*GATAD2A*
Out probe position (hg19)	52721840	52721840	43663766	19558189	19558189	19558189
Top SNP	rs2256332	rs6445541	rs1724390	rs10426780	rs2074295	rs2074295
Top SNP chromosome	3	3	17	19	19	19
Top SNP position (hg19)	52855865	52880128	43663247	19375883	19369435	19369435
effect allele	G	G	A	C	A	A
non-effect allele	A	T	C	T	G	G
effect allele frequency	0.61	0.60	0.24	0.32	0.79	0.79
Beta (*cis*-eQTL)	0.39	0.42	0.60	-0.29	0.27	0.27
Beta se (*cis*-eQTL)	0.05	0.05	0.11	0.04	0.04	0.04
p-value (*cis*-eQTL)	3.76×10^{-15}	2.86×10^{-17}	3.60×10^{-8}	1.00×10^{-14}	1.75×10^{-10}	1.75×10^{-10}
Beta (mQTL)	-0.57	-0.36	1.40	-0.31	0.50	0.44
Beta se (mQTL)	0.06	0.04	0.05	0.04	0.05	0.05

p-value (mQTL)	1.91×10^{-23}	1.90×10^{-16}	1.08×10^{-203}	2.76×10^{-12}	1.11×10^{-25}	4.47×10^{-20}
Beta (SMR)	-0.68	-1.15	0.43	0.94	0.54	0.61
Beta se (SMR)	0.11	0.20	0.08	0.18	0.10	0.12
p-value (SMR)	6.59×10^{-10}	3.73×10^{-9}	5.92×10^{-8}	2.14×10^{-7}	5.03×10^{-8}	1.61×10^{-7}
p-value (HEIDI)	0.079	0.11	0.046	0.031	0.028	0.14
n of SNPs after HEIDI	12	20	16	19	20	15
Exp ID (mQTL)	cg14021871	cg01262667	cg17414380	cg26162025	cg26732615	
Exp chromosome	19	19	19	19	19	
Exp probe position (hg19)	19384381	19385393	19431394	19616502	19648335	
Out ID (eQTL)	ENSG00000167491	ENSG00000167491	ENSG00000167491	ENSG00000167491	ENSG00000167491	
Out Chromosome	19	19	19	19	19	
Out Gene	*GATAD2A*	*GATAD2A*	*GATAD2A*	*GATAD2A*	*GATAD2A*	
Out probe position (hg19)	19558189	19558189	19558189	19558189	19558189	
Top SNP	rs2905425	rs2074303	rs7247309	rs4808198	rs4808208	
Top SNP chromosome	19	19	19	19	19	
Top SNP position (hg19)	19475717	19381755	19439631	19533630	19650096	
effect allele	G	T	A	C	G	
non-effect allele	C	C	T	T	A	
effect allele frequency	0.32	0.32	0.33	0.33	0.32	
Beta (*cis*-eQTL)	-0.30	-0.29	-0.29	-0.29	-0.28	
Beta se (*cis*-eQTL)	0.04	0.04	0.04	0.04	0.04	
p-value (*cis*-eQTL)	4.23×10^{-15}	2.00×10^{-14}	2.02×10^{-14}	8.08×10^{-15}	1.66×10^{-13}	
Beta (mQTL)	-0.56	1.16	0.42	0.70	0.74	
Beta se (mQTL)	0.06	0.03	0.04	0.06	0.04	
p-value (mQTL)	4.84×10^{-19}	0	3.51×10^{-22}	9.86×10^{-32}	3.90×10^{-81}	
Beta (SMR)	0.53	-0.25	-0.68	-0.42	-0.37	
Beta se (SMR)	0.09	0.03	0.11	0.06	0.05	
p-value (SMR)	3.84×10^{-9}	5.45×10^{-14}	1.94×10^{-9}	9.53×10^{-11}	6.07×10^{-12}	
p-value (HEIDI)	0.24	0.025	0.13	0.029	0.21	
n of SNPs after HEIDI	20	20	17	19	20	

SNP: single nucleotide polymorphism. se: standard error. GWAS: genome-wide association study. *cis*-eQTL: *cis*-expression quantitative trait loci. mQTL: DNA methylation quantitative trait loci. SMR: Summary-data-based Mendelian randomisation. HEIDI: HEterogeneity In Dependent Instruments.

Table S47. Bonferroni-significant SMR associations between brain-based DNA methylation (shown in Table S46) and specific NPDs (shown in Table S45), related to Figure 5 and STAR Methods.

probe ID	cg07148594	cg16977858	cg17372223	cg05564831	cg24629711	cg14449575	cg13364410	cg14021871	cg17414380	cg26162025	cg26732615
Chromosome	3	3	3	3	3	19	19	19	19	19	19
Probe position (hg19)	52565909	52567510	52568218	52568323	52869263	19373743	19373755	19384381	19431394	19616502	19648335
Top SNP chromosome	rs4282054	rs7639267	rs12489828	rs12489828	rs2256332	rs2074295	rs2074295	rs2905425	rs7247309	rs4808198	rs4808208
Top SNP chromosome	3	3	3	3	3	19	19	19	19	19	19
Top SNP position (hg19)	52566065	52568805	52567014	52567014	52855865	19369435	19369435	19475717	19439631	19533630	19650096
effect allele	T	G	G	G	G	A	A	G	A	C	G
non-effect allele	C	T	T	T	A	G	G	C	T	T	A
effect allele frequency	0.44	0.43	0.45	0.45	0.61	0.79	0.79	0.32	0.33	0.33	0.32
Trait	Schizophrenia	Schizophrenia	Schizophrenia	Schizophrenia	Schizophrenia	Schizophrenia	Schizophrenia	Schizophrenia	Schizophrenia	Schizophrenia	Schizophrenia
Beta (GWAS)	0.06	0.07	0.07	0.07	0.07	-0.06	-0.06	0.07	0.07	0.07	0.07
Beta se (GWAS)	0.01	0.01	0.01	0.01	0.01	0.01	0.01	0.01	0.01	0.01	0.01
p-value (GWAS)	3.94×10^{-13}	2.47×10^{-13}	2.51×10^{-13}	2.51×10^{-13}	4.53×10^{-16}	1.02×10^{-9}	1.02×10^{-9}	4.78×10^{-15}	1.47×10^{-13}	1.43×10^{-15}	2.36×10^{-14}
Beta (mQTL)	0.59	0.37	-0.40	-0.51	-0.57	0.50	0.44	-0.56	0.42	0.70	0.74
Beta se (mQTL)	0.04	0.04	0.04	0.04	0.06	0.05	0.05	0.06	0.04	0.06	0.04
p-value (mQTL)	3.25×10^{-47}	4.05×10^{-17}	9.53×10^{-21}	2.18×10^{-35}	1.91×10^{-23}	1.11×10^{-25}	4.47×10^{-20}	4.84×10^{-19}	3.51×10^{-22}	9.86×10^{-32}	3.90×10^{-81}
Beta (SMR)	0.11	0.18	-0.16	-0.13	-0.13	-0.13	-0.15	-0.13	0.16	0.11	0.10
Beta se (SMR)	0.02	0.03	0.03	0.02	0.02	0.02	0.03	0.02	0.03	0.02	0.01
p-value (SMR)	9.37×10^{-11}	3.49×10^{-8}	8.74×10^{-19}	3.08×10^{-10}	3.22×10^{-10}	1.21×10^{-7}	3.43×10^{-7}	4.37×10^{-9}	4.56×10^{-9}	4.78×10^{-11}	1.77×10^{-12}
p-value (HEIDI)	0.064	0.23	0.034	0.033	0.25	0.019	0.16	0.26	0.33	0.012	0.19
n of SNPs after HEIDI	20	14	12	20	12	20	15	20	17	19	20

NPD: neurological and psychiatric disorder. SNP: single nucleotide polymorphism. se: standard error. GWAS: genome-wide association study. mQTL: DNA methylation quantitative trait loci. SMR: Summary-data-based Mendelian randomisation. HEIDI: HEterogeneity In Dependent Instruments.

Table S48. Estimated correlations among significant brain-based DNA methylation probes shown in Table S47, related to Figure 5 and STAR Methods.

correlation	cg07148594	cg16977858	cg17372223	cg05564831	cg24629711	cg14449575	cg13364410	cg14021871	cg17414380	cg26162025	cg26732615
cg07148594	1.00	1.00	-0.96	-0.96	-0.85	-	-	-	-	-	-
cg16977858	1.00	1.00	-0.96	-0.96	-0.84	-	-	-	-	-	-
cg17372223	-0.96	-0.96	1.00	1.00	0.88	-	-	-	-	-	-
cg05564831	-0.96	-0.96	1.00	1.00	0.88	-	-	-	-	-	-
cg24629711	-0.85	-0.84	0.88	0.88	1.00	-	-	-	-	-	-
cg14449575	-	-	-	-	-	1.00	1.00	0.79	-0.81	-0.77	-0.82
cg13364410	-	-	-	-	-	1.00	1.00	0.80	-0.81	-0.77	-0.82
cg14021871	-	-	-	-	-	0.79	0.80	1.00	-0.98	-0.97	-0.97
cg17414380	-	-	-	-	-	-0.81	-0.81	-0.98	1.00	0.97	0.97
cg26162025	-	-	-	-	-	-0.77	-0.77	-0.97	0.97	1.00	0.99
cg26732615	-	-	-	-	-	-0.82	-0.82	-0.97	0.97	0.99	1.00

Table S49. Candidate gene lists for specific pairs of traits used in gene set enrichment analysis, related to Figure 5 and STAR Methods.	
Trait Pair	Gene list
Multiple sclerosis - Eosinophil count	*CD5 FCRL2 FCRL3 MYO19 PRXL2B ZNHIT3*
Multiple sclerosis - Lymphocyte count	*ABCB9 AC100854.1 BACH2 BANF1 GPR25 TNFSF14 ZMIZ1*
Multiple sclerosis - Neutrophil percentage of white cells	*ABCB9 AC100854.1 AHI1 BACH2 SCO2 ZC2HC1A ZMIZ1*
Multiple sclerosis - Red cell distribution width	*BANF1 GGNBP2 MAST3 MYO19 TYMP ZNHIT3*
Schizophrenia - Eosinophil count/Eosinophil percentage of white cells	*AC005829.1 AC091132.1 GATAD2A MAPK8IP1P1 MAPK8IP1P2*
Schizophrenia - Lymphocyte count	*ABCB9 AL360001.33 DDHD2 KANSL1-AS1 LRRC37A2 MAPK8IP1P1 RABEP1 WHSC1L1 ZNF664*
Schizophrenia - Lymphocyte percentage of white cells	*AC005829.1 AC091132.16 DDHD2 DND1P1 KANSL1-AS1 MAPK8IP1P1 MAPK8IP1P2 PPP2R3C*
Schizophrenia - Monocyte percentage of white cells	*AC005829.1 EP300 GATAD2A MAP1A STRCP1*
Schizophrenia - Neutrophil percentage of white cells	*ABCB9 AC005829.1 AC091132.16 MAPK3 MAPK8IP1P1 MAPK8IP1P2*
Schizophrenia - Reticulocyte count	*ABCB9 ARL6IP4 GATAD2A OGFOD2 ZNF664*
Schizophrenia - Reticulocyte fraction of red cells	*ABCB9 AC091132.1 AC091132.16 ARL6IP4 GATAD2A INO80E LRRC37A2 MAPK8IP1P1 MAPK8IP1P2 OGFOD2 ZNF664*

Table S50. Summary of significant pathways identified in the gene set enrichment analysis using ShinyGO, related to Figure 5 and STAR Methods.

Trait Pair	Pathway database	Pathway	Enrichment FDR	n of Genes	n of Pathway Genes	Enrichment Fold	Involved Genes
Schizophrenia - Monocyte percentage of white cells	GO: Molecular Function	Tau protein binding	4.68×10^{-4}	2	45	337.72	*EP300 MAP1A*
Schizophrenia - Reticulocyte fraction of red cells	GO: Cellular Component	SWI/SNF superfamily-type complex	5.87×10^{-3}	2	94	69.29	*GATAD2A INO80E*
Schizophrenia - Reticulocyte fraction of red cells	GO: Cellular Component	ATPase complex	5.87×10^{-3}	2	95	68.56	*GATAD2A INO80E*
Schizophrenia - Lymphocyte count	GO: Cellular Component	Centrosome	6.52×10^{-3}	2	658	34.64	*DDHD2 PPP2R3C*
Schizophrenia - Lymphocyte count	GO: Cellular Component	Microtubule organizing center	6.52×10^{-3}	2	868	26.26	*DDHD2 PPP2R3C*
Schizophrenia - Monocyte percentage of white cells	GO: Molecular Function	Protein-macromolecule adaptor activity	8.48×10^{-3}	2	283	53.70	*MAP1A GATAD2A*
Schizophrenia - Monocyte percentage of white cells	GO: Molecular Function	Molecular adaptor activity	8.48×10^{-3}	2	353	43.05	*MAP1A GATAD2A*
Schizophrenia - Lymphocyte count	GO: Cellular Component	Microtubule cytoskeleton	0.011	2	1391	16.39	*DDHD2 PPP2R3C*
Schizophrenia - Neutrophil percentage of white cells	GO: Molecular Function	ATP binding	0.014	2	1662	13.72	*MAPK3 ABCB9*
Schizophrenia - Neutrophil percentage of white cells	GO: Molecular Function	Adenyl nucleotide binding	0.014	2	1743	13.08	*MAPK3 ABCB9*
Schizophrenia - Neutrophil percentage of white cells	GO: Molecular Function	Adenyl ribonucleotide binding	0.014	2	1730	13.18	*MAPK3 ABCB9*
Schizophrenia - Lymphocyte count	GO: Cellular Component	Golgi apparatus	0.014	2	1812	12.58	*DDHD2 PPP2R3C*
Schizophrenia - Monocyte percentage of white cells	GO: Cellular Component	Transcription regulator complex	0.016	2	465	32.68	*EP300 GATAD2A*
Schizophrenia - Monocyte percentage of white cells	GO: Molecular Function	Zinc ion binding	0.016	2	942	16.13	*EP300 GATAD2A*
Schizophrenia - Monocyte percentage of white cells	GO: Molecular Function	Cytoskeletal protein binding	0.017	2	1050	14.47	*EP300 MAP1A*
Schizophrenia - Monocyte percentage of white cells	GO: Molecular Function	Transition metal ion binding	0.019	2	1238	12.28	*EP300 GATAD2A*
Multiple sclerosis - Eosinophil count	GO: Cellular Component	Cell surface	0.020	3	960	11.87	*CD5 FCRL2 FCRL3*
Multiple sclerosis - Eosinophil count	GO: Molecular Function	Phosphatase binding	0.023	2	224	33.92	*FCRL2 FCRL3*
Multiple sclerosis - Eosinophil count	GO: Molecular Function	Protein phosphatase binding	0.023	2	170	44.70	*FCRL2 FCRL3*
Schizophrenia - Monocyte percentage of white cells	GO: Cellular Component	Nuclear protein-containing complex	0.031	2	1379	11.02	*EP300 GATAD2A*
Schizophrenia - Monocyte percentage of white cells	GO: Cellular Component	Catalytic complex	0.031	2	1540	9.87	*EP300 GATAD2A*
Schizophrenia - Lymphocyte count	GO: Biological Process	Positive regulation of developmental process	0.032	2	1373	16.60	*DDHD2 PPP2R3C*
Multiple sclerosis - Red cell distribution width	GO: Biological Process	Mitochondrion organization	0.040	2	605	12.56	*TYMP MYO19*
Multiple sclerosis - Red cell distribution width	GO: Biological Process	Organelle fission	0.040	2	584	13.01	*BANF1 MYO19*
Schizophrenia - Reticulocyte fraction of red cells	GO: Cellular Component	Nuclear speck	0.041	2	481	13.54	*GATAD2A ARL6IP4*
Schizophrenia - Monocyte percentage of white cells	GO: Biological Process	Learning or memory	0.041	2	273	55.67	*EP300 MAP1A*
Schizophrenia - Monocyte percentage of white cells	GO: Biological Process	Cognition	0.041	2	327	46.48	*EP300 MAP1A*
Schizophrenia - Reticulocyte count	GO: Cellular Component	Nuclear speck	0.043	2	481	18.96	*GATAD2A ARL6IP4*
Schizophrenia - Monocyte percentage of white cells	GO: Cellular Component	Chromosome	0.044	2	1918	7.92	*EP300 GATAD2A*
Multiple sclerosis - Eosinophil count	GO: Cellular Component	Integral component of plasma membrane	0.045	3	1881	6.06	*CD5 FCRL2 FCRL3*
Multiple sclerosis - Eosinophil count	GO: Cellular Component	Intrinsic component of plasma membrane	0.045	3	1965	5.80	*CD5 FCRL2 FCRL3*

Table S51. Drug targets identified for shared candidate genes (listed in Tables S36-37) underlying PDW - PD and PCT - stroke, respectively, related to Figure 4 and STAR Methods.

Trait Pair	Gene	Drug	Sources*
PDW - PD	*CTNNB1*	TEMSIROLIMUS	JAX-CKB
PDW - PD	*CTNNB1*	CYCLOPHOSPHAMIDE	PharmGKB
PDW - PD	*CTNNB1*	LENALIDOMIDE	PharmGKB
PDW - PD	*CTNNB1*	LETROZOLE	CGI
PDW - PD	*CTNNB1*	EVEROLIMUS	CGI
PDW - PD	*CTNNB1*	EOSIN_Y	DTC
PDW - PD	*CTNNB1*	THALIDOMIDE	PharmGKB
PDW - PD	*CTNNB1*	VANTICTUMAB	JAX-CKB
PDW - PD	*CTNNB1*	CELECOXIB	PharmGKB
PDW - PD	*CTNNB1*	CHEMBL410484	DTC
PDW - PD	*CTNNB1*	DEXAMETHASONE	PharmGKB
PDW - PD	*CTNNB1*	IMATINIB	JAX-CKB
PDW - PD	*CTNNB1*	FLUORESCEIN SODIUM	DTC
PDW - PD	*CTNNB1*	DITHIAZANINE IODIDE	DTC
PDW - PD	*CTNNB1*	CHEMBL2172378	DTC
PDW - PD	*CTNNB1*	TRICIRIBINE	JAX-CKB
PDW - PD	*CTNNB1*	CHEMBL533293	DTC
PDW - PD	*CTNNB1*	TRAMETINIB	JAX-CKB
PDW - PD	*CTNNB1*	CHEMBL91638	DTC
PDW - PD	*FXR2*	METHYLPHENIDATE	PharmGKB
PDW - PD	*GGCX*	PHYTONADIONE	TdgClinicalTrial|TEND|TTD
PDW - PD	*GGCX*	ANISINDIONE	TdgClinicalTrial|TEND|GuideToPharmacology
PDW - PD	*GGCX*	MENADIONE	TdgClinicalTrial|TEND
PDW - PD	*GGCX*	ACENOCOUMAROL	PharmGKB
PCT - Stroke	*KCNK5*	QUINIDINE	GuideToPharmacology
PCT - Stroke	*KCNK5*	HALOTHANE	GuideToPharmacology
PDW - PD	*MAP3K5*	HYDROXYUREA	PharmGKB
PDW - PD	*MAP3K5*	SELONSERTIB	ChemblInteractions|GuideToPharmacology|TTD
PDW - PD	*PRKD1*	QUERCETIN	MyCancerGenome
PDW - PD	*PRKD1*	GSK-690693	ChemblInteractions
PDW - PD	*PRKD1*	MIDOSTAURIN	ChemblInteractions
PDW - PD	*PRKD1*	UCN-01	ChemblInteractions
PDW - PD	*PRKD1*	SOTRASTAURIN	ChemblInteractions
PDW - PD	*PRKD1*	CEP-2563	ChemblInteractions
PDW - PD	*PRKD1*	BRYOSTATIN	TdgClinicalTrial
PDW - PD	*PRKD1*	VASOPRESSIN	NCI
PDW - PD	*PRKD1*	RESVERATROL	NCI
PDW - PD	*PSMB10*	BORTEZOMIB	DTC|MyCancerGenome|ChemblInteractions
PDW - PD	*PSMB10*	OPROZOMIB	ChemblInteractions
PDW - PD	*PSMB10*	IXAZOMIB CITRATE	ChemblInteractions
PDW - PD	*PSMB10*	CARFILZOMIB	DTC|MyCancerGenome|ChemblInteractions
PDW - PD	*PSMB10*	MARIZOMIB	ChemblInteractions
PDW - PD	*PTK2*	PF-00562271	TALC|DTC|ChemblInteractions|GuideToPharmacology|TTD
PDW - PD	*PTK2*	GSK-2256098	ChemblInteractions|TTD
PDW - PD	*PTK2*	VS-4718	ChemblInteractions|GuideToPharmacology|TTD
PDW - PD	*PTK2*	CEP-37440	ChemblInteractions|GuideToPharmacology|TTD
PDW - PD	*PTK2*	ENMD-2076	TdgClinicalTrial|GuideToPharmacology
PDW - PD	*PTK2*	DEFACTINIB	TdgClinicalTrial|ChemblInteractions
PDW - PD	*PTK2*	HESPERADIN	DTC
PDW - PD	*PTK2*	BI-853520	ChemblInteractions|TTD
PDW - PD	*PTK2*	MASITINIB	MyCancerGenome
PDW - PD	*PTK2*	SNS-314	DTC
PDW - PD	*PTK2*	CHEMBL456559	DTC
PDW - PD	*PTK2*	LINIFANIB	DTC
PDW - PD	*PTK2*	GW843682X	DTC
PDW - PD	*PTK2*	CHEMBL2333445	DTC
PDW - PD	*PTK2*	PD-0166285	DTC
PDW - PD	*PTK2*	ALISERTIB	DTC
PDW - PD	*PTK2*	RG-1530	DTC
PDW - PD	*PTK2*	DEFACTINIB HYDROCHLORIDE	TTD
PDW - PD	*PTK2*	ENTRECTINIB	DTC
PDW - PD	*PTK2*	PAZOPANIB	DTC
PDW - PD	*PTK2*	ADAVOSERTIB	DTC
PDW - PD	*PTK2*	ILORASERTIB	DTC
PDW - PD	*PTK2*	R-406	DTC

PDW - PD	*PTK2*	CHEMBL1997335	DTC
PDW - PD	*PTK2*	CHLORPYRAMIN HYDROCHLORIDE	DTC
PDW - PD	*PTK2*	MLN-8054	DTC
PCT - Stroke	*PXN*	CHEMBL456559	DTC
PCT - Stroke	*PXN*	LOVASTATIN	NCI
PDW - PD	*RHD*	ROZROLIMUPAB	ChemblInteractions
PDW - PD	*RHD*	ROLEDUMAB	ChemblInteractions|TTD
PDW - PD	*RHD*	ATOROLIMUMAB	ChemblInteractions
PDW - PD	*SENP3*	METHYLPHENIDATE	PharmGKB
PDW - PD	*SREBF1*	INSULIN	NCI
PDW - PD	*SREBF1*	FLUVASTATIN	PharmGKB
PDW - PD	*SYK*	CERDULATINIB	ChemblInteractions|GuideToPharmacology|TTD
PDW - PD	*SYK*	APITOLISIB	GuideToPharmacology
PDW - PD	*SYK*	FOSTAMATINIB	MyCancerGenome|TdgClinicalTrial|ChemblInteractions|TTD
PDW - PD	*SYK*	R-343	ChemblInteractions
PDW - PD	*SYK*	ENTOSPLETINIB	ChemblInteractions|GuideToPharmacology|TTD
PDW - PD	*SYK*	R-112	ChemblInteractions
PDW - PD	*SYK*	R-406	DTC|ChemblInteractions
PDW - PD	*SYK*	LANRAPLENIB	GuideToPharmacology
PDW - PD	*SYK*	PRT-2607	ChemblInteractions|GuideToPharmacology|TTD
PDW - PD	*SYK*	HMPL-523	ChemblInteractions
PDW - PD	*SYK*	R-348	ChemblInteractions
PDW - PD	*SYK*	TAK-659	ChemblInteractions|TTD
PDW - PD	*SYK*	R-333	ChemblInteractions
PDW - PD	*SYK*	ENTRECTINIB	DTC
PDW - PD	*SYK*	CEDIRANIB	DTC
PDW - PD	*SYK*	ERLOTINIB	DTC
PDW - PD	*SYK*	SP-600125	DTC
PDW - PD	*SYK*	CHEMBL535331	DTC
PDW - PD	*SYK*	PD-0166285	DTC
PDW - PD	*SYK*	RG-1530	DTC
PDW - PD	*SYK*	ILORASERTIB	DTC
PDW - PD	*SYK*	ADAVOSERTIB	DTC
PDW - PD	*SYK*	IMATINIB MESYLATE	TTD
PDW - PD	*SYK*	GW441756X	DTC
PDW - PD	*SYK*	TAE-684	DTC
PDW - PD	*SYK*	PACLITAXEL	CIViC
PDW - PD	*SYK*	CYC-116	DTC
PDW - PD	*SYK*	CENISERTIB	DTC
PDW - PD	*SYK*	DASATINIB	DTC
PDW - PD	*SYK*	CHEMBL379975	DTC

*Sources are based on the drug-gene interaction database (DGIdb; https://www.dgidb.org/). PCT: plateletcrit. PDW: platelet distribution width. PD: Parkinson's disease.

Supplemental Data

Data S1. Phenotypic correlations for BCT-NPD trait pairs with putative causal relationships, related to STAR Methods.

Using individual-level data from the UK Biobank (UKB) cohort, we estimated phenotypic correlations for the three blood cell trait (BCT)-neurological and psychiatric disorder (NPD) pairs found to have a putative or suggestive causal relationship on the basis of Mendelian randomisation (MR): plateletcrit ("PCT") and stroke, platelet distribution width ("PDW") and Parkinson's disease (PD), and lymphocyte count (LYMPH#) and multiple sclerosis (MS). After restricting to unrelated Europeans (genetic relatedness < 0.05) and removing individuals with missing data on sex and age at recruitment, nearly 348K individuals remained. Individuals were coded with information on PCT (UKB field ID: 30090), PDW (UKB field ID: 30110), LYMPH# (UKB field ID: 30120), stroke-related variables (UKB field ID: 42007 [hospital admission, exclude self-report only], 42009 [hospital admission, exclude self-report only], 41270-I64 [10th revision of the International Statistical Classification of Diseases (ICD10)-based stroke status]), PD status (UKB field ID: 41270-G20 [ICD10-based PD status]), and MS status (UKB field ID: 41270-G35 [ICD10-based MS status]).

We defined stroke cases (hospital admission and ICD10-based stroke, n = 5,288, UKB field ID: 42007 + 42009 + 41270-I64), PD cases (ICD10-based PD, n = 1,323, UKB field ID: 41270-G20), and MS cases (ICD10-based MS, n = 1,238, UKB field ID: 41270-G35). For each diagnostic group (i.e., stroke, PD or MS cases, respectively), we randomly selected healthy controls from individuals without the respective diagnosis (i.e., non-stroke, non-PD or non-MS), matching by sex and age (+/- 2 years). We then evaluated the phenotypic correlations (r_P) for these three pairs of traits, using the full sample and lists of sub-samples at an assumed prevalence of 1% (for PD and MS), 2% (for PD and MS), 5% (for all three diseases) and 10% (for stroke only), respectively. We observed significant phenotypic correlations between PCT and stroke, regardless of the definition used to define the prevalence, with estimated r_P at around 0.01 ($p < 0.05$; Table S28). We also observed marginally significant phenotypic correlations between PDW and PD ($r_P \sim 0.01$, $p < 0.07$; Table S28). Conversely, we failed to observe any evidence for a significant phenotypic correlation between LYMPH# and MS, potentially due to the modest number of MS cases in the UKB (Table S28).

Data S2. Investigating the role of inflammatory response in mediating the causal relationship between platelet distribution width and Parkinson's disease, related to STAR Methods.

Published studies[2-6] support a critical role for the inflammatory response on both PD and platelet hyperactivity. On the basis of these findings, we hypothesised that C-reactive protein (CRP, used as a 'proxy' of inflammatory response) might be relevant to the putative causal effect of PDW on PD.

We investigated the role of CRP using a conditional MR approach. First, we utilised multi-trait-based conditional & joint analysis (mtCOJO)[7] to condition genome-wide association study (GWAS) summary data of PDW and PD on the GWAS of CRP[8], based on the in-house UKB genotype reference of unrelated Europeans. Here, we used summary data from the GWAS of CRP by Ligthart et al.[8], which was generated from 204,402 individuals of European ancestry using fixed-effect inverse-variance-weighted meta-analysis. Second, we re-estimated the causal relationship between PD and PDW on the basis of the conditional GWAS summary statistics using CAUSE[9]. Notably, the results from these conditional CAUSE analyses were highly consistent with the original analyses, both with PDW as an exposure for PD (odds ratio [OR_{CAUSE}] = 1.07, 95% confidence interval [CI] = 1.02-1.12, $p_{OR} = 1.37\times10^{-3}$; $p = 0.04$ for testing if the causal model is a better fit than the sharing model or null model) and PD as an exposure for PDW ($OR_{CAUSE} = 0.99$, 95% CI = 0.98-1.00, $p_{OR} = 0.06$; $p = 0.27$) (Table S26). This suggests a limited contribution of the inflammatory response on the putative causality of PDW on risk of PD. This conclusion is also supported by the absence of support for a significant genome-wide genetic correlation (estimated by linkage disequilibrium score regression[10]) between CRP and PDW ($r_g = 0.07$, se = 0.06, $p = 0.11$), or between CRP and PD ($r_g = -0.06$, se = 0.05, $p = 0.10$).

Supplemental References

1. Lloyd-Jones, L.R., Zeng, J., Sidorenko, J., Yengo, L., Moser, G., Kemper, K.E., Wang, H., Zheng, Z., Magi, R., Esko, T., et al. (2019). Improved polygenic prediction by Bayesian multiple regression on summary statistics. Nat Commun *10*, 5086. 10.1038/s41467-019-12653-0.
2. Park, S.M., Jung, H.Y., Kim, H.O., Rhim, H., Paik, S.R., Chung, K.C., Park, J.H., and Kim, J. (2002). Evidence that alpha-synuclein functions as a negative regulator of Ca(++)-dependent alpha-granule release from human platelets. Blood *100*, 2506-2514. 10.1182/blood.V100.7.2506.
3. Rawish, E., Nording, H., Munte, T., and Langer, H.F. (2020). Platelets as Mediators of Neuroinflammation and Thrombosis. Front Immunol *11*, 548631. 10.3389/fimmu.2020.548631.
4. Wang, Q., Liu, Y., and Zhou, J. (2015). Neuroinflammation in Parkinson's disease and its potential as therapeutic target. Transl Neurodegener *4*, 19. 10.1186/s40035-015-0042-0.
5. Koupenova, M., Clancy, L., Corkrey, H.A., and Freedman, J.E. (2018). Circulating Platelets as Mediators of Immunity, Inflammation, and Thrombosis. Circ Res *122*, 337-351. 10.1161/CIRCRESAHA.117.310795.
6. Morrell, C.N., Aggrey, A.A., Chapman, L.M., and Modjeski, K.L. (2014). Emerging roles for platelets as immune and inflammatory cells. Blood *123*, 2759-2767. 10.1182/blood-2013-11-462432.
7. Zhu, Z., Zheng, Z., Zhang, F., Wu, Y., Trzaskowski, M., Maier, R., Robinson, M.R., McGrath, J.J., Visscher, P.M., Wray, N.R., and Yang, J. (2018). Causal associations between risk factors and common diseases inferred from GWAS summary data. Nat Commun *9*, 224. 10.1038/s41467-017-02317-2.
8. Ligthart, S., Vaez, A., Vosa, U., Stathopoulou, M.G., de Vries, P.S., Prins, B.P., Van der Most, P.J., Tanaka, T., Naderi, E., Rose, L.M., et al. (2018). Genome Analyses of >200,000 Individuals Identify 58 Loci for Chronic Inflammation and Highlight Pathways that Link Inflammation and Complex Disorders. Am J Hum Genet *103*, 691-706. 10.1016/j.ajhg.2018.09.009.
9. Morrison, J., Knoblauch, N., Marcus, J.H., Stephens, M., and He, X. (2020). Mendelian randomization accounting for correlated and uncorrelated pleiotropic effects using genome-wide summary statistics. Nat Genet *52*, 740-747. 10.1038/s41588-020-0631-4.
10. Bulik-Sullivan, B.K., Loh, P.R., Finucane, H.K., Ripke, S., Yang, J., Schizophrenia Working Group of the Psychiatric Genomics, C., Patterson, N., Daly, M.J., Price, A.L., and Neale, B.M. (2015). LD Score regression distinguishes confounding from polygenicity in genome-wide association studies. Nat Genet *47*, 291-295. 10.1038/ng.3211.